USING *N*-ALKANE AS A PROXY TO RECONSTRUCT PALEOENVIRONMENT IN THALE NOI, PHATTHALUNG PROVINCE

Miss Assuma Sainakum

จุฬาลงกรณ์มหาวิทยาลัย
CHULALONGKORN UNIVERSITY

A Thesis Submitted in Partial Fulfillment of the Requirements
for the Degree of Master of Science in Earth Sciences
Department of Geology
Faculty of Science
Chulalongkorn University
Academic Year 2018
Copyright of Chulalongkorn University

การใช้ เอ็น แอลเคน เป็นตัวบ่งชี้เพื่อจำลองสภาพแวดล้อมบรรพกาล บริเวณทะเลน้อย จังหวัดพัทลุง

น.ส.อัสสุมา สายนาคำ

วิทยานิพนธ์นี้เป็นส่วนหนึ่งของการศึกษาตามหลักสูตรปริญญาวิทยาศาสตรมหาบัณฑิต
สาขาวิชาโลกศาสตร์ ภาควิชาธรณีวิทยา
คณะวิทยาศาสตร์ จุฬาลงกรณ์มหาวิทยาลัย
ปีการศึกษา 2561

Thesis Title	USING *N*-ALKANE AS A PROXY TO RECONSTRUCT PALEOENVIRONMENT IN THALE NOI, PHATTH ALUNG PROVINCE
By	Miss Assuma Sainakum
Field of Study	Earth Sciences
Thesis Advisor	Assistant Professor AKKANEEWUT CHABANGBORN, Ph.D.
Thesis Co Advisor	Assistant Professor Piyada Jittangprasert, Ph.D.

Accepted by the Faculty of Science, Chulalongkorn University in Partial Fulfillment of the Requirement for the Master of Science

.... Dean of the Faculty of Science
(Professor POLKIT SANGVANICH, Ph.D.)

THESIS COMMITTEE

.... Chairman
(Associate Professor Srilert Chotpantarat, Ph.D.)
.... Thesis Advisor
(Assistant Professor AKKANEEWUT CHABANGBORN, Ph.D.)
.... Thesis Co-Advisor
(Assistant Professor Piyada Jittangprasert, Ph.D.)
.... Examiner
(Assistant Professor Penjai Sompongchaiyakul, Ph.D.)
.... External Examiner
(Assistant Professor Krit Won-in, Ph.D.)

จุฬาลงกรณ์มหาวิทยาลัย

CHULALONGKORN UNIVERSITY

อัสสุมา สายนาคำ : การใช้ เอ็น แอลเคน เป็นตัวบ่งชี้เพื่อจำลองสภาพแวดล้อมบรรพกาล บริเวณทะเลน้อย จังหวัดพัทลุง. (USING *N*-ALKANE AS A PROXY TO RECONSTRUCT PALEOENVIRONMENT IN THALE NOI, PHATTHALUNG PROVINCE) อ.ที่ปรึกษาหลัก : ผศ. ดร.อัคนีวุธ ชะบางบอน, อ.ที่ปรึกษาร่วม : ผศ. ดร.ปิยะดา จิตรตั้งประเสริฐ

สารประกอบไฮโดรคาร์บอนอิ่มตัวโซ่ตรง (เอ็น แอลเคน) เป็นตัวบ่งชี้ไฮโดรคาร์บอนที่ถูกใช้อย่างแพร่หลายในการศึกษาสภาพแวดล้อมบรรพกาล เนื่องจากมีลักษณะเฉพาะและความทนทานต่อการถูกย่อยสลายโดยจุลินทรีย์ เอ็น-แอลเคนในแท่งตะกอน TLN-CP5 และ TLN-CP7 จากทะเลน้อย จังหวัดพัทลุง ถูกนำมาใช้ในการศึกษาครั้งนี้ โดยการศึกษานี้ได้ทำการสกัดเอ็น แอลเคน จากตัวอย่างตะกอน แล้วนำไปเปรียบเทียบกับเอ็น แอลเคน ที่สกัดได้จากพืชปัจจุบัน ซึ่งพืชเหล่านี้เก็บมาจากกลุ่มพืชป่าชายเลน ได้แก่ ป่าชายเลนที่แท้จริง (true mangrove) ป่าบริเวณหลังแนวป่าชายเลน (back mangrove) และป่าชายเลนทั่วไป (mangrove associate) โดยอ้างอิงจากการวิเคราะห์ละอองเรณูในทะเลน้อยจากการศึกษาก่อนหน้านี้ การกระจายตัวของเอ็น-แอลเคน ค่าเฉลี่ยช่วงน้ำหนัก (ACL) ค่าอัตราส่วนปริมาณคาร์บอนอะตอมเลขคี่ต่อปริมาณคาร์บอนอะตอมเลขคู่ (CPI) และอัตราส่วนของปริมาณพืชน้ำ (P_{aq}) ได้ถูกนำมาวิเคราะห์เพื่อใช้จำลองการเปลี่ยนแปลงของสภาพแวดล้อมบรรพกาล สำหรับในตัวอย่างพืชปัจจุบันพบว่าการกระจายตัวของเอ็น-แอลเคน ค่า ACL และ CPI ในพืชแต่ละกลุ่มนั้นค่อนข้างหลากหลายและมีการกระจายตัวสูง ซึ่งผลลัพธ์ที่คลุมเครือนี้อาจเกิดจากสภาพแวดล้อมที่พืชเจริญเติบโตในแต่ละพื้นที่มีผลต่อการสร้างเอ็น แอลเคนที่แตกต่างกัน และตัวอย่างพืชมีน้อยเกินไปจนไม่สามารถเป็นตัวแทนของกลุ่มพืชทั้งหมดได้ ตรงกันข้ามกับในตะกอนทะเลสาบที่การกระจายตัวของเอ็น-แอลเคน ค่า ACL และ CPI มีความสอดคล้องกับการเปลี่ยนแปลงของสภาพแวดล้อมบรรพกาลอย่างชัดเจน ผลการศึกษานี้แนะให้เห็นว่าการเปลี่ยนแปลงของ C_{21} C_{27} C_{29} และ C_{31} บ่งบอกการเปลี่ยนแปลงของพืชพรรณและระดับน้ำในทะเลสาบได้ โดย C_{21} สัมพันธ์กับระดับน้ำที่ค่อนข้างสูงซึ่งตรงข้ามกับ C_{27} C_{29} และ C_{31} ที่สัมพันธ์กับระดับน้ำที่ต่ำกว่า ส่วนค่า ACL CPI และ P_{aq} สามารถนำมาใช้บ่งบอกความผันผวนของระดับน้ำทะเลได้ โดยการเพิ่มขึ้นของค่า ACL และ CPI บ่งบอกถึงการถดถอยของน้ำทะเลในช่วงประมาณ 8,300 ถึง 8,000 ปีก่อนปัจจุบัน จากนั้นค่า ACL และ CPI ค่อย ๆ ลดลงตอนประมาณ 7,600 ถึง 7,200 ปีก่อนปัจจุบัน ซึ่งสอดคล้องกับการเพิ่มขึ้นของระดับน้ำทะเล ค่า P_{aq} ที่สูงและการเพิ่มขึ้นของ ACL และ CPI ที่พบบริเวณผิวตะกอนแสดงให้เห็นว่าน้ำจืดมีอิทธิพลมากกว่าน้ำทะเลหลังจากช่วง 7,200 ปีก่อนปัจจุบันจนมาถึงปัจจุบัน

จุฬาลงกรณ์มหาวิทยาลัย
CHULALONGKORN UNIVERSITY

สาขาวิชา	โลกศาสตร์	ลายมือชื่อนิสิต ....
ปีการศึกษา	2561	ลายมือชื่อ อ.ที่ปรึกษาหลัก ....
		ลายมือชื่อ อ.ที่ปรึกษาร่วม ....

Assuma Sainakum : USING *N*-ALKANE AS A PROXY TO RECONSTRUCT PALEOENVIRONMENT IN THALE NOI, PHATTHALUNG PROVINCE. Advisor: Asst. Prof. AKKANEEWUT CHABANGBORN, Ph.D. Co-advisor: Asst. Prof. Piyada Jittangprasert, Ph.D.

Normal alkane (*n*-alkane) is the widely used hydrocarbon proxy for the paleoenvironmental study because of their specific characteristic and resistance to microbial degradation. The *n*-alkanes from the sediment cores TLN-CP5 and TLN-CP7 from Thale Noi, Phatthalung Province, were analyzed and subsequently compared with those derived from the recent plant samples. The plant samples were taken from mangrove forests, i.e. true mangrove, back mangrove, and mangrove associate, based on the previous study on pollen analysis. The *n*-alkane distributions, the average chain length (ACL), the carbon preference index (CPI) and the proportion of aquatic components (P_{aq}) were further analyzed in order to reconstruct past environmental changes. For the modern plant samples, the *n*-alkane distributions, ACL and CPI values in each plant group are diverse and high uncertainty. These ambiguity results are possibly caused by growing environment influent on *n*-alkane synthesis and too small sample size to represent the entire plant groups. In contrast, the *n*-alkanes distribution and their parameters in lake sediment have obviously corresponded to change of paleoenvironment. Our results suggest that the change of C_{21}, C_{27}, C_{29}, and C_{31} abundances of *n*-alkane indicate the dynamic of vegetations and water level in the lake. C_{21} relate to the high-water level that opposing to C_{27}, C_{29}, and C_{31}. The ACL, CPI, and P_{aq} can be used to indicate a sea-level fluctuation. During about 8,300 to 8,000 cal yr BP, the ACL and CPI gradually increase that suggest a sea level regression. And then the ACL and CPI gradually decrease about 7,600 to 7,200 cal yr BP that correspond to a transgression. A high P_{aq} and increasing of ACL and CPI presence in the surface sediment demonstrate that freshwater has more influence than seawater after 7,200 cal yr BP to recent.

จุฬาลงกรณ์มหาวิทยาลัย

CHULALONGKORN UNIVERSITY

Field of Study:	Earth Sciences	Student's Signature ....
Academic Year:	2018	Advisor's Signature ....
		Co-advisor's Signature ....

ACKNOWLEDGEMENTS

TABLE OF CONTENTS

Page

จุฬาลงกรณ์มหาวิทยาลัย

CHULALONGKORN UNIVERSITY

LIST OF TABLES

จุฬาลงกรณ์มหาวิทยาลัย

CHULALONGKORN UNIVERSITY

LIST OF FIGURES

จุฬาลงกรณ์มหาวิทยาลัย

CHULALONGKORN UNIVERSITY

CHAPTER I
INTRODUCTION

1.1 Rationale

Climate is an average of weather, which is a modulation of many atmospheric variables, e.g. temperature, humidity, atmospheric pressure, and wind speed and direction, over a given period of time (Easterling et al., 1993). The gradual increase in temperature plays a key role in environmental changes, e.g. long frost-free season, violent droughts, heat wave, and strengthen and frequent hurricanes (Hoegh-Guldberg et al., 2007). The sea level change is also a potential indicator of global temperature variability because it has a closed relationship with the disruption of the ocean thermal and the continental ice sheets (Hoegh-Guldberg et al., 2007). In addition, recent studies point to the accelerating on sea level rise between 19th and 21st century under global warming (Hoegh-Guldberg et al., 2007). This transgression allows the saline intrusion into groundwater and surface water, which is caused by a decrease in the agricultural products (Easterling et al., 1993). Moreover, the accelerated rise in sea level triggers coastal erosion and coastal wetland loss (Wenner and Simmons, 2009). These physical impacts can be led to socio-economic problems, e.g. unemployment, food resources, and a decline in the gross domestic product. Despite the physical impact on the sea level rise are well known, the information on long-term sea level changes are necessary for the proper adaptation and application in the future.

The reconstruction of the past environment based on the geological archives, e.g. ice cores, speleothems, marine or lake sediments and evolution of geomorphology, can provide a longer time record than the instrumental observation (Fairall et al., 2003). This indirect information can be used to validate climate simulation for a better understanding of the environmental response on climate changes. The lake sediments are widely used for environmental reconstruction because of their simple chronology and deposition with various proxies (Meyers, 1997, 2003; Meyers and Ishiwatari, 1993). The lake sediments are generally not disturbed by external factors after deposition. Therefore, the sediment sequences have followed the law of superposition that the lower strata are older than their overlaid

layer (Jackson, 2006). Moreover, many proxies deposit with the sediments in the lake that can be classified into three groups: physical, biological and chemical proxies. The physical proxies are sediment characteristics including their composition, texture, structure, color, density or magnetic property (Last and Smol, 2006). The biological proxies are non-living organisms from plants and animals, such as pollen, spore, plant macrofossil, charcoal, ostracod, and diatom (Last and Smol, 2006). And the chemical proxies are fossil substances derived from living organisms that preserved in sediments, e.g. elemental composition, biogenic silica, and organic matter (Last and Smol, 2006).

Organic matter is complex organic compound, which generally consist of carbon, hydrogen and other elements that derived from the decomposition of living organisms by microbial activities (Meyers, 2003). The organic compounds are, for example, fatty acids, aliphatic hydrocarbons, isoprenoid compounds, alcohols and ketones, pentacyclic triterpenoid acids, steranes and triterpenes, sterols, carbohydrates, amino acids, and amino sugars, pigments, purines and pyrimidines (Hao et al., 2015; Peters et al., 2004). Among those organic matters, the biomarkers are organic compounds, which are commonly found in a specific organism, and contain stable structure under the sediment processes (Peters et al., 2004). Most of the biomarkers are lipid hydrocarbon that is generally divided into the saturated and unsaturated hydrocarbons. Normal alkanes (*n*-alkanes) are the saturated hydrocarbons consisting of carbon and hydrogen atoms that the carbon atoms arranged in a straight chain. The *n*-alkane have widely used as a proxy because of their resistance to microbial degradation (Meyers and Ishiwatari, 1993). Since the *n*-alkanes can be survived in the sediments for tens of millions of years and different organisms create a specific range of *n*-alkanes, they can be used to classify the provenance of organic matter in the sediments. These hydrocarbon proxies were here using to reconstruct the past environment in Thale Noi, Phatthalung Province.

Since plants surrounding the lake are a major source of organic matters in the sediments, the *n*-alkanes in the sediments are possibly derived from those vegetation (Pu et al., 2017). Furthermore, the vegetation dynamics in regarding to pollen analysis have been assumed to be recorded in the *n*-alkanes.

1.2 The objectives of this study consist of

      1. To construct a database of *n*-alkanes distribution of mangrove plants in the tropical zone.

      2. To reconstruct the paleoenvironment in Thale Noi, Phatthalung Province.

1.3 Expected outcome

      1. Information of *n*-alkane distribution and their parameters of mangrove plants in the tropical zone.

      2. Information on paleoenvironmental change around Thale Noi, Phatthalung Province.

1.4 Scope of works

      Eight sediment cores were taken from Thale Noi during the field experiment in January 2015 (Yoojam, 2015). These sediment successions suggest that Thale Noi possibly consists of two sub-basins. Core TLN-CP5, which represent the east sub-basin, were studied in detail by using pollen analysis by Nudnara (2016), and physical and chronological analysis by Phountong (2016). However, the detailed study in the west sub-basin has not available. The site description and previous studies were reported in detail in Chapter 2.

      The *n*-alkanes were using here as a proxy in order to understand the environmental history in Thale Noi. This study consists of two parts, i.e. modern leaf wax and sediments analysis. The methodology is presented in detail in Chapter 3. In order to cover all plant species classified by pollen in core TLN-CP5 by Nudnara (2016), the modern plant samples were taken from Thale Noi, Pattalung Province, Kung Krabaen Bay Royal Development Study Center (KKB), Chantaburi Province, and Khun Samut Chin Temple (KSC) and Pom Phra Chulachomklao (PPC), Samut Prakan Province. For the sediment analysis, cores TLN-CP5 and TLN-CP7 were selected in order to represent the western and eastern sedimentary sequences. Macroplant remains from TLN-CP7 were dated by radiocarbon dating technique using the accelerate mass spectrometer (AMS). The results of plant and sediment

analysis were present in Chapter 4. The reconstruction of environmental changes in the study area was discussed in Chapter 5 and concluded in Chapter 6.

LITERATURE REVIEWS

FIELD WORK
- Site survey
- Sampling
  - Core sampling (Yoojam, 2015)
  - Modern leaf sampling

LABORATORY WORK
- Chemical experiment : GC/MS
- Radiocarbon dating : AMS ^{14}C dating

DATA ANALYSIS
- Biomarker analysis
- Chronological analysis

INTERPRETATION
- *n*-Alkane distribution data of mangrove plants
- Paleoenvironmental change around Thale Noi
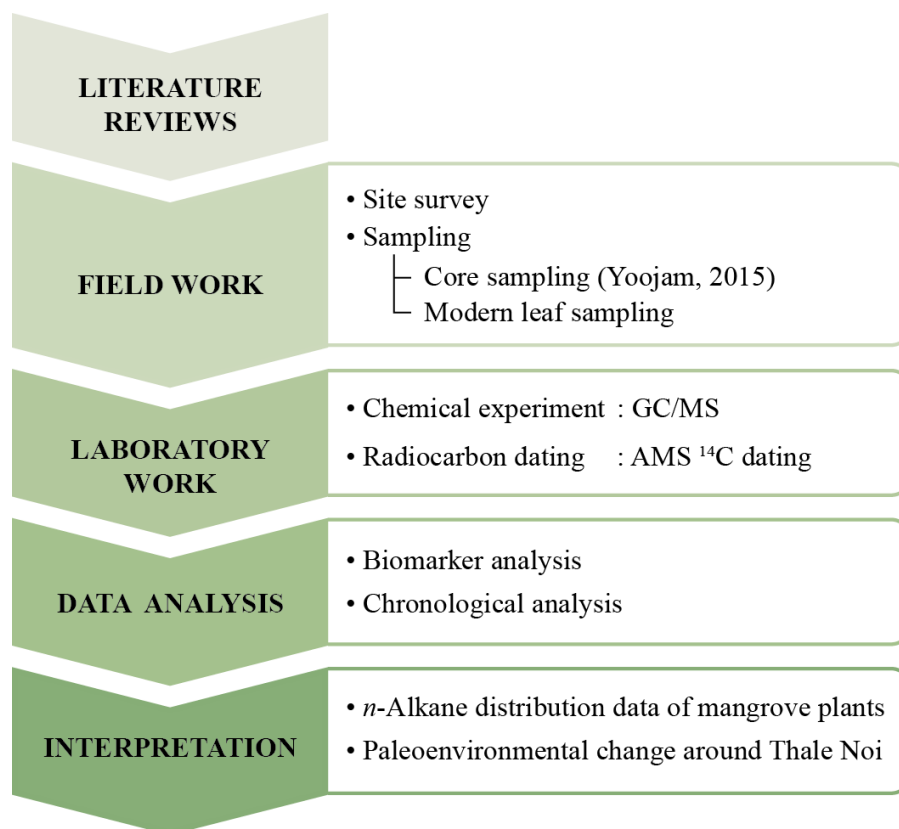
Figure 1 Thesis workflow.

CHAPTER II
LITERATURE REVIEWS

2.1 Study area

Thale Noi (7°50′N, 100°08′E) is a shallow freshwater lake that connects to the northern part of The Great Songkhla Lake, which is a lagoon on the east coast of Thai–Malay Peninsula (Fig. 2). The lake level in Thale Noi is possibly affected by not only runoff but also the sea-level changes in the Gulf of Thailand. Since this area is located in a tropical climate, and a tectonically stable region, it is a crucially important area for investigating the long-term fluctuation in the sea-level (Tjia and Liew, 1996).

Thale Noi is approximately 20 km far from the coast and covering the area of about 25 km^2 (Chaimanee et al., 1986). It is surrounded by flat plain with approximately 2 to 3 m above mean sea level (MSL) (Chaimanee et al., 1986; Somboon, 1990). The western part of the area is the Cretaceous granite mountain range and an undulated plain (Chaimanee et al., 1986; Pramojanee et al., 1986). The limestone mountain and clastic sedimentary rock can be found in the north and south, and scatter around the lake (Chaimanee et al., 1986) (Figure 3). Meanwhile, the eastern part of the lake is a flat plain and a strand plain next to the coastline. Consequently, the sediments are potentially eroded and transported from the western highland to the eastern lowland. The modern lake level is mainly supplied by precipitation, and many small canals in the north, east and west direction. The southern part of the lake is connected to the great Songkhla lake through 3 canals, i.e. Khlong Nang Riam, Khlong Ban Klang and Klong Yuan (Figure 2).

The climate in Thailand is mainly controlled by the northeast (winter) and southwest (summer) monsoons (Chawchai et al., 2013). The southwest monsoon transports humidity from the Indian Ocean and increases rainfall in Thailand from May to October. However, the precipitation in the study area is relatively low during the strengthening of the southwest monsoon. The precipitation gradual increases from October to February caused the transportation of humidity from the Gulf of Thailand to the study area by the northeast monsoon. The mean annual precipitation in this area is approximately 1,500-2,000 mm/yr (Horton et al., 2005).
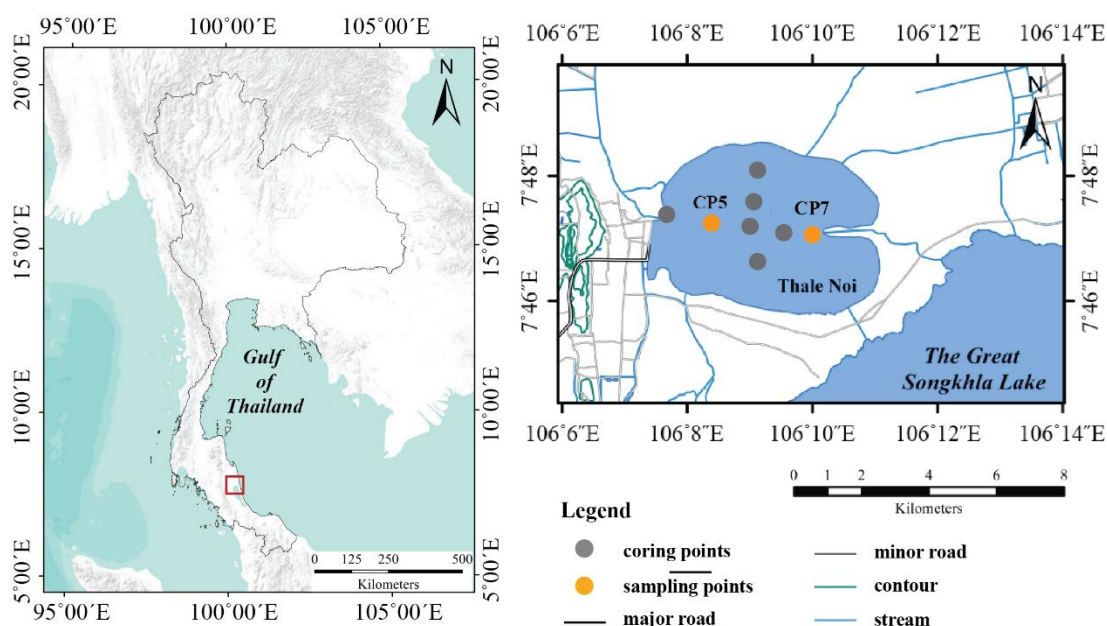
Figure 2 Topography around Thale Noi and the location of coring points.

2.2 Sea-level fluctuation

Since Thale Noi is located on tropical climate and a tectonically stable region, the tectonic movement and glacial isostatic adjustment on sea-level change are possibly negligible (Tjia and Liew, 1996). These all together make this an interesting area for the long-term investigation in sea-level changes.

According to the Quaternary sediment analysis, the Great Songkhla Lake and its surrounding area including Thale Noi was a part of the Sundaland during the late Pleistocene (Chaimanee et al., 1986; Somboon, 1990). And it became flooding caused by a gradual sea level rise at about 8500 cal yr BP (Chaimanee et al., 1986; Pradit et al., 2009; Pramojanee et al., 1986). This transgression can be assessed by pollen and sediment analysis from nearshore Thale Noi by Horton et al. (2005) (Figure 5). However, the recent study of sediment sequences suggests two different lithostratigraphic between the western and eastern Thale Noi (Yoojam, 2016) (Figure 4). Moreover, the study of radiocarbon dating associated with pollen and sediment analysis by Nudnara (2017) and Phountong (2017) propose that Thale Noi had submerged under marine environment before 8300 cal yr BP (Figure 6). Regarding to Nudnara (2017) and Phountong (2017), the sea-level decreased from 8,300 - 8,050 cal

yr BP. The transgression from 8,050 - 7,600 cal yr BP can be reconstructed, while Horton et al. (2005) mention a gradual regression from 7,780 - 2,535 cal yr BP. These discrepancies can be explained by the low dating resolution of the record from nearshore Thale Noi, which makes it difficult to capture the abrupt environmental change (Horton et al., 2005). Moreover, Nudnara (2017) and Phountong (2017) suggest the subsequent stillstand of sea-level from 7,600 - 7,200 cal yr BP. Unfortunately, the radiocarbon dating results from Nudnara (2017) and Phountong (2017) are limited at 7,200 cal yr BP. However, Chaimanee et al. (1986) found that the sea-level was lowering near the study area at approximately 6,490 – 6,758 cal yr BP. Pollen and sediment records from nearshore Thale Noi further suggest the transformation from a mangrove swamp to a freshwater lake during 2,720-2,350 cal year BP (Horton et al., 2005).
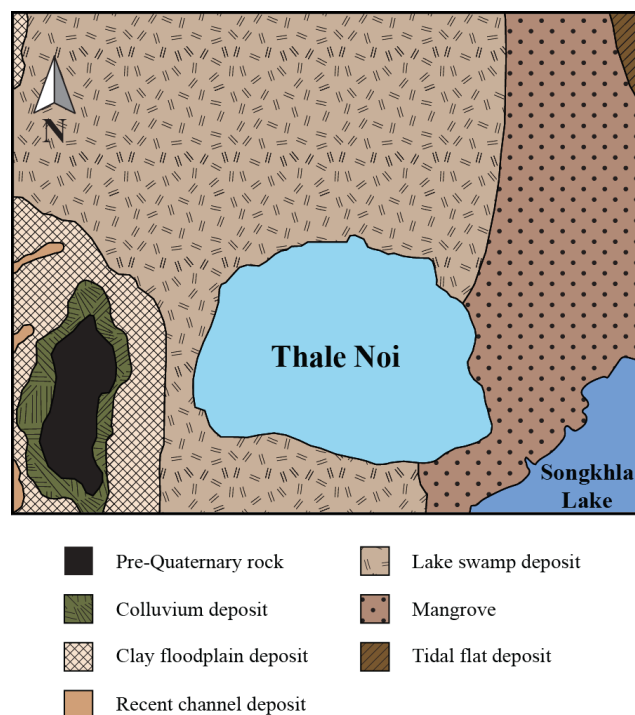
Figure 3 Quaternary geologic map of Cha-uat district, Phatthalung Province (Chaimanee., 1986).

Figure 4 Correlation of sediment cores in a west-east direction, Thale Noi (Yoojam, 2015).
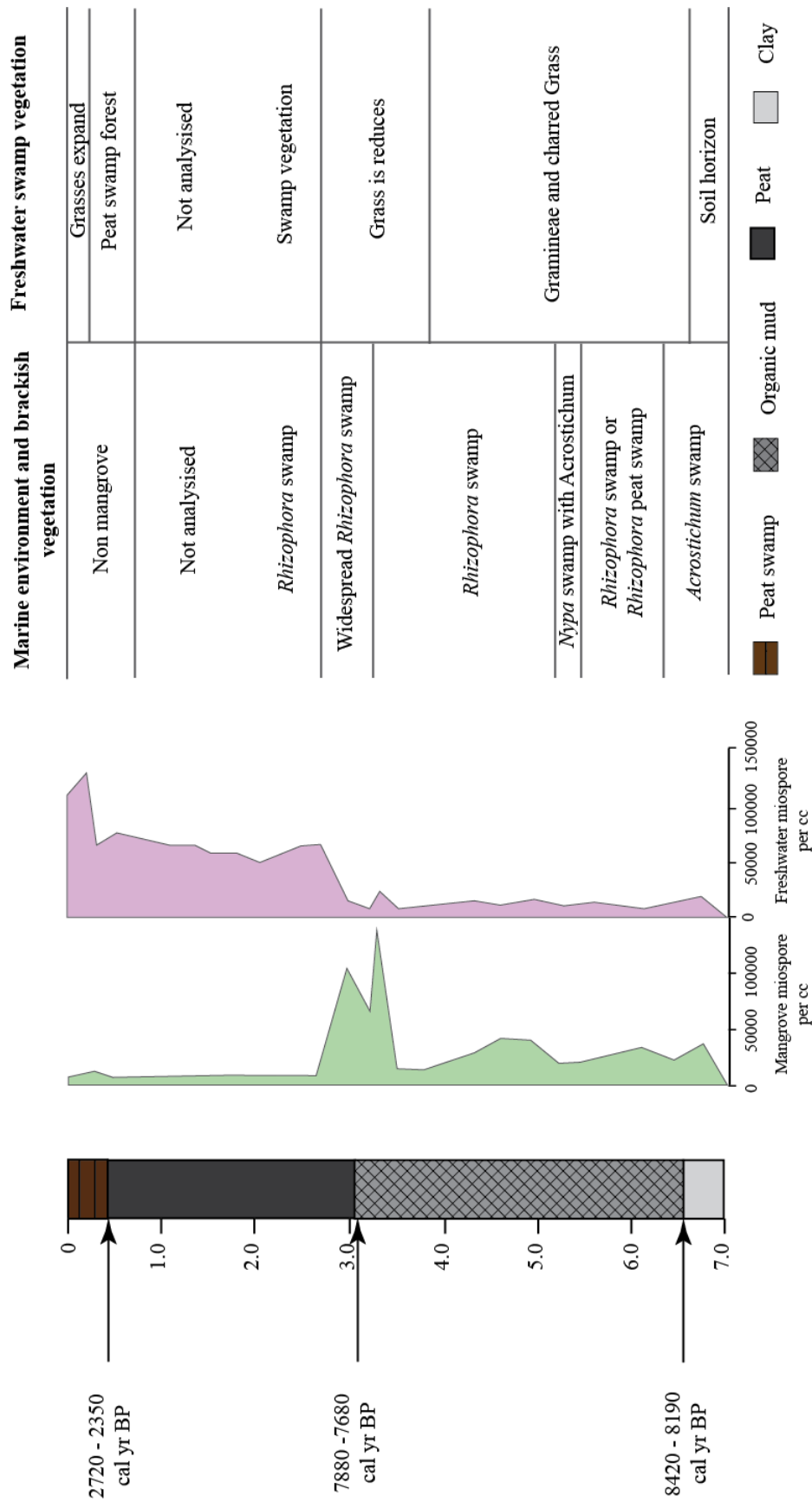
Figure 5 Thale Noi Core 3 (TN-3) paleoenvironmental interpretation based on sedimentological and palynological data (Horton et al., 2005). The coring point (TN-3) was shown in figure 2.
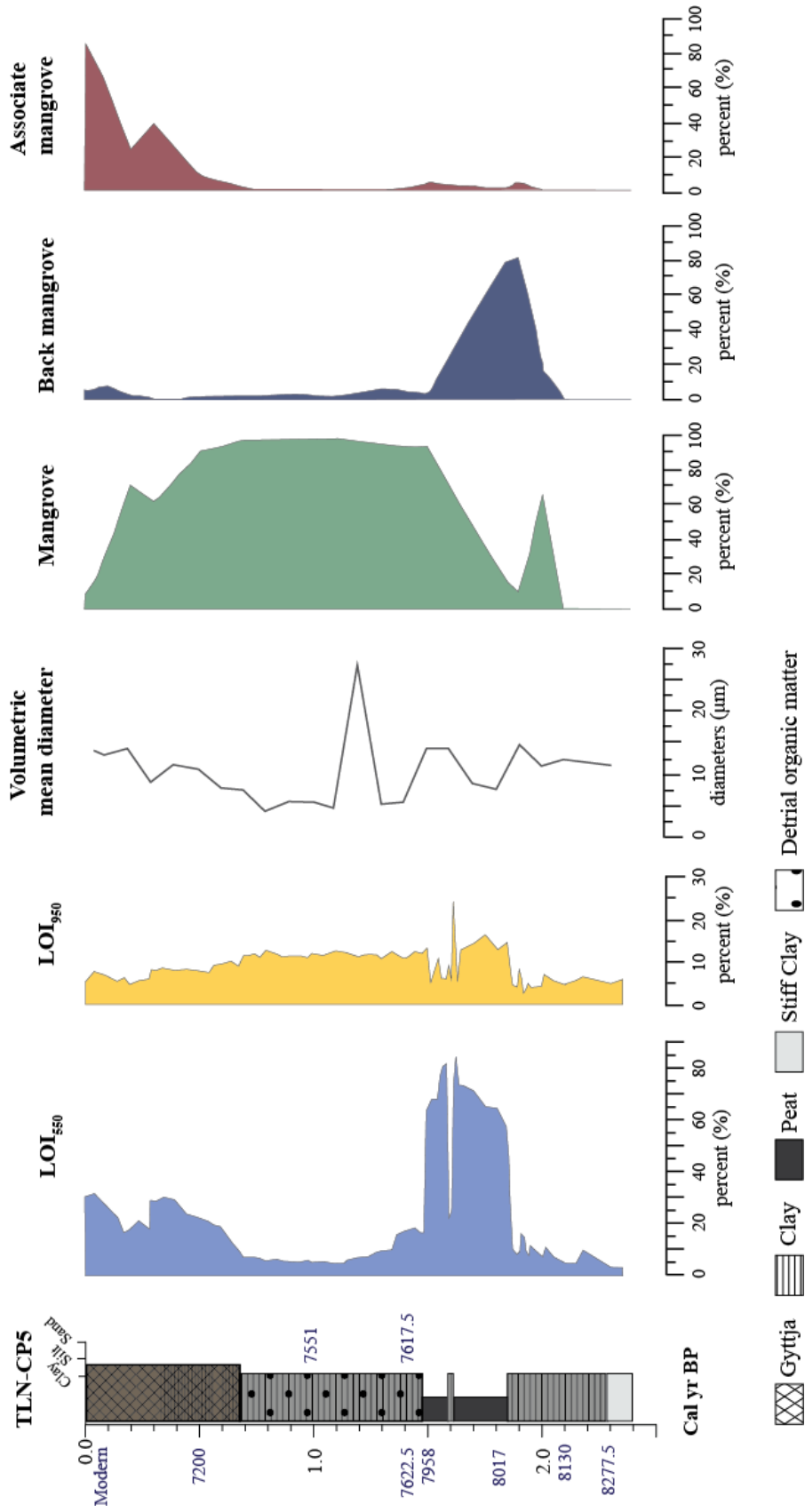
Figure 6 Graph compares lithostratigraphic column with age depth model, LOI$_{550}$, PSD and pollen assemblage distributions reported by Phountong (2016) and Nudnara (2016).

2.3 Biomarker

Biomarkers are complex organic compounds consist of carbons, hydrogens, and other elements such as oxygens, and nitrogen, etc., which are derived from diverse living organisms and stored in soil and sediment organic matter (Eglinton and Hamilton, 1967; Eglinton and Eglinton, 2008). The living organisms are classified into three major domains, including archaea, eubacteria, and eukarya (Peters et al., 2004). Archaea and eubacteria are prokaryotic cells that lack a nuclear membrane, unlike eukarya, that contains a nuclear membrane and complex organelles(Peters et al., 2004). The difference of morphology, biochemistry and metabolic pathway in the three domains organisms control the kinds of biomarkers that originated by the organisms.

The metabolism in an organism can be described as an autotrophic, heterotrophic, chemotrophic and phototrophic term (Peters et al., 2004) that rely on carbon and energy sources. Autotrophs use carbon dioxide (CO_2) as a carbon source for their thriving and obtain energy from sunlight or the oxidation of inorganic compounds to use in the process of converting CO_2 into organic compounds and create a store of chemical energy (Peters et al., 2004). In contrast, heterotrophs use organic compounds from the decomposition process from other organisms as carbon and energy sources for their growth (Peters et al., 2004). Chemotrophs take carbon and energy from the oxidation of inorganic compounds, such as H_2, H_2S, and NH_3 (Peters et al., 2004). Phototrophs are organisms which use sunlight for their metabolic process. They have the substrates for either anoxygenic photosynthesis/non-O_2 producing, which is a process that generates sulfur instead of oxygen, or oxygenic photosynthesis/ O_2-producing.

Table 1 Classification of organisms based on their metabolisms (Peters et al., 2004).

	Sources	Types of producers	
Energy sources	Sunlight	Phototroph	-
	Preformed molecules	Chemotroph	-
Carbon sources	Inorganic compounds	-	Autotroph
	Organic compound	-	Heterotroph

Table 2 Organism can be classified by carbon nutrients (left column) and energy metabolism (top row) (Peters et al., 2004).

	Phototroph	**Chemotroph**
Autotroph	Photoautotroph	Chemoautotroph
	green-plant, bacteria, algae	nitrogen-fixing bacteria, iron bacteria, methanogen
Heterotroph	Photoheterotroph	Chemoheterotroph
	purple non-sulfur bacteria, green non-sulfur bacteria, and heliobacteria	fungi, lithotrophic bacteria

Consequently, chemical compositions or biomarkers that are specific component can be used in many fields, such as pharmacology, plant taxonomy, and further ecological or environmental reconstruction.

2.3.1 Biomarker for chemotaxonomy

The chemotaxonomy is the classification of plants based on their specific chemical constituents, which are produced from their biosynthetic pathways (Singh, 2016). The chemical constituents are often specific and limited to taxonomically related organisms and consequently useful in classification (Singh, 2016). In recent studies, chemical compositions of epicuticular wax from leaves have been widely used for chemotaxonomy (Pu et al., 2017).

Epicuticular waxes of higher plants are a first protective barrier to reduce the loss of water, reflect or attenuated ultraviolet radiation and control leaf temperature, and defend against attack by harmful pathogens (Peters et al., 2004). The most common epicuticular wax components are hydrocarbons, e.g. wax esters, fatty acids and fatty alcohols, ketones, primary alcohols, diols, and aldehydes (Herbin and Robins, 1969; Kolattukudy, 1970; Singh, 2016; Zeisler-Diehl et al., 2018). Aliphatic hydrocarbon have been widely used for chemotaxonomy, particular *n*-alkanes (Bush

and McInerney, 2013; Nikolić et al., 2013; Phountong, 2016) because they are widespread in cuticular waxes of higher plants, and easier to analyze than others (Eglinton and Hamilton, 1967) and further they can be used to apply in many fields e.g. paleoenvironment (Andersson et al., 2011; Meyers, 1997, 2003; Ratnayake et al., 2017), and air pollutant studies (Percy et al., 2009).

The *n*-alkanes of epicuticular wax are a mixture of straight-chain hydrocarbons consists of major carbon atoms (C_{21} - C_{37}), especially C_{29} and C_{31} and minor carbon atoms (C_{20} - C_{34}) (Eglinton and Hamilton, 1967; Herbin and Robins, 1969; Kuhn et al., 2010; Rao et al., 2011). They are usually synthesized from elongated fatty acid precursors by decarbonylation pathway (Fig 7) (Guo et al., 2014; Kolattukudy, 1970; Kunst and Samuels, 2003). The *n*-alkanes have been proposed to serve as a chemotaxonomy index among different plant types, mostly at the genus and species levels (Nikolić et al., 2013).
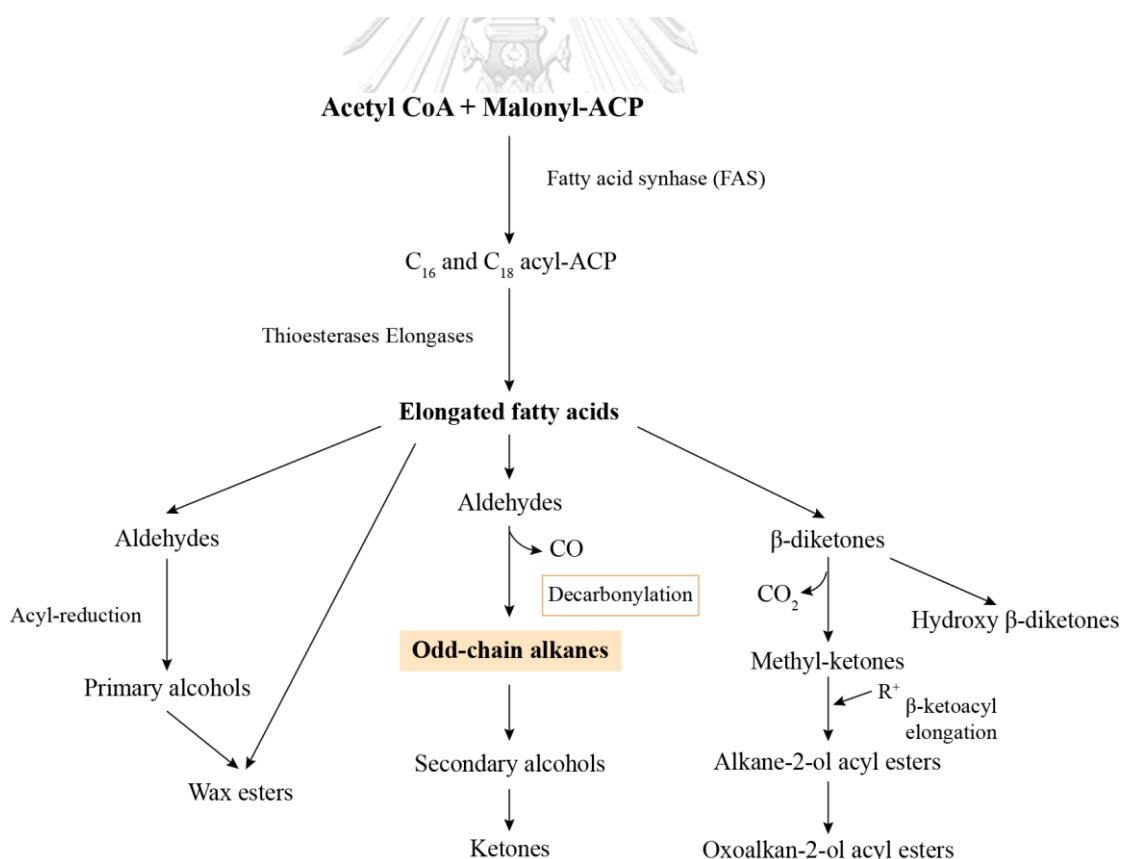
Figure 7 Biosynthetic pathway of epicuticular waxes. Odd-chain alkanes derived from decarbonylation by their biosynthetic pathway (Peters et al., 2004).

The epicuticular waxes of the higher plants generally consist of a long-chain n-alkanes range from C_{21} to C_{35} with the predominance of odd carbon number (Zeisler-Diehl et al., 2018). The shorter-chain n-alkanes lengths are mostly produced by other organisms. C_{17} or C_{19}, for example, are produced by aquatic algae and photosynthetic bacteria (Cranwell, 1973). C_{27}, C_{29}, and C_{31} n-alkanes are commonly originated by terrestrial plant epicuticular waxes (Cranwell, 1973; Meyers, 1997), and in particular, C_{31} can be used to separate grasses from other land plants.

However, recent studies suggest more complication in the chemotaxonomy based on n-alkanes. Angiosperms, for example, generally synthesize more n-alkane than gymnosperms (Bush and McInerney, 2013). C_{23} and C_{25} are representative of Sphagnum mosses (Bush and McInerney, 2013). However, C_{23} is the most abundant n-alkanes in the leaves of *Salix oritrepha,* which is a deciduous shrub. And C_{25} has been found in the highest concentration in *Ajuga ovalifolia*, which is herb and submerged and floating aquatic plants (Ficken et al., 2000; Pu et al., 2017). The recent studies also indicate that woody plants cannot be distinguished from graminoids by n-alkane abundances because both groups are dominated by all C_{27}, C_{29}, and C_{31} (Bush and McInerney, 2013). C_{27}, $C_{29,}$ and C_{31} are common in herb and shrub (Bush and McInerney, 2013; Vogts et al., 2009). However, this result was argued by Rao et al. (2010) that similar n-alkane distribution patterns do not contain a clear specific pattern among grasses, shrubs, and trees. The n-alkane ratio, e.g. average chain length (ACL), carbon preferent index (CPI), and proportion of aquatic plant (P_{aq}) were subsequently introduced to classify vegetation types in several studies (Bush and McInerney, 2013; Ficken et al., 2000; Pu et al., 2017).

ACL is an average value of n-alkane chain length that is a specific character in the higher plants (Bush and McInerney, 2013; Ficken et al., 2000; Pu et al., 2017). They show the significant difference among the same plant genera (Li et al., 2013). The CPI is a ratio of odd and even carbon chain length and generally high and wide range of CPI values are always found in the modern plant (Bush and McInerney, 2013; Li et al., 2013). Because aquatic plants commonly synthesize middle-chain n-alkane, the separation between macrophytes and land plants are simple. P_{aq} is a ratio of middle- and long-chain that is a potential proxy for aquatic plant separation (Ficken et al., 2000).

Many studies, however, proposed that the environmental conditions play a key role on the relative concentrations of hydrocarbon in the plants (Andersson et al., 2011; Baker, 1974; Guo et al., 2014; Herbin and Robins, 1969; Pitty, 1988). The environmental effect on epicuticular waxes has been investigated and reported that the production of waxes both their chemical contents and quantity are controlled by radiation, photoperiod, air temperature, moisture stress, relative humidity, or even leaf age (Norström et al., 2017; Pitty, 1988). For example, the production of epicuticular waxes in Brussel sprouts (*Brassica oleracea*) is mainly controlled by solar radiation (Baker, 1974). Ketone can be formed in Brussel sprouts when solar radiation is 80 W/m^2 (Baker, 1974). The same plant, however, produces alkane, if they receive the solar radiation of about 38 W/m^2. In contrast, the formation of epicuticular waxes in tobacco have been not related to radiation but depends on photoperiods (Wilkinson, 1972). C_{31} in epicuticular waxes of tobacco increase from 4.5% to 11.7% of the total hydrocarbons, when decreasing the photoperiods from 16 to 12 hours (Wilkinson, 1972). In addition, the barley leaves grown under light can produce C_{29}, C_{31}, and C_{33} summing 64% of the total hydrocarbons. But the hydrocarbon chain length becomes predominance of C_{21}, C_{23}, and C_{25}, which is about 46% of the total hydrocarbons, in the leave grown in dark (Wilkinson, 1974). Baker (1974) also suggested the influence of temperature on the epicuticular waxes that the plant growing at 15°C can produce a higher concentration of alkanes than that at 35°C. Hogg (1984) suggested that portion of hydrocarbons and fatty acids from a leaf of true mangrove plant are potentially reflected their environment. In contrast, the average chain length (ACL) values do not significant differences in both angiosperms and gymnosperms that are growing under the sun and shade, or in summer and fall (Bush and McInerney, 2013).

2.3.2 Biomarker for environmental reconstruction

The detritus of plants that grow in and around the lake are major sources of organic matter in the sediments (Meyers, 2003; Pu et al., 2017). Therefore, the aliphatic hydrocarbon in sediment is widely used for environmental reconstruction, especially *n*-alkanes compositions because of their high resistance to microbial degradation after sedimentation (Meyers and Ishiwatari, 1993).

The *n*-alkane can be used to assess the source of organic matter. For example, the short-chain *n*-alkanes, which commonly have a major component at C_{17}, C_{15} or C_{13}, derived from algae and bacteria (Gelpi et al., 1970; Han et al., 1968). However, the long-chain *n*-alkane, which generally compose of C_{27}, C_{29} or C_{31}, are mainly derived from higher plants (Cranwell, 1973; Eglinton and Hamilton, 1967; Han et al., 1968; Meyers, 1997, 2003; Meyers and Ishiwatari, 1993). Floating and submerged plants contain a broad range of *n*-alkanes from C_{13} to C_{31}. The floating plants are dominated by C_{25} or C_{27} (Nishimoto, 1974), while C_{19} or C_{21} or C_{25} are predominances in the submerged plants (Ficken et al., 2000).

In addition, *n*-alkane ratios, which are including average chain length (ACL), the carbon preference index (CPI), and the proportion of aquatic components (P_{aq}), have been further proposed in order to classify the provenance of organic matter. The ACL values are generally an indicator of organic matter input derived from diverse organisms, i.e. phytoplankton, aquatic plant, and terrestrial plant, in the sediments (Bush and McInerney, 2013; Ficken et al., 2000; Meyers, 2003; Zhang et al., 2017). Alternatively, ACL values had been used as paleohydrology proxy in Arctic bog (Andersson et al., 2011).

The *n*-alkanes found in sediment are not only abundance of the odd carbon number but also those of the even carbon number can be predominance (Kuhn et al., 2010; Nishimura and Baker, 1986). The CPI values are the relationship between odd and even carbon number that is usually used to assess even over odd carbon number predominance (EOP) and odd over even carbon number predominance (OEP) (Marzi et al., 1993). Since EOP is depended on the degree of maturity of source rocks and degradation level of sediment, this value is commonly used in petroleum geochemistry in order to estimate (Eglinton and Hamilton, 1967). However, the *n*-alkane distributions with a remarkable EOP ($C_{16} - C_{24}$) were found in surface marine sediment that is possibly directly obtained from marine bacteria (Nishimura et al., 1985). Wang et al (2010) reported that the *n*-alkane from Linxia Basin showed a bimodal distribution which the *n*-alkanes is characterized by a range from $C_{16} - C_{20}$ in a short-chain length, while a long-chain length is dominated by range from $C_{27} - C_{31}$. Autochthonous bacteria are also a possible provenance of EOP because of a high production rate under arid deposition environment.

P$_{aq}$ was frequently applied to the study of sediment. The relative proportion of middle-chain length (C$_{23}$, C$_{25}$) to long-chain length (C$_{29}$, C$_{31}$) can be used to separate submerge/floating plant from emergent and terrestrial plant (Ficken et al., 2000). High P$_{aq}$ indicates freshwater swamp or lake environment. Anderson et al (2011) applied P$_{aq}$ values that have been used to indicator for the water level in a peat bog.

As the mention to the *n*-alkanes in lake sediment derived from multiple inputs and consequently are likely to reflect different aspects of past environmental conditions. Hence, consideration of the possible origins has to rely on various potential biomarkers to expand and refine paleoenvironmental reconstructions.

2.4 Gas chromatography-mass spectrum technique

Gas chromatography-mass spectrum technique (GCMS) can be utilized to detect and identify compounds by relative gas chromatographic retention times, and the mass spectral fragmentation patterns characteristic of their structures.

A known amount of the hydrocarbon fraction was injected into the gas chromatograph. The injection was selected to split, split-less, solvent-split, or direct injection mode. The selection of the injection mode is depended on the portion and concentration of the sample. Each injected sample is vaporized and mixed with an inert carrier gas, such as helium or hydrogen. The vaporized mixture of sample and carrier gas then moves through a capillary column. The temperature of the column is raised gradually using a temperature-programmed oven. The gas (mobile phase) and sample mixture move through a long, thin capillary column (typically 0.20–0.25mm ID, 30–60m long) which inner surface is coated with a film (∼0.25 μm thick) of non-volatile liquid (stationary phase). Different components were separated during their moving down in the column. They are repeatedly retained by the stationary phase and released into the mobile phase depend on their volatility and affinity for each phase.

The separated compounds were eluted and directly pass to the ionizing chamber in the mass spectrometer. At this point, the electron impact mode was selected for the ionization in GCMS. Most mass spectrometry systems ionize the eluting compounds in the electron-impact mode using 70 eV since molecules are ionized most efficiently in the range 50–90 eV based on the empirical experiment.

Then fragment ions generated in the ion source chamber are accelerated toward the detector through the mass analyzer by a high differential voltage. Ions formed in the source of the mass spectrometer are analyzed according to their mass/charge ratio using a magnetic or quadrupole mass spectrometer. An electron multiplier detects positive ions. Mass analyzer can be analyzed ion beam by two principle methods including magnets and quadrupole rods. But here only mention to quadrupole. Single or triple quadrupole and three-dimensional ion trap instruments all make use of quadrupole radio frequency (RF)/electrical fields to select ions of a given mass/charge ratio. Quadrupole mass filters use no focusing at all but achieve mass selection because, for a given set of conditions, only ions with a narrow range of mass/charge ratios are able to remain within the instrument during mass analysis. The only those ions of interest are trapped and detected.

Gas Chromatograph
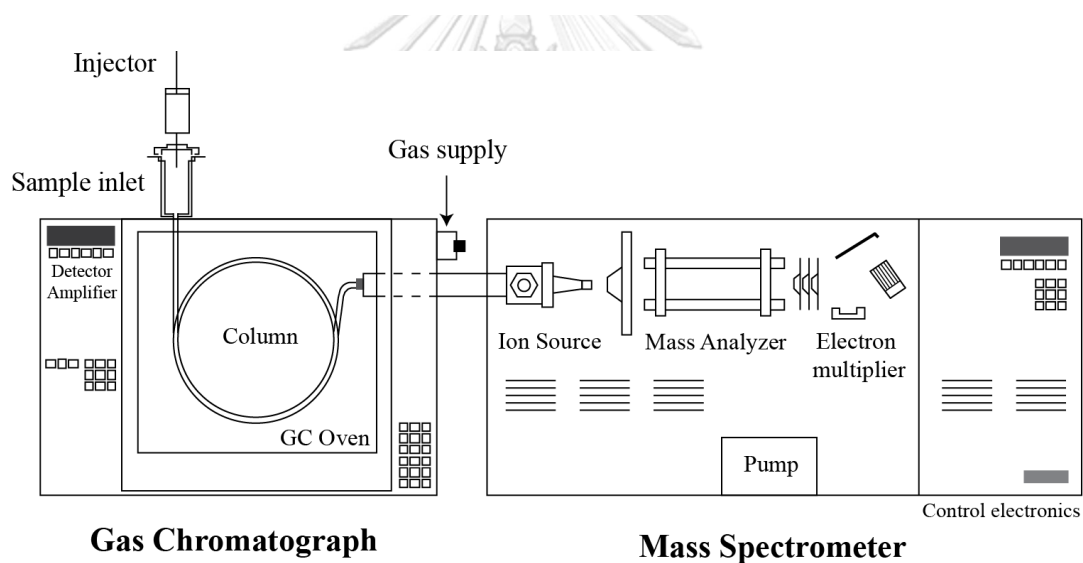
Mass Spectrometer

Figure 8 A typical gas chromatograph/mass spectrometer performs six functions (from left to right): (1) compound separation by gas chromatography; (2) transfer of separated compounds to the ionizing chamber of the mass spectrometer; (3) ionization and acceleration of the compounds down the flight tube; (4) mass analysis of the ions; (5) detection of the focused ions by the electron multiplier; and (6) acquisition, processing, and display of the data by computer. Modified from (Peters et al., 2004).

CHAPTER III
METHODOLOGY

The leaves of modern plants and lake sediments were collected in order to analyze *n*-alkanes and subsequently reconstruct the paleoenvironment in the study area. The method of study consists of sample collection and preparation, lipid extraction and purification, and eventually biomarker analysis by using gas chromatography-mass spectrometry (GC/MS) technique (Fig 8).
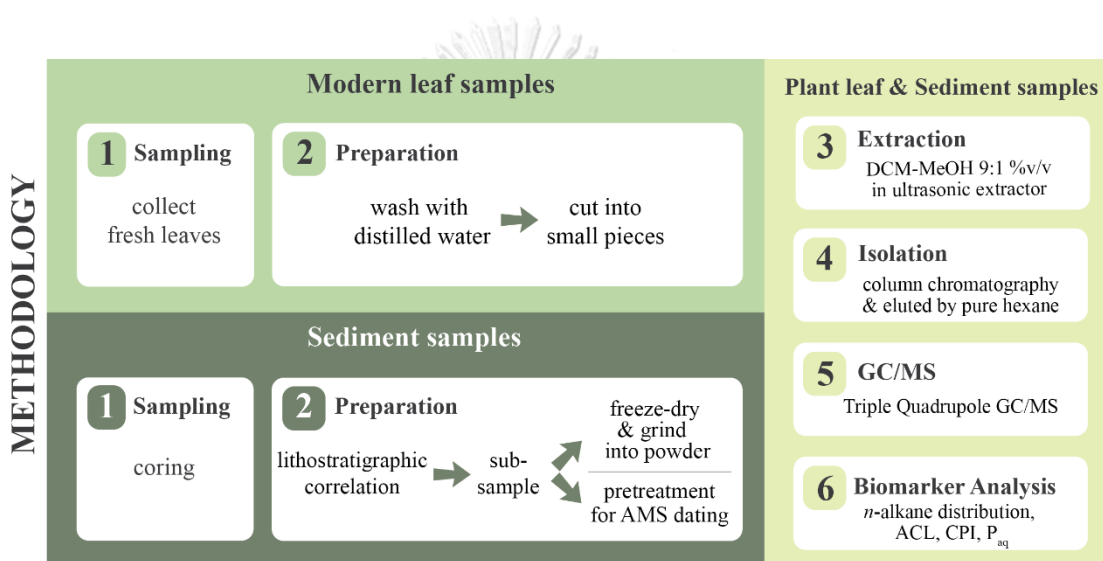
Figure 9 Diagram of the methodological procedure.

3.1 Sample collection and preparation

The leaf and sediment samples were taken in this study (Fig. 10).

3.1.1 Modern leaf samples

The leaves of modern plants from different environments were collected in regarding to pollen analysis in core TLN-CP5 between January and March in 2018 (Nudnara, 2016). The leaves of true mangrove and back mangrove plants were taken from Kung Krabaen Bay Royal Development Study Center (KKB), Chantaburi Province, Khun Samut Chin Temple (KSC) and Pom Pra Chulachomklao (PPC),

Samut Prakan Province, and Thale Noi (TLN), Phattalung Province. The leaves of mangrove associate plants were obtained from KKB and TLN (Fig 10).
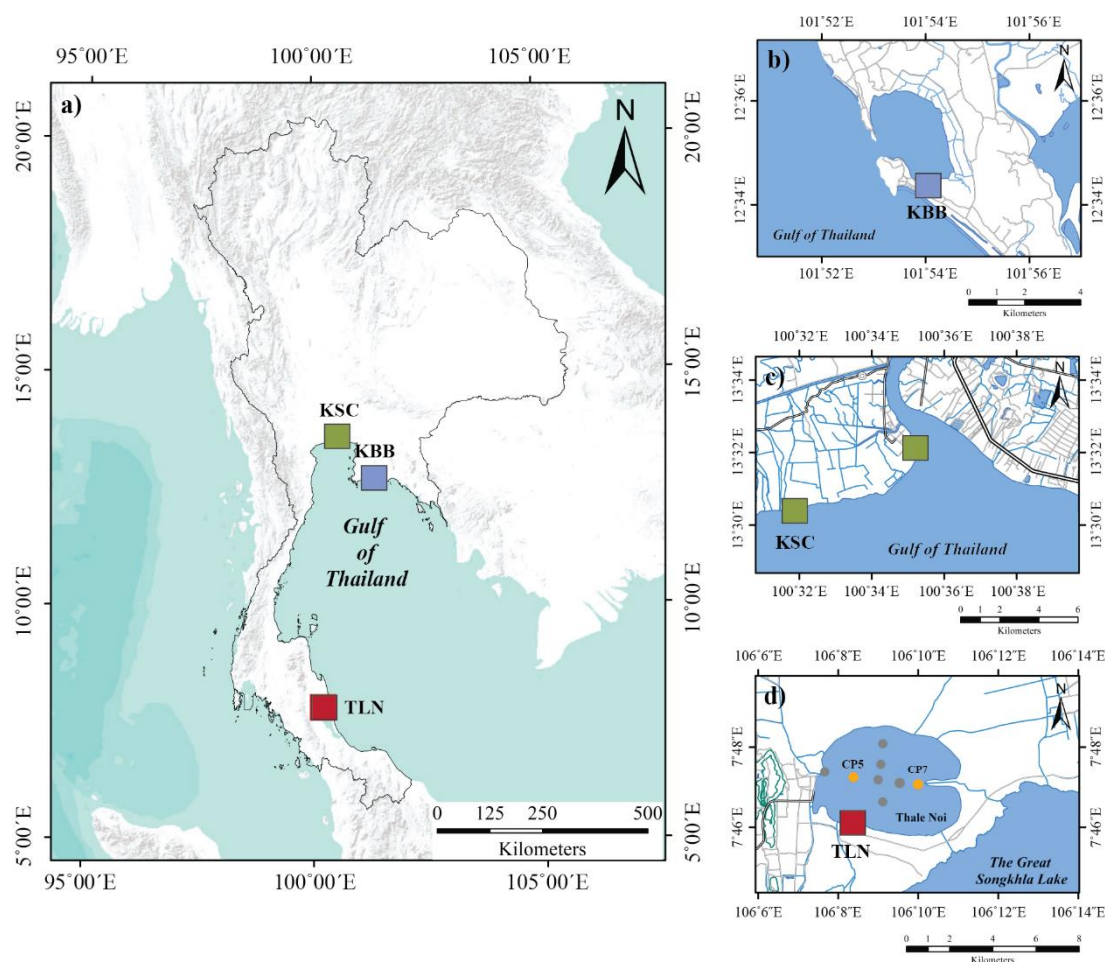
Figure 10 Location map of leaf sampling sites a) including Kung Krabaen Bay Royal Development Study Center (KKB), Chantaburi Province b) , Khun Samut Chin Temple (KSC) c) , Samut Prakan Province, and Thale Noi (TLN), Phatthalung Province d).

The seventeen leaf samples here can be assigned to 11 families (Table 3). The leaves were collected from at least five different trees for each species in the same location (Bush and McInerney, 2013). Moreover, the samples of *Barringtonia asiatica*, *Casuarina equisetifolia*, *Rhizophora mucronate* and *Sonneratia caseolaris* were taken from different locations in order to validate the *n*-alkane analysis. The

samples were placed in zipped plastic bags and stored in the refrigerator at the Department of Geology, Chulalongkorn University before further analysis.

The samples were prepared by carefully clean several times with deionized water and then cut into small pieces by scissors.

Table 3 The leaf samples were collected from Khun Samut Chin Temple (KSC), Kung Krabaen Bay Royal Development Study Center (KKB), and Thale Noi (TLN) (Fig. 10).

Location	Species	Plant groups
KSC	*Acrostichum aureum*	Back mangrove
	Avicennia marina	True mangrove
	Rhizophora apiculate	True mangrove
	Rhizophora mucronate	True mangrove
	Sesuvium portulacastrum	True mangrove
	Sonneratia caseolaris	True mangrove
KKB	*Barringtonia asiatica*	True mangrove
	Bruguira gymnorrhiza	True mangrove
	Casuarina equisetifolia	Mangrove associate
	Oncusperma tigllarium	Back mangrove
	Rhizophora mucronate	True mangrove
	Xylocarpus granatum	Back mangrove
TLN	*Barringtonia asiatica*	True mangrove
	Casuarina equisetifolia	Mangrove associate
	Poaceae (*Bambusoideae*)	Mangrove associate
	Sonneratia caseolaris	True mangrove

3.1.2 Sediment samples

Sediment cores were taken from eight locations in Thale Noi, Phatthalung Province during January 2016 by using a modified Russian corer (7.5 cm diameter, 1 m length). To achieve a continuous sequence, sediment cores were taken 50 cm overlapping at each coring site. The sediment cores were wrapped in plastic and

placed in PVC tubes for transport to the Department of Geology, Chulalongkorn University. The sediment samples were then described in detail, correlation, constructed the composited depth, sub-sample, and stored in a refrigerator until analyses (Fig. 4).

The lithostratigraphy of the sediment cores was described and correlated by Yoojam (2015). According to the lithostratigraphy, Thale Noi possibly consists of two sub-basins in the eastern and the western parts of the lake (Yoojam, 2015). This result agrees well with Chaimanee (1986) that point to the deposition under freshwater swamp and true mangrove environments in the west and east Thale Noi, respectively. Core TLN-CP5 and CP7 are the longest sediment sequences from the western and eastern sub-basins (Fig. 4). They possibly record the long-term variability of environmental changes in this lake.

Sediment cores were subsampled every 1 cm interval and these samples were selected every 10 cm for the biomarker analysis. The selected samples were freeze-dried at Department of Marine Science, Chulalongkorn University, and then grind for homogenization and increase their surface area for the lipid extraction.
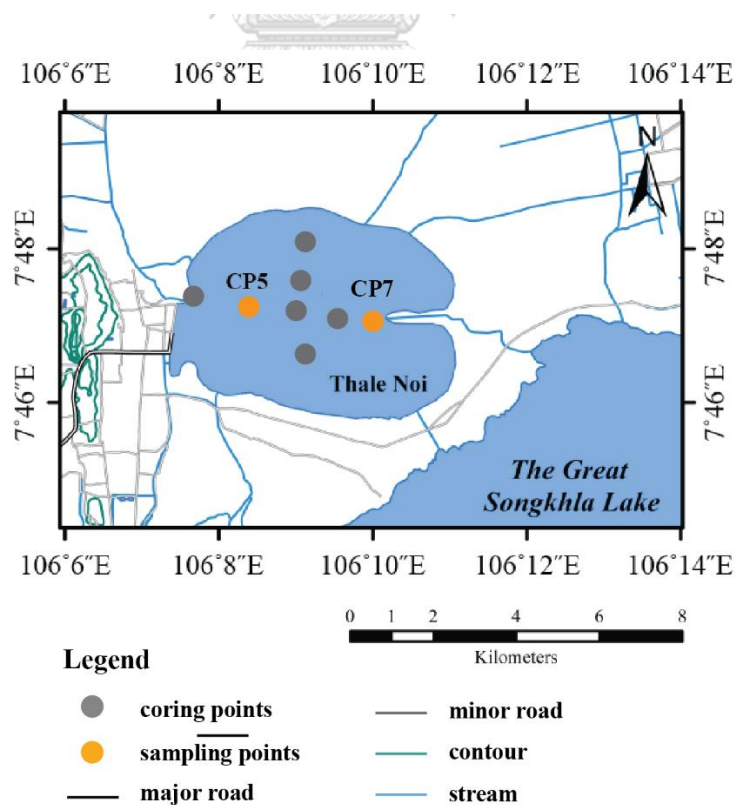
Figure 11 Location of sediment cores sampling in Thale Noi, Phatthalung Province.

3.2 Lipid extraction and purification

The prepared samples were put in 20 ml of a mixture of dichloromethane and methanol (DCM-MeOH 9:1%v/v) and left them in the ultrasonic extractor for 10 minutes for the lipid extraction (Pu et al., 2017). This process was repeated for 3 times. The mixture of solvent and total lipid was then put together and then evaporated by rotary evaporator. The evaporation had been continued until approximately 2 ml of mixture remaining in the round bottom flask. These prepared samples were transferred to a glass vial and left them under room temperature till all solvent evaporates. The total lipid was left in a vial glass in this step.

The non-polar fraction was further separated from the total lipid by silica column chromatography. Silica gels were weighed 10 times higher than that of the total lipid weight (10X of total lipid weight) and loaded them in a glass column. The total lipid was transferred to the silica gel column by an autopipette. The non-polar or *n*-alkane fraction was eluted by three to four column volume of hexane. All fractions were again poured into the round bottom flask and evaporated by rotary evaporator before transferring to the glass vial. Finally, hexane/ethyl acetate (1:1 % v/v) was added to the *n*-alkane fraction and sent to Scientific and Technological Research Equipment Center (STREC), Chulalongkorn University for further analysis.

3.3 Gas chromatography-mass spectrum analysis

The *n*-alkane fractions were analyzed by gas chromatography-mass spectrometer (GC/MS) on Triple Quadrupole GC/MS (GC-QQQ) Agilent Technologies, equipped with Agilent 7633 ALS Autosampler at Scientific and Technological Research Equipment Centre (STREC), Chulalongkorn University.

The 1.2 µl of samples were injected in the split mode and passed through HP-5ms column (30 m × 0.25 mm i.d., film thickness 0.25 µm) into the GC oven by helium, which is a carrier gas (Pu et al., 2017). The oven temperature was increased from 100 to 320°C with 11°C/min and hold at 100°C and 320°C for 4 and 12 min, respectively. The gas of *n*-alkane fraction was then transferred to an ion source which temperature was set at 280°C to emit electrons, and the 70eV electron impact mass

spectra were acquired over the mass per charge (m/z) scan ranged from 35 to 650 (Fig. 8).

The individual n-alkanes were identified by an external standard of the mass spectrum of C12-C40 alkane D.

3.4 Biomarker analysis

The n-alkanes ranging from C_{15} to C_{20}, and from C_{21} to C_{35} were defined to the short- and long-chain n-alkanes (Pu et al., 2017). The relative abundances of n-alkanes were calculated from the peak area of chromatogram. The distributions of n-alkanes were here classified into three patterns; the predominance in long- and short-chain n-alkanes, and bimodal patterns. The predominance in long-chain (short-chain) n-alkanes is here referred to the summary of the abundant intensity of the long-chain n-alkanes is higher (less) than 60% of those in the short-chain n-alkanes. The bimodal distribution is classified when the concentration of the dominant n-alkanes ranging from C_{15} to C_{20} is almost the same as those ranging from C_{21} to C_{35}. Since the short-chain n-alkanes are possibly produced by microbial activity, the long-chain n-alkanes were solely considered in the sediments (Hao et al., 2015; Pu et al., 2017).

Moreover, the ratio between relative abundances of n-alkanes, e.g. average chain length (ACL) and carbon preference index (CPI) was introduce in order to classify plants and assess the source of organic matter in the sediments.
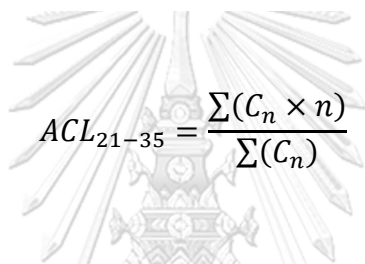
The ACL of hydrocarbon in leaf wax is a specific character in the individual plant species (Bush and McInerney, 2013; Ficken et al., 2000; Pu et al., 2017). The specific value of ACL makes it frequently used for a group of plant classification (Bush and McInerney, 2013). Moreover, the ACL is generally an indicator of organic matter input derived from diverse organisms such as phytoplankton, aquatic plant and terrestrial plant into the sediments (Bush and McInerney, 2013; Ficken et al., 2000; Meyers, 2003; Zhang et al., 2017).

The ACL was here calculated into two ranges; total average chain length (ACL_T) and average chain length of C_{21} to C_{35} (ACL_{21-35}) (Bush and McInerney, 2013). The plant group classification was referred from the ACL_T, which can be calculated by equation (1);

$$ACL_T = \frac{\sum(C_n \times n)}{\sum(C_n)} \tag{1}$$

Where C_n are the relative abundance of individual n-alkane from C_{15} to C_{35} and n are the number of carbon atoms (15-35), respectively.

Since the long-chain n-alkane is more resistance in microbial activity, the ACL_{21-35} was separated from ACL_T in order to assess the source of organic matter in the sediments (Bush and McInerney, 2013; Pu et al., 2017). ACL_{21-35} is weight mean of the carbon chain lengths from C_{21} to C_{35} that is generally used to assess the dominant proportions of n-alkanes chain length in the leaf waxes and sediments (Bush and McInerney, 2013; Pu et al., 2017). ACL_{21-35} can be calculated by equation (2);

$$ACL_{21-35} = \frac{\sum(C_n \times n)}{\sum(C_n)} \tag{2}$$

Where C_n are the relative abundance of individual n-alkane from C_{21} to C_{35} and n are the carbon atoms (21-35), respectively.

The ACL_{21-35} values in sediments and in leaf plants were compared in order to investigate the source of organic matter reflecting vegetation dynamics around the lake.

Carbon preference index (CPI) is the relationship between odd and even carbon number that is usually used to measure the relative abundance of odd to even carbon chain lengths (Marzi et al., 1993). This value is frequently used in petroleum geochemistry in order to estimate the degree of maturity of source rocks (Eglinton and Hamilton, 1967). The CPI in modern plants is mostly greater than 1 or odd over even predominance. However, even over odd predominance n-alkane can be produced under high degradation (Kuhn et al., 2010). Alternately, environmental conditions influence on the shift of n-alkane distribution (Herbin and Robins, 1969).

Here, we calculated two range of CPI that are CPI_T and CPI_{21-35}. The CPI_T is the ratio of odd over even carbon number chain length of C_{15} to C_{35}, which can be calculated by equation (3);

$$CPI_T = \frac{[\sum_{odd}(C_{15-33}) + \sum_{odd}(C_{17-35})]}{(2\sum_{even} C_{16-34})} \tag{3}$$

Where C_{15-33}, C_{17-35} and C_{16-34} are the relative abundance of n-alkane between C_{15} and C_{33}, between C_{17} and C_{35}, and between C_{16} and C_{34}, respectively.

CPI$_{21-35}$ is the ratio of odd over even carbon chain lengths of C_{21} to C_{35} (Marzi et al., 1993) that can be calculated by equation (4);

$$CPI_{21-35} = \frac{[\sum_{odd}(C_{21-33}) + \sum_{odd}(C_{23-35})]}{(2\sum_{even} C_{22-34})} \tag{4}$$

Where C_{21-33}, C_{23-35} and C_{22-34} are the relative abundance of n-alkane between C_{21} and C_{33}, between C_{23} and C_{35}, and between C_{22} and C_{34}, respectively.

The CPI$_{21-35}$ value in modern plants and sediments are further used to examine the relationship between organic matters in the lake and its surrounding plant. While Furthermore, low CPI$_T$ also indicate the degree of organic origin decomposition and degradation.

Submerged/floating plants often create a middle-chain length of n-alkane in particularly between C_{23} and C_{25} (Ficken et al., 2000). This work P$_{aq}$ was applied to the study of sediment samples followed Ficken (2000). The relative proportion of middle-chain length (C_{23}, C_{25}) to long-chain length (C_{29}, C_{31}) or proportion of aquatic components (P$_{aq}$) can be used to separate submerge/floating plant from emergent and terrestrial plant (Ficken et al., 2000). P$_{aq}$ can be calculated by equation (5);

$$P_{aq} = \frac{C_{23} + C_{25}}{C_{23} + C_{25} + C_{29} + C_{31}} \tag{5}$$

P$_{aq}$ are generally less than 0.1 in the terrestrial plants, while P$_{aq}$ of 0.1 - 0.4 and 0.4 – 1 are reflecting emergent and submerged/floating macrophytes, respectively

(Ficken et al., 2000). Alternatively, the P_{aq} of 0.1 - 0.4 in sediment can be assessed to a mixture of inputs from terrestrial, emergent and submerged/floating aquatic macrophytes (Ficken et al., 2000). Furthermore, P_{aq} can also be used to estimate the *n*-alkane distribution, for example, P_{aq} less than 0.1 is related to long-chain predominance, 0.1 to 0.4 is related to middle-chain and long-chain predominance or bimodal distribution, and 0.4 to 1 is related to middle-chain predominance.

3.5 Radiocarbon dating and age-depth model

The sufficient age control is necessitated to insight into the regional environmental changes. Among various dating techniques, the radiocarbon is possibly the most widely used to construct a chronology of the lake sediments. However, the pretreatment of dating sample is necessary in order to reduce any sources of error (Björk and Wohlfarth, 2001).

The selected sediment samples were deflocculation by 5% sodium hexametaphosphate or Calgon. The defflocculated samples were then sieved under running water with a mesh size of 500 μm. The sieved plant remains were identified under a stereomicroscope. Plant roots were excluded but leaves, teak, charcoal, and seed were here selected. The selected samples were cleaned several times by distilled water and then dried in an oven at 60°C for overnight. After that, the dried samples were treated by acid-base-acid technique (ABA) (Brock et al., 2010). A 1 M hydrochloric acid (HCl) was added and put the samples in an oven at 80°C for 20 minutes in order to eliminate the carbonate content. After that, the samples were rinsed by distilling water 3 times. To remove organic acids such as humic and fulvic acid, the sample was then treated by a 0.2 M sodium hydroxide (NaOH) and put them in an oven at 80°C for 20 minutes. The sample was subsequently cleaned 3 times by the distilled water. The 1 M HCl was again added to the treated samples and put them in an oven at 80°C for 1 hour in order to eliminate the dissolved atmospheric CO_2 and then washed them by the distilled water 3 times. The samples were dried in an oven at 60°C for an overnight before putting them in the glass vials and eventually sending to Direct AMS for the radiocarbon dating. The radiocarbon dating results were calibrated by using InCal13 (Reimer et al., 2013), and the age-depth models were

subsequently constructed by using computer software called BACON (the Bayesian accumulation histories of deposits) (Blaauw and Christen, 2011).

An age-depth model of sediment TLN-CP5 core was constructed by Phountong (2016) based on nine C-14 dating results (Table 7). The age of sediment sequence TLN-CP5 extends from 8300 to 7200 cal yr. BP. The detailed chronology of core TLN-CP5 will be present in the discussion. Furthermore, four samples from TLN-CP7 core were sent to analyze the radiocarbon dating. However, there are only two samples were used for the construction of chronology for core TLN-CP7. These new results were also presented in detail in Chapter 4.

CHAPTER IV
RESULTS

The results were here divided into 3 parts including *n*-alkane analyses in the modern leaf waxes, and in the sediments from core TLN-CP5 and TLN-CP7 (Fig. 11).

4.1 The *n*-alkane analysis in the modern leaf waxes

The modern leaf samples were taken in regarding to pollen analysis by Nudnara (2017) that compose of true mangrove, back mangrove and mangrove associate from Kung Krabaen Bay Royal Development Study Center (KKB), Chantaburi Province, Khun Samut Chin Temple (KSC) and Pom Pra Chulachomklao (PPC), Samut Prakan Province, and Thale Noi (TLN), Phattalung Province (Fig. 10). The *n*-alkanes analysis in the modern leaf wax was further compared with these in the sediment sequence from Thale Noi, Phatthalung Province in order to insight into the past environmental changes.

True mangrove plants

True mangrove plants are vegetation growing in tidal environments or the brackish environment (Tomlinson, 1986; Duke, 1992; Giesen et al., 2007). The modern leaf samples of mangrove plants were here collected from KKB, KSC and PPC, and TLN that consisted of *Avicennia marina*, *Barringtonia asiatica*, *Bruguiera gymnorrhiza, Rhizophora apiculate, Rhizophora mucronate, Sesuvium portulacastrum, and Sonneratia caseolaris*.

Avicennia marina, *Rhizophora apiculate* and *Sonneratia caseolaris* are the predominances in the long-chain *n*-alkanes (Fig. 12). C_{33} and C_{31} are the highest concentration of about 45% in *Avicennia marina*, and 40% in *Rhizophora apiculate*. However, C_{31} is the most abundantof 40% in *Sonneratia caseolaris* from KSC but C_{33} is about 30% and more dominant in this kind of plant from TLN. The short-chain *n*-alkanes are generally less than 5% in *Avicennia marina*, *Rhizophora apiculate* and *Sonneratia caseolaris*.
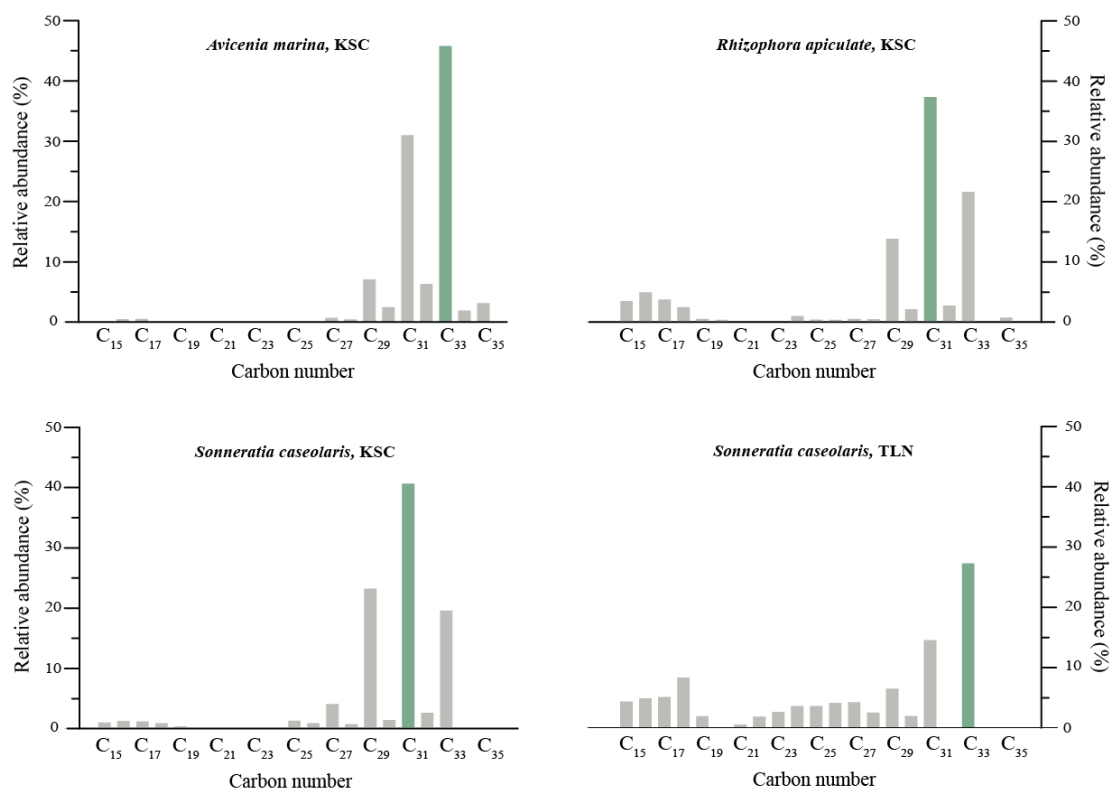
Figure 12 The predominance of long-chain *n*-alkane in true mangrove plants consisting of *Avicennia marina*, *Rhizophora apiculate* and *Sonneratia caseolaris*.

The predominance in the short-chain *n*-alkanes can be found in the sample of *Bruguiera gymnorrhiza* and *Sesuvium portulacastrum* (Fig. 13). The long-chain *n*-alkanes abundances are lower than 5% in *Sesuvium portulacastrum* and *Bruguiera gymnorrhiza*. C_{16} are the most abundant *n*-alkanes in *Sesuvium portulacastrum* and *Bruguiera gymnorrhiza* that their concentrations are approximately 20%.
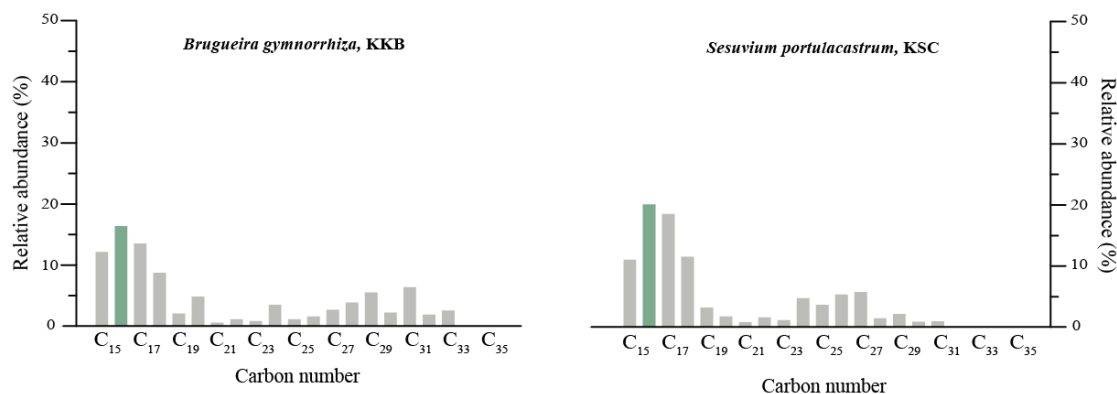
Figure 13 The predominance of short-chain *n*-alkane in true mangrove plants consisting of *Bruguiera gymnorrhiza* and *Sesuvium portulacastrum*.

Interestingly, the, unlike *n*-alkanes distribution, can be found in *Rhizophora mucronate* and *Barringtonia asiatica* from different sits. C_{29} is the most abundant of more than 50% in *Rhizophora mucronate* from KSC (Fig. 14). The short-chain *n*-alkanes have been found in a low concentration of less than 5% in this sample. However, C_{29} and other long-chain *n*-alkanes become less than 10% in *Rhizophora mucronate* from KKB. The most predominate *n*-alkane in the *Rhizophora mucronate* from KKB is C_{17}, which is approximately 19%. The *n*-alkanes distribution of *Rhizophora mucronate* from KSC and KKB can be classified to the predominance of long- and short-chain *n*-alkanes, respectively (Fig. 14).
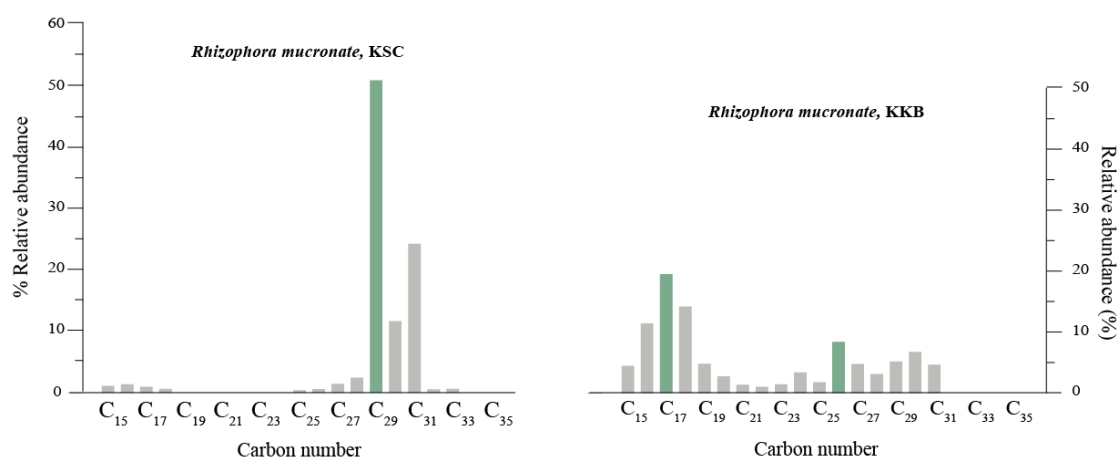
Figure 14 The predominance of long-chain *n*-alkanes in *Rhizophora mucronate* from KSC (left) and the bimodal distribution of *n*-alkanes *Rhizophora mucronate* from KKB (right).

The different pattern of *n*-alkanes distribution can be also found in *Barringtonia asiatica*. The sample from TLN is the predominance in the short-chain *n*-alkanes (Fig. 15), while the bimodal distribution is in the samples from KKB (Fig. 15). C_{17} and C_{18} are the most abundant short-chain *n*-alkanes of about 18% in the *Barringtonia asiatica* from TLN. The *n*-alkanes ranging form C_{21} to C_{31} have been found only less than 10% in this sample. C_{16} and C_{24} are about 10% and 15% and they the highest concentration of the short- and long-chain *n*-alkanes in *Barringtonia asiatica* from KKB.
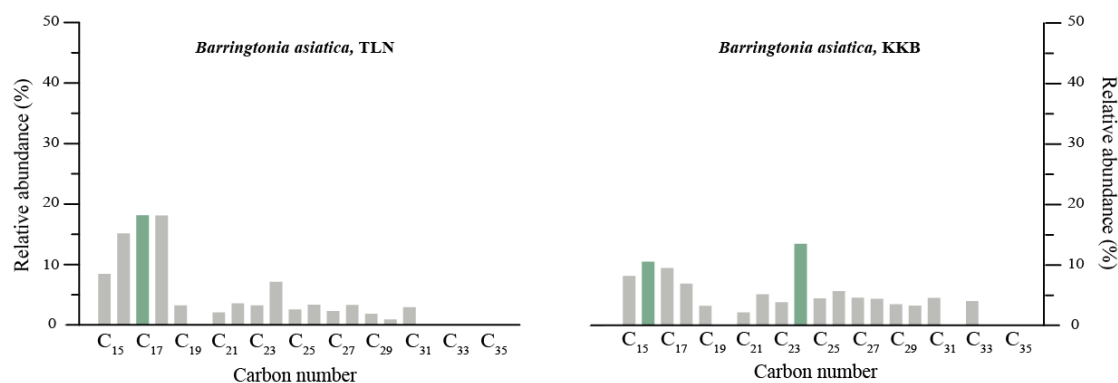
Figure 15 The *n*-alkanes distribution in *Barringtonia asiatica* from TLN is the predominance in the short-chain *n*-alkanes (left), while the bimodal distribution is in the samples from KKB (right).

The ACL_T and ACL_{21-35} values are varied from 19.55 to 31.90, and from 26 to 32 (Table 4). According to the ACL_T, the mangrove plants are generally dominated by the long-chain *n*-alkanes. The exceptions are *Sesuvium portulacastrum* from KSC and *Barringtonia asiatica* from TLN that is prevailed by the short-chain *n*-alkane (Table 4).

The CPI_T and CPI_{21-35} values are ranged from 0.79 to 11.30, and from 0.76 to 15.29 (Table 4). According to the CPI_T, *Avicennia marina*, *Rhizophora apiculate,* and *Sonneratia caseolaris* can be assigned to the odd over even predominance (Table 4). The CPI_T values are less than 1 in the modern leaf samples of *Barringtonia asiatica*, *Bruguiera gymnorrhiza,* and *Sesuvium portulacastrum*. CPI_T of *Rhizophora mucronate* however is higher than 1 in the sample from KSC, while the value became less than l in the sample from KKB (Table 4). The classification of odd over even or

even over odd predominance based on CPI_{21-35} is generally similar to those in regarding to CPI_T. However, *Bruguiera gymnorrhiza* and *Sesuvium portulacastrum* can be assigned to odd over even predominance based on CPI_{21-35} (Table 4).

Back mangrove

The back mangrove plants are the plant community that is located landward next to true mangrove. These plants can be distinguished from true mangrove vegetation by their appearance in peripheral mangrove habitats (Berlyn, 1986). The modern leaf samples of back mangrove plants consisting of *Acrostichum aureum*, *Oncusperma tigllarium,* and *Xylocarpus granatum* were collected from KKB and KSC.

The long-chain *n*-alkanes are predominated in the *Acrostichum aureum*, but *Oncusperma tigllarium* and *Xylocarpus granatum* are dominated by the short-chain *n*-alkanes (Fig. 16, 17). C_{33} is the most abundant of more than 40% in *Acrostichum aureum* while the short-chain *n*-alkane are generally less than 10% (Fig. 16). C_{17} is about 20%, which is the most abundant in *Oncusperma tigllarium*. However, the most dominant *n*-alkanes in *Xylocarpus granatum* is C_{17}, which is approximately 20%. In *Oncusperma tigllarium* and *Xylocarpus granatum*, the short-chain *n*-alkanes have been found in a low concentration of less than 5% (Fig. 17).
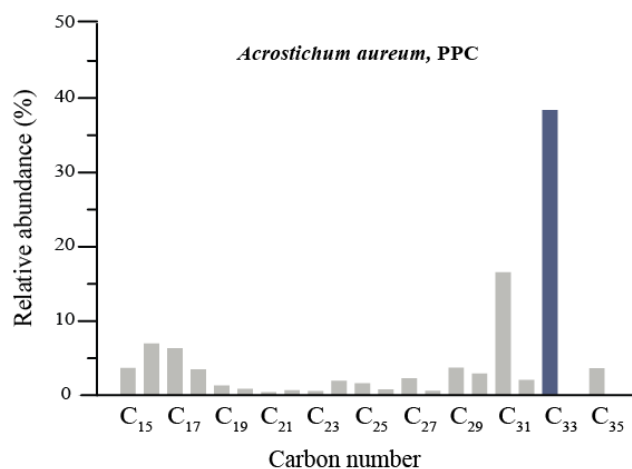
Figure 16 The predominance of long-chain *n*-alkanes in *Acrostichum aureum*.
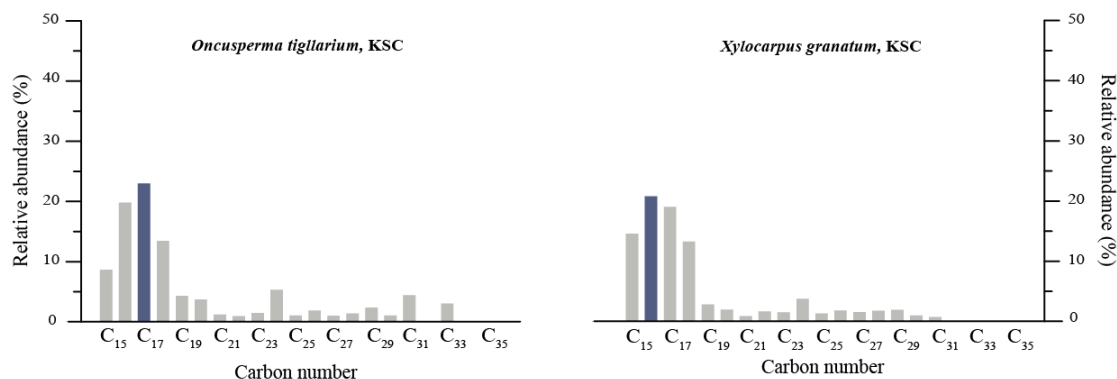
Figure 17 The predominance of short-chain *n*-alkanes in *Oncusperma tigllarium* (left) and *Xylocarpus granatum* (right).

ACL$_T$ are about 29.63, 20.21 and 18.10 in *Acrostichum aureum*, *Oncusperma tigllarium,* and *Xylocarpus granatum*, respectively (Table 4). The ACL$_T$ in *Oncusperma tigllarium,* and *Xylocarpus granatum* show the short-chain predominance that agrees well with the distribution of *n*-alkanes (Fig. 17). The ACL$_{21-35}$ in *Acrostichum aureum*, *Oncusperma tigllarium,* and *Xylocarpus granatum* are 31.63, 28.74 and 26.10, respectively (Table 4).

According to the CPI$_T$ values, *Acrostichum aureum* can be classified to odd over even predominance, but *Oncusperma tigllarium* and *Xylocarpus granatum* are even over odd predominance (Table 4). However, *Oncusperma tigllarium* can be recognized as the odd over even predominance based on CPI$_{21-35}$ (Table 4).

Mangrove associate

The mangrove associate is vegetation that is mainly distributed in a terrestrial or aquatic habitat but also occurs in the mangrove ecosystem. The mangrove associate here consists of *Casuarina equisetifolia* and Poaceae (*Bambusoideae*).

The distribution of *n*-alkanes in Poaceae (*Bambusoideae*) demonstrates the predominance in long-chain *n*-alkanes, which C$_{33}$ concentration is about 25% (Fig. 18). The highest concentration of the short-chain *n*-alkanes in this plant is C$_{17}$ that is about 10%. The predominance in short-chain *n*-alkane and the bimodal distribution can be found in *Casuarina equisetifolia* from KKB and TLN, respectively. C$_{16}$ and C$_{24}$ are the most abundant short- and long-chain *n*-alkanes in *Casuarina equisetifolia*

from KKB that is about 20 and 5%, respectively. However, *Casuarina equisetifolia* from TLN is mainly consisted of C_{18} and C_{24} which their concentration are approximately 15 and 10% (Fig. 19).
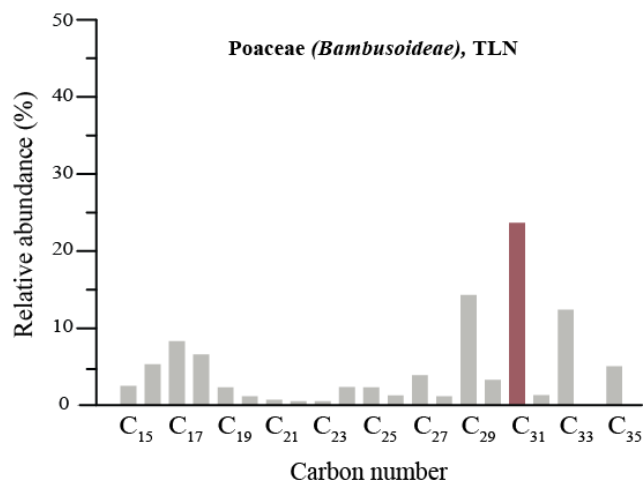
Figure 18 The predominance of long-chain *n*-alkanes in Poaceae (*Bambusoideae*).
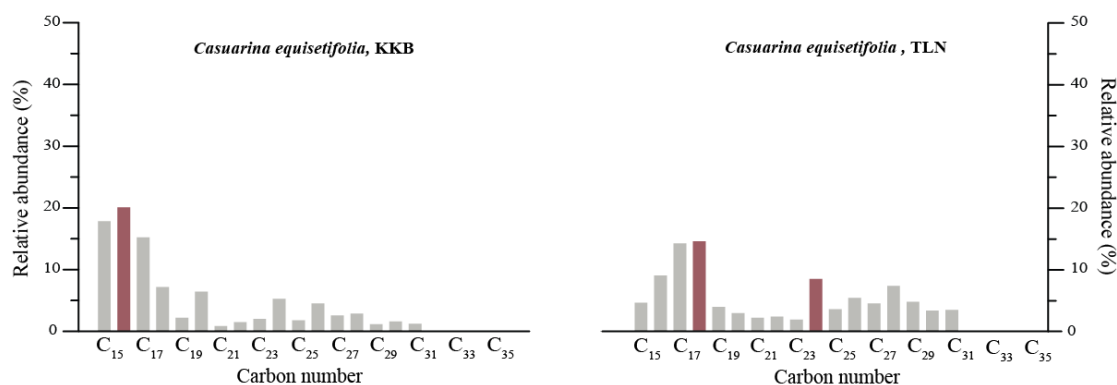
Figure 19 The predominance of short-chain *n*-alkanes in *Casuarina equisetifolia* from KKB (left) and a bimodal distribution of *n*-alkanes in *Casuarina equisetifolia* from TLN (right).

The distribution of *n*-alkane in the same kind of plant species (*Casuarina equisetifolia*) from different sits (from KKB and TLN, respectively).

The ACL_T in *Casuarina equisetifolia* from KKB and TLN are 18.22 and 21.60 that suggest the short-chain *n*-alkane predominance (Table 4). However, ACL_T is about 28.24 in Poaceae (*Bambusoideae*) that is prevailed by the long-chain *n*-alkane (Table 4).

CPI$_T$ and CPI$_{21-35}$ of *Casuarina equisetifolia* are between 0.6 and 0.7 that can be classified to the even over odd predominance (Table 4.1). However, CPI$_T$ and CPI$_{21-35}$ of Poaceae (*Bambusoideae*) are 3.14 and 6.04 which indicate the odd over even predominance group (Table 4).

Table 4 Biomarker values of modern plants divide into three groups consist of true mangrove, back mangrove, and mangrove associate. LOQ = ppt

Plant groups	Species	Locations	Maximum Peak	ACL_T[a]	ACL_{21-35}[b]	CPI_T[c]	CPI_{21-35}[d]
	Avicennia marina	KSC	C_{33}	31.90	31.99	7.41	7.68
	Barringtonia asiatica	KKB	C_{16}, C_{24}	22.70	27.45	0.89	0.82
		TLN	C_{17}	19.78	25.99	0.79	0.76
	Bruguiera gymnorrhiza	KKB	C_{31}	21.63	29.17	0.94	1.36
	Rhizophora apiculate	KSC	C_{31},	29.77	31.19	5.43	10.74
True mangrove	*Rhizophora mucronate*	KKB	C_{17}, C_{26}	21.24	27.61	0.89	0.81
		KSC	C_{29}	29.23	29.59	4.58	5.08
	Sesuvium portulacastrum	KSC	C_{16}	19.55	26.40	0.88	1.00
	Sonneratia caseolaris	KSC	C_{31}	30.23	30.64	11.30	15.29
		TLN	C_{33}	28.33	30.59	2.51	4.18
	Acrostichum aureum	KSC	C_{33}	29.63	31.83	3.68	7.20
Back mangrove	*Oncusperma tigllarium*	KKB	C_{17}	20.21	28.74	0.97	1.32
	Xylocarpus granatum	KKB	C_{16}	18.10	26.10	0.81	0.75
	Casuarina equisetifolia	KKB	C_{16}	18.22	26.02	0.73	0.58
Mangrove associate		TLN	C_{18}, C_{24}	21.60	26.76	0.77	0.72
	Poaceae (*Bambusoideae*)	TLN	C_{31}	28.24	30.60	3.14	6.04

[a] $ACL_T = (15C_{15} + 17C_{17} + \ldots + 35C_{35})/(C_{15} + C_{17} + \ldots + C_{35})$

[b] $ACL_{21-35} = (21C_{21} + 23C_{23} + \ldots + 35C_{35})/(C_{21} + C_{23} + \ldots + C_{35})$

[c] $CPI_T = (C_{15} + C_{17} + \ldots + C_{33}) + (C_{17} + C_{19} + \ldots + C_{35})/2(C_{16} + C_{18} + \ldots C_{34})$

[d] $(C_{21} + C_{23} + \ldots + C_{33}) + (C_{23} + C_{25} + \ldots + C_{35})/2(C_{22} + C_{24} + \ldots C_{34})$

4.2 The *n*-Alkane analysis in sediments from TLN-CP5

      The sediment sequence TLN-CP5 was described in detail by Yoojam (2015) based on Wohlfarth (2012) classification. The TLN-CP5 core can be divided into five sediment units (Fig 20). The basal unit is the stiff light gray clay of unit A (385.0 − 368.0 cm depth below water surface), which is overlaid by the dark grey clay of unit B (368.0 – 333.5 cm depth below water surface). The sediment unit B gradually transfers to peat layer of unit C (333.5 – 289.5 cm depth below water surface). The sharp boundary can be observed between the top of the peat layer and bottom of dark grey clay with detrital organic matter of unit D (289.5 – 217 cm depth below water surface). The uppermost unit E (217 – 150 cm depth below water surface) is the dark gray to dark brown sediments called gyttja. Since the short-chain is possibly decomposed by microbial activities, the *n*-alkanes analysis in sediments has been here considered from C_{21} to C_{35} (Bush and McInerney, 2013). The lithostratigraphic column of core TLN-CP5 was further compared with the distribution of *n*-alkane, ACL_{21-35}, CPI_{21-35}, and P_{aq} for the past environmental reconstruction.

จุฬาลงกรณ์มหาวิทยาลัย

CHULALONGKORN UNIVERSITY

Table 5 Lithostratigraphic description of TLN-CP5 sediment core (Yoojam, 2015).

Depth below water surface (cm)	Lithostratigraphic description	Layers	Units
168.0 – 150.0	Dark brown gyttja	20	E
179.5 – 168.0	Dark brown clayey gyttja	19	E
182.0 – 179.5	Dark brown gyttja	18	E
205.0 – 32.0	Dark brown clayey gyttja	17	E
209.0 – 205.0	Dark brown gyttja	16	E
217.0 – 209.0	Dark brown clayey gyttja	15	E
227.5 – 217.0	Dark grey clay	14	D
248.0 – 227.5	Grey clay	13	D
264.0 – 248.0	Dark grey clay	12	D
278.0 – 264.0	Dark grey clay with detrital organic matter	11	D
286.0 – 278.0	Dark grey clay	10	D
298.5 – 286.0	Dark grey clay with detrital organic matter	9	D
298.5	Possibly hiatus		
308.5 – 298.5	Peat	8	C
311.0 – 308.5	Peaty clay	7	C
333.5 – 311.0	Peat	6	C
340.5 – 333.5	Dark grey clay	5	B
344.0 – 340.5	Peat	4	B
350.5 – 344.0	Dark grey clay	3	B
368.0 – 350.5	Dark grey clay with detrital organic matter, found the root.	2	B
385.0 – 368.0	Stiff and light grey clay	1	A
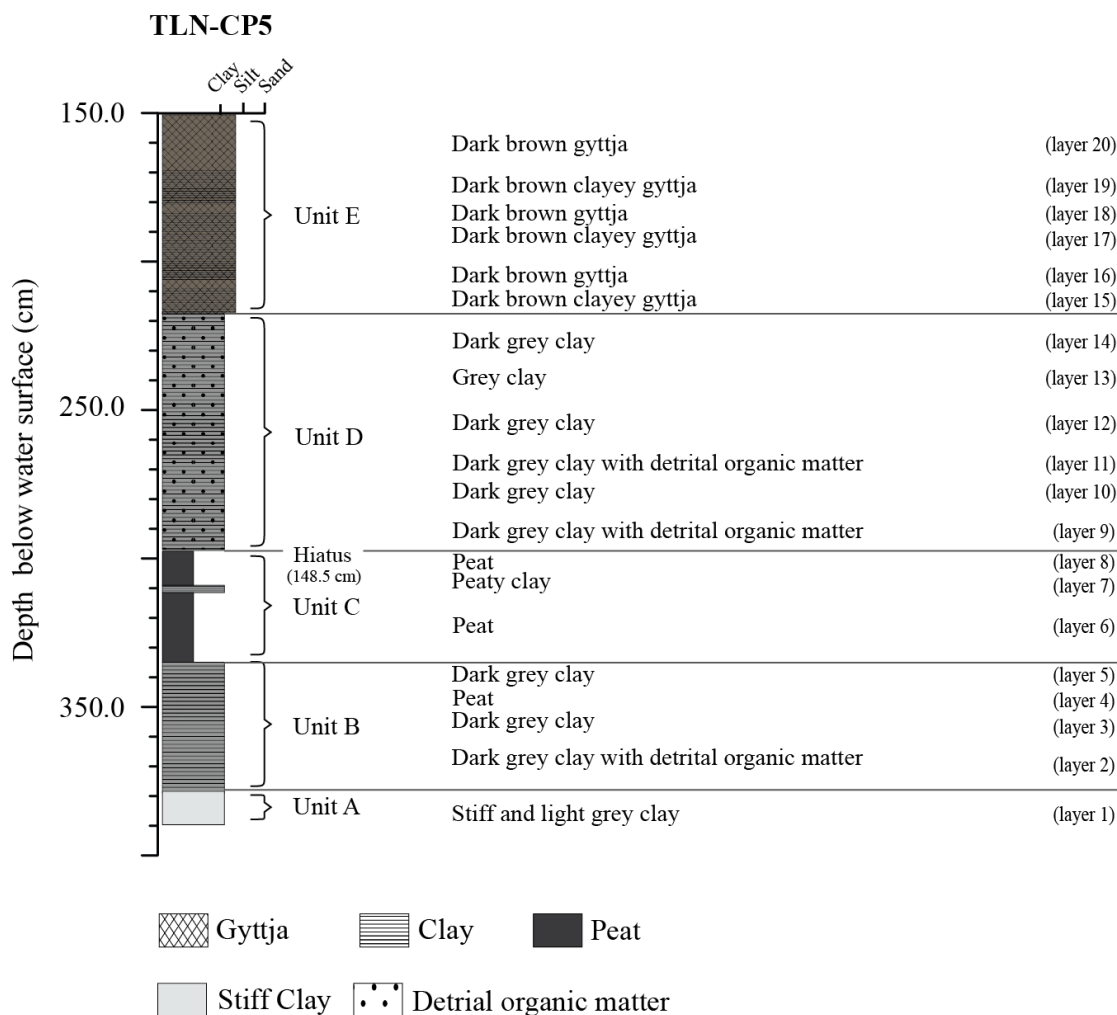
Figure 20 Lithostratigraphy of core TLN-CP5 (Yoojam, 2015). The coring point is shown in figure 11.

4.2.1 Distributions of *n*-alkane in TLN-CP5

C_{28} is the most abundant *n*-alkanes of about 15% in the stiff light grey clay of unit A (Fig. 21). The predominant *n*-alkanes are diverse in sediment unit B, which consist of 4 layers (Fig. 22 and Table 4). C_{25} is the highest concentration in dark grey clay with detrital organic matter of layer 2. However, the dark grey clay of layer 3 and 5 are dominated by C_{29} and C_{31}. C_{25}, $C_{29,}$ and C_{31} are about 15% at 360, 350 and 340 cm depth, respectively (Fig. 22). In the peat layer of unit C, C_{31} is the most abundance, especially at 320 and 310 cm depth, which its concentration is higher than 30% (Fig. 23). C_{31} is relatively less abundance than that at 320 and 310 cm depth

which is about 17.5% at 330 cm depth. However, the dominance of C_{31} is replaced by C_{27} in the uppermost peat layer (layer 8) at 300 cm depth. C_{31} have been found only 10%, while the relative abundance of C_{27} is about 15%.

For unit D, C_{31} become again prevailing in the dark grey clay with detrital organic matter at 290 and 270 cm depth (layer 9 and 11) (Fig. 24, D-1), and in the dark grey at 280 cm depth (layer 10). However, the relative abundance of C_{31} is less than that in unit C.

This layer is overlaid by the dark grey clay (layer 12 and 14) and grey clay (layer 13) layers (Table 5). C_{21} is a dominance of about 20 and 15% at 260 and 250 cm depth in layer 12 (Fig. 25, D-2). It is also found in high concentration in the lower part of layer 11, while the upper part of layer 12 become predominance of C_{26}. The dark grey clay of layer 14 is dominated by C_{31}, which its abundance is about 20% (Fig. 26, D-3).

Unit E is dominated by C_{31} from 210 to 200 cm depth, which relative abundance is approximately 20%. The predominance of C_{31} was occupied by C_{27} in the upper part of unit E from 190 to 155 cm depth. The concentration of C_{27} is about 15%.

จุฬาลงกรณ์มหาวิทยาลัย
CHULALONGKORN UNIVERSITY
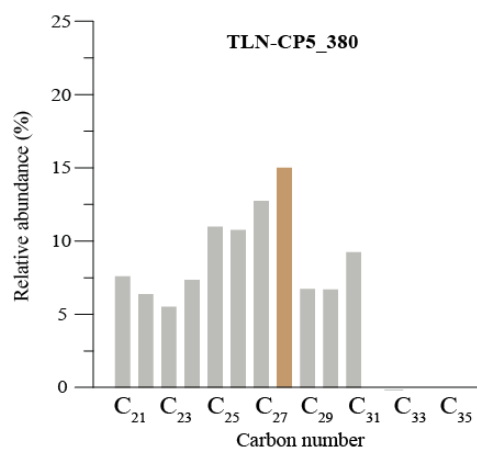
Unit A

Figure 21 The distribution of *n*-alkane in the stiff light grey clay of unit A.

Unit B
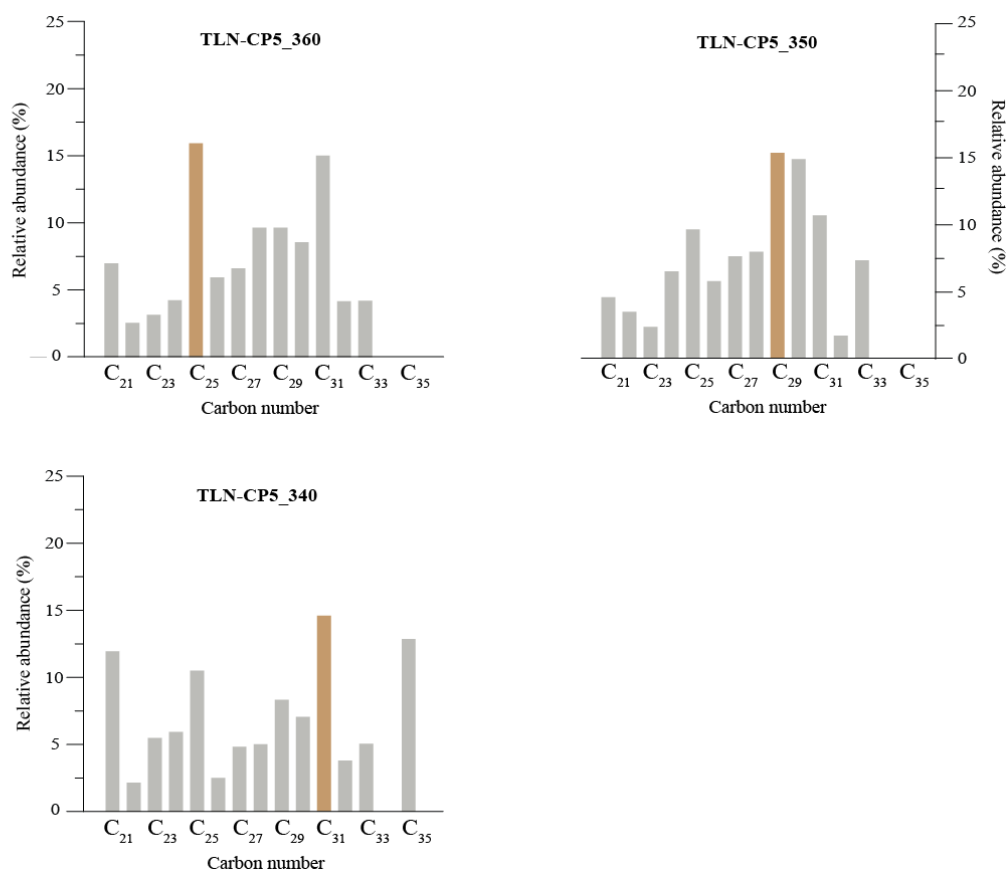
Figure 22 The distributions of *n*-alkane in the dark grey clay of unit B.

Unit C

Figure 23 The distributions of *n*-alkane in the peat layer of unit C.

Unit D-1

Figure 24 The distributions of *n*-alkane in the dark grey clay with detrital organic matter of unit D-1.

Unit D-2

Figure 25 The distributions of *n*-alkane in the dark grey clay with detrital organic matter of unit D-2.

Unit D-3

Figure 26 The distributions of *n*-alkane in the dark grey clay with detrital organic matter of unit D-3.
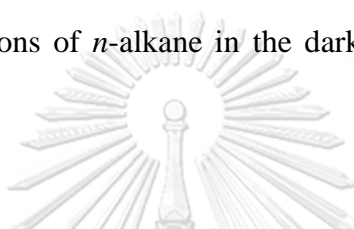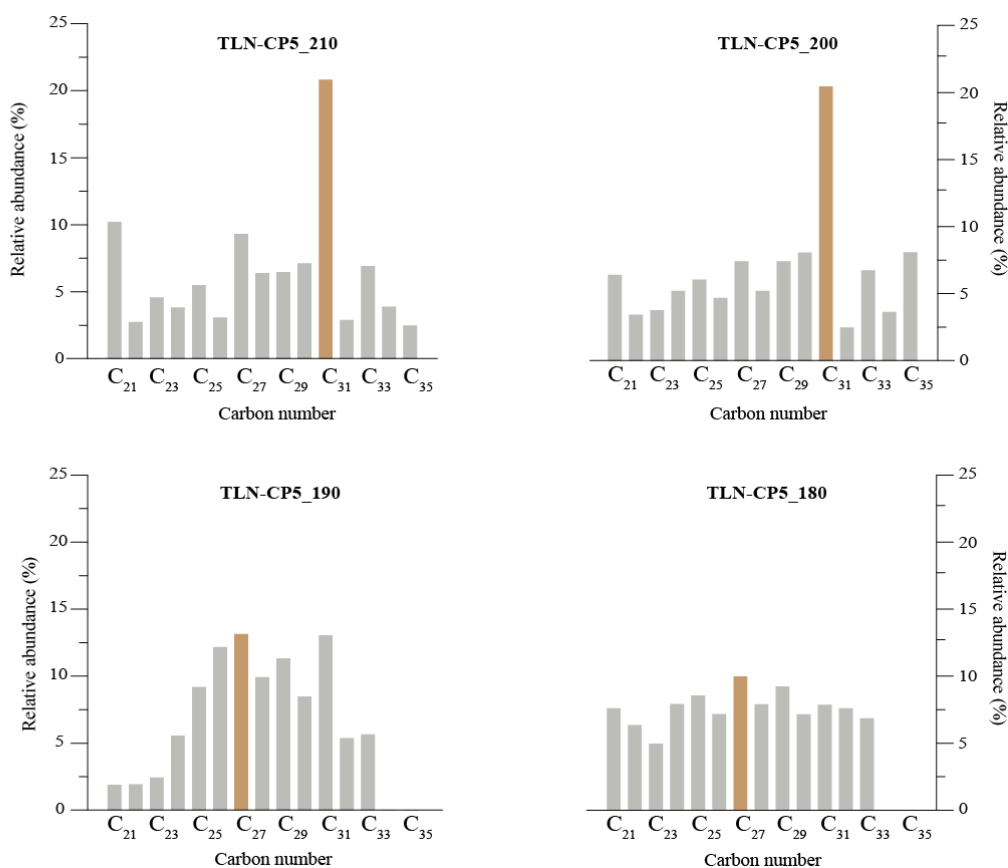
Unit E

Unit E
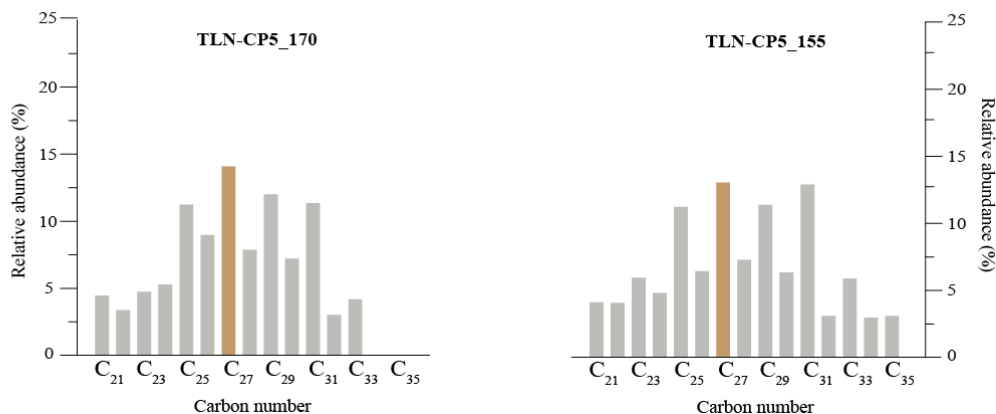
Figure 27 The distributions of *n*-alkane in the clayey gyttja and gyttja of unit E.

4.2.2 Average chain length, carbon preference index and proportion of aquatic macrophyte

The ACL_{21-35} values are varied from 25.0 to 30.0, respectively. Despite the ACL_{21-35} gradually increase from 26.0 to 28.0 in sediment unit A and C, The ACL_{21-35} generally decrease from 30.0 to 26.0 in from the bottom to middle of unit D before gradually increase to about 28.0 in the lowermost layer of unit E. The increases in ACL_{21-35} values are in the bottom to middle part of unit E. The ACL_{21-35} values are approximately 28.0 at the uppermost part of the sedimentary sequence (Fig. 28).

The variability of CPI_{21-35} relatively resembles with those in ACL_{21-35}. CPI_{21-35} varies from 1.0 to 3.0. CPI_{21-35} enhance from 1.0 to 3.0 in unit A and the middle part of unit C. CPI_{21-35} gradually decline from 3.0 to 1.0 in the upper part of unit C. It slightly changes of about 1.0 in unit D and the unit E (Fig. 28).

P_{aq} gradually decrease from 0.4 to 0.2 in unit A and lower part of unit C. It becomes increase from 0.2 to 0.4 at the upper layer of unit C and varies from 0.4 to 0.2 through unit D. A gradual increase in P_{aq} from 0.2 to 0.4 can be found in the lower part of unit E before it becomes an insignificant change in the upper part of this unit (Fig. 28).

Figure 28 Derived the *n*-alkane biomarker parameters ACL_{21-35}, $CPI_{21-35,}$ and P_{aq} from core TLN-CP5 along with depth (cm).

4.3 The *n*-Alkane analysis in sediments from TLN-CP7

The sedimentary sequence of core TLN-CP7 core contains three sedimentary units which were described in detail by Yoojam (2015) (Table 6). The basal unit of the core is very similar to unit C in the TLN-CP5 core. But the peat in this unit is very well compaction and can be split into thin sheets. This unit, therefore, was distinguished and called unit C* (439.0 – 436.0 cm depth below water surface). The compacted peat was overlaid by grey clay with dark plant detritus of unit D (436 – 189 cm depth below water surface), which is the longest unit in this core. The uppermost unit E is gyttja (189 – 150 cm depth below water surface). The lithostratigraphic column of core TLN-CP7 was here compared with the *n*-alkane, ACL_{21-35}, CPI_{21-35}, and P_{aq} (Fig. 29).

Table 6 Lithostratigraphic description of TLN-CP7 sediment core (Yoojam, 2015).

| Depth below water surface (cm)	Lithostratigraphic description	Layers	Units
162.0 – 150.0	Dark brown gyttja	18	E
168.0 – 162.0	Dark brown clayey gyttja	17	E
175.0 – 168.0	Dark brown gyttja	16	E
179.0 – 175.0	Dark brown clayey gyttja	15	E
182.0 – 179.0	Dark brown gyttja clay	14	E
189.0 – 182.0	Brown gyttja clay	13	E
195.0 – 189.0	Brown clay	12	D
200.0 – 195.0	Dark grey clay with detrital organic matter	11	D
277.0 – 200.0	Grey clay with detrital organic matter	10	D
233.0 – 277.0	Grey clay with detrital organic matter	9	D
270.0 – 233.0	Light grey clay with detrital organic matter	8	D
392.0 – 270.0	Light grey clay	7	D
441.0 – 392.0	Light grey clay with detrital organic matter more than layer 8	6	D
425.0 – 441.0	Light grey clay with detrital organic matter more than layer 8	5	D
430.0 – 425.0	Grey clay with detrital organic matter more than layer 9 and 10	4	D
434.0 – 430.0	Dark grey clay with detrital organic matter more than layer 11	3	D
436.0 – 434.0	Dark grey clay with detrital organic matter more than layer 11	2	D
439.0 – 436.0	Compacted peat	1	C[*]
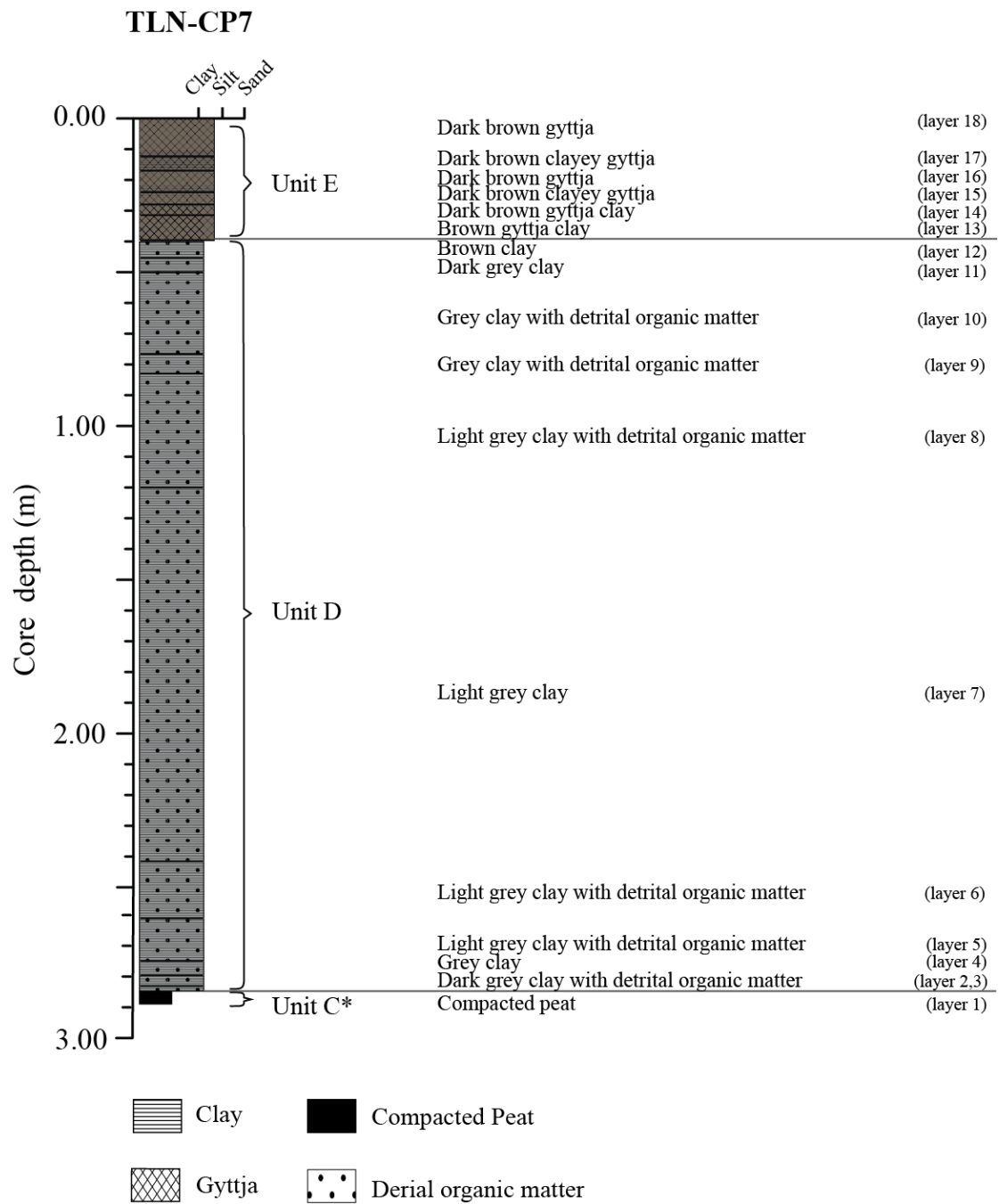
Figure 29 Lithostratigraphy of core TLN-CP7 (Yoojam, 2015). The coring point is shown in figure 11.

4.3.1 Distributions of *n*-alkane in TLN-CP7

Samples at 437 cm depth below water surface were here selected to represent the compacted peat of unit C*. The most abundant *n*-alkane is C_{29} (Fig 30).

The *n*-alkanes distribution in unit D, which is about 390 cm thick, are generally diverse. C_{21} is the most dominant of higher than 15% in the sample at 433 and 430 cm depth below water surface (layer 1 and 3), which is the lowermost layer of unit D (Fig. 31). C_{26} is the highest concentration of about 14% at 410 cm depth below water surface (layer 6).

At 380 cm depth below water surface (layer 7), the most abundant *n*-alkanes is C_{24}, which is about 17%. Notably, the relative abundance of C_{21} is about 16%, which is slightly lower than C_{24}, in this sample. C_{21} become the most dominant *n*-alkanes of about 17.5% in the samples at 360, 340 and 320 cm depth below water surface (layer 7).

For the middle part of unit D (unit D-2), C_{26} is the most abundant about 12.5% in the light grey clay at 300 cm depth below water surface (Fig 32). C_{26} is slightly less than C_{29}, which its abundance is about 12%, at 280 cm depth. It became again predominance at 260 cm depth below water surface that is about 12%. At 240 cm depth below water surface, the highest abundant *n*-alkanes is C_{27}, which is about 15%.

The dominant *n*-alkane the upper part of unit D (unit D-3) between 220 and 190 cm depth below water surface are different (Fig. 33; D-3). At 220 cm depth below water surface (layer 9) are the dark grey clay, which is dominated by C_{29}. Whereas the dark grey clay (layer 11) and the brown clay (layer 12) are dominated by C_{26} and C_{24}, respectively.

The most abundant *n*-alkanes of unit E are C_{29} (layer 14) and C_{27}, which are about 15% and 20% at 170 and 160 cm depth below water surface (layer 16 and 18) (Fig. 34).
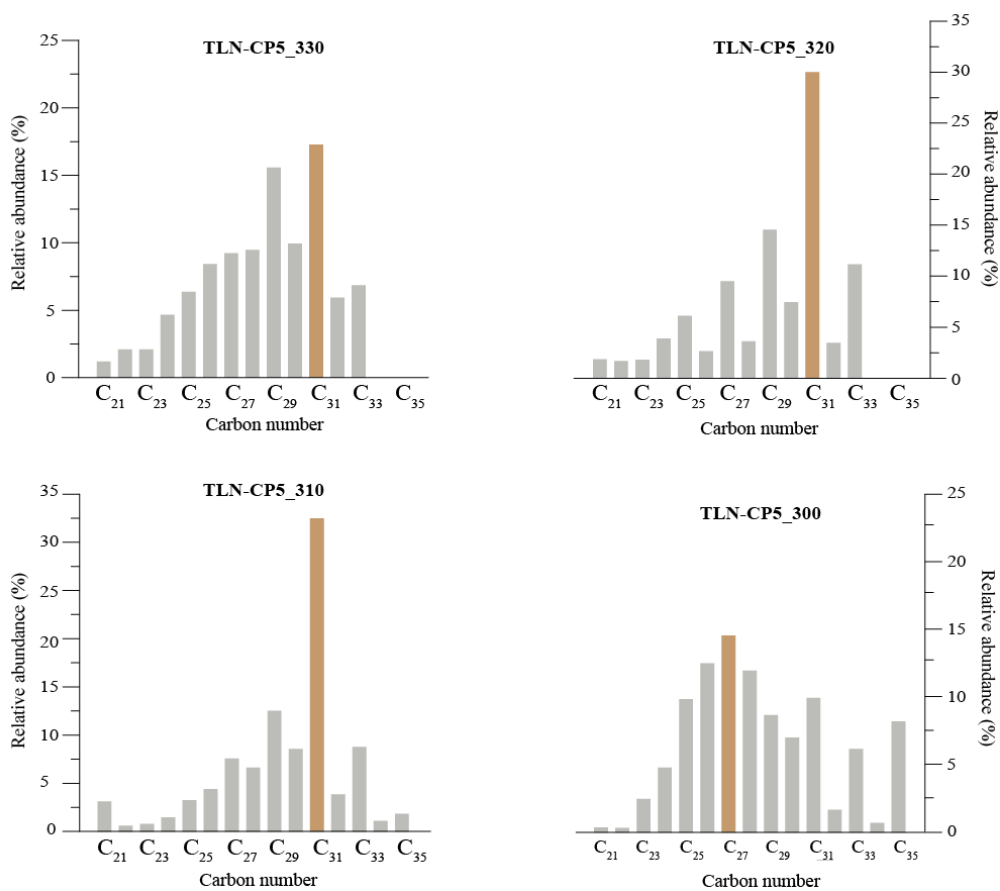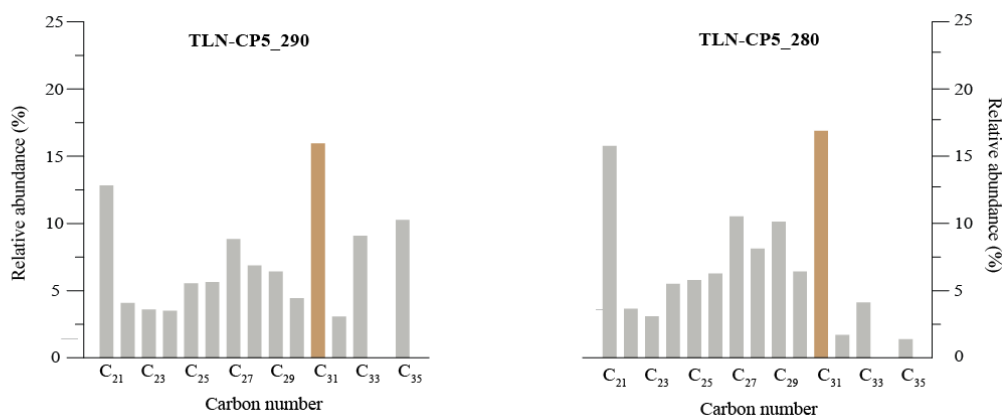
Unit C*
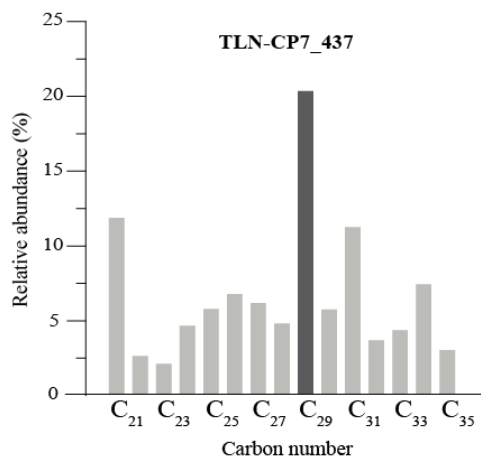
Figure 30 The distribution of *n*-alkane in compacted peat of unit C*.
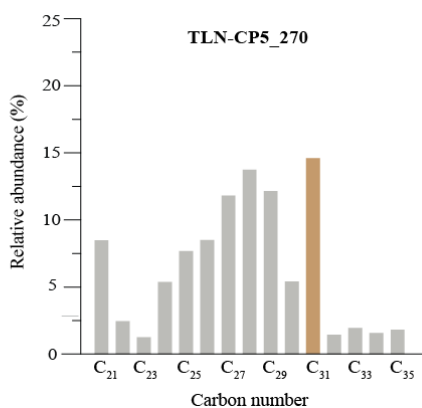
Unit D-1
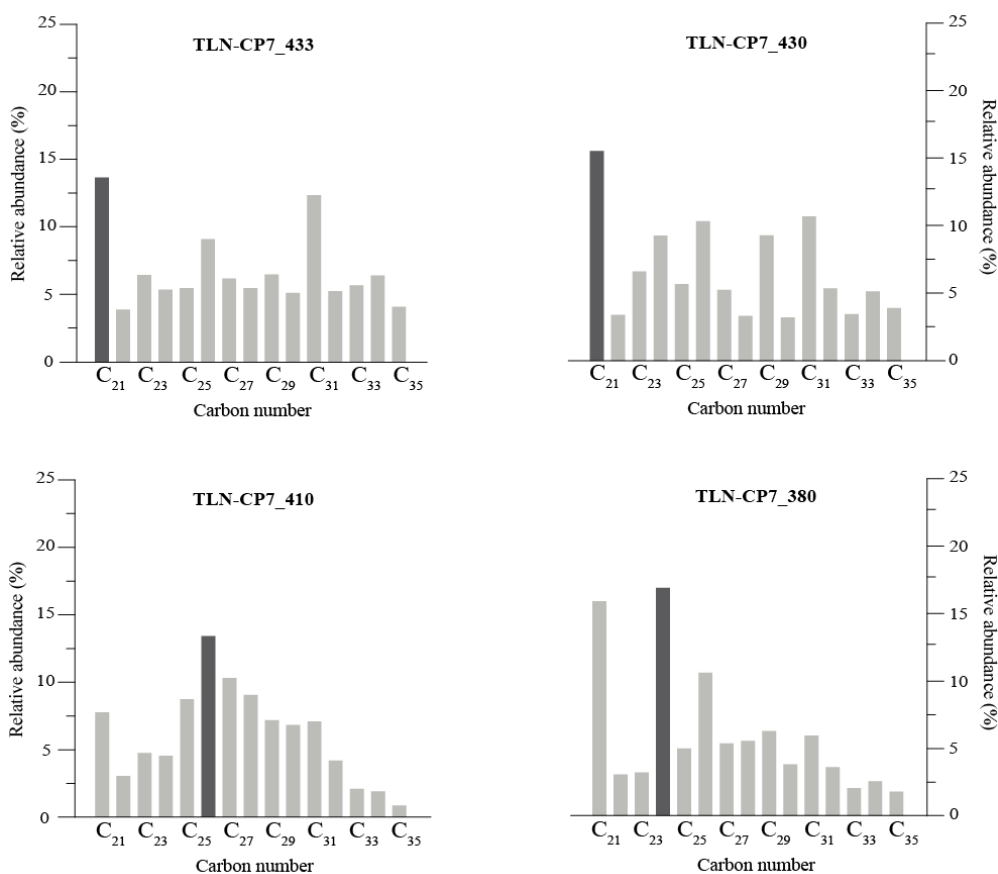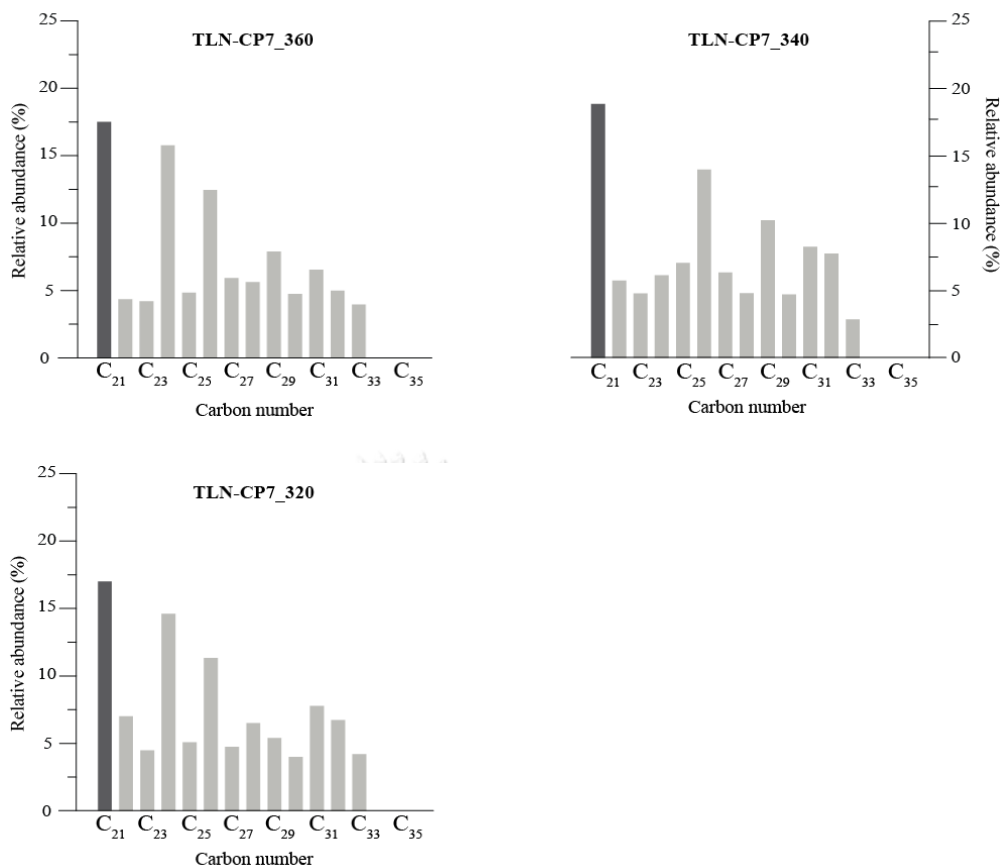
Figure 31 The distributions of *n*-alkane in the dark grey clay with detrital organic matter of unit D-1.
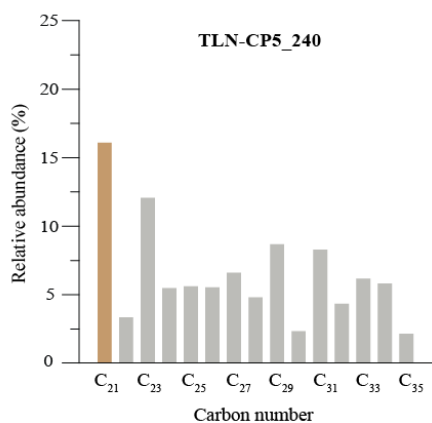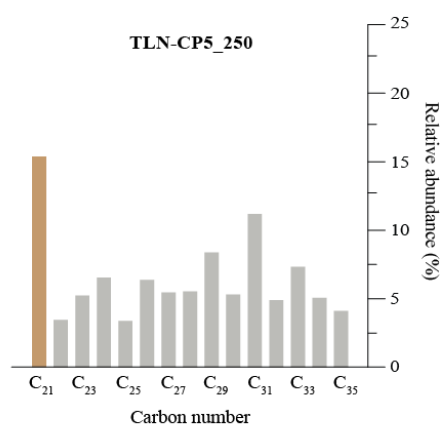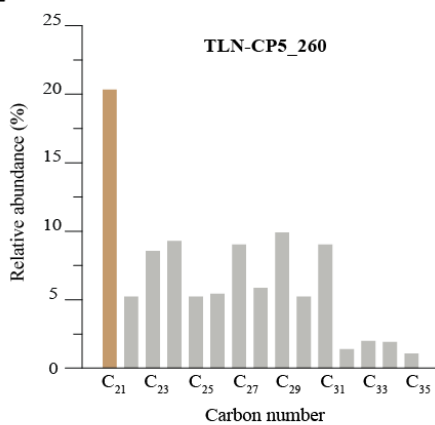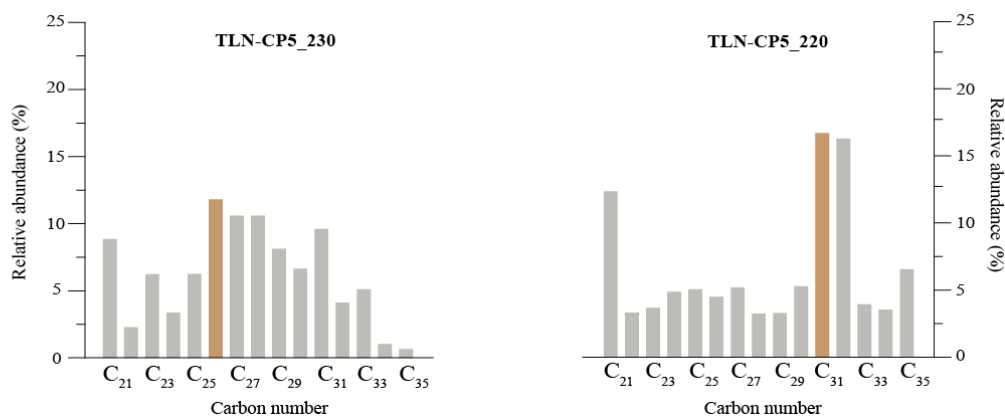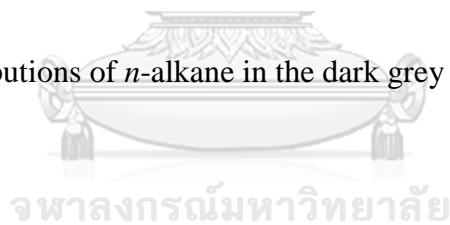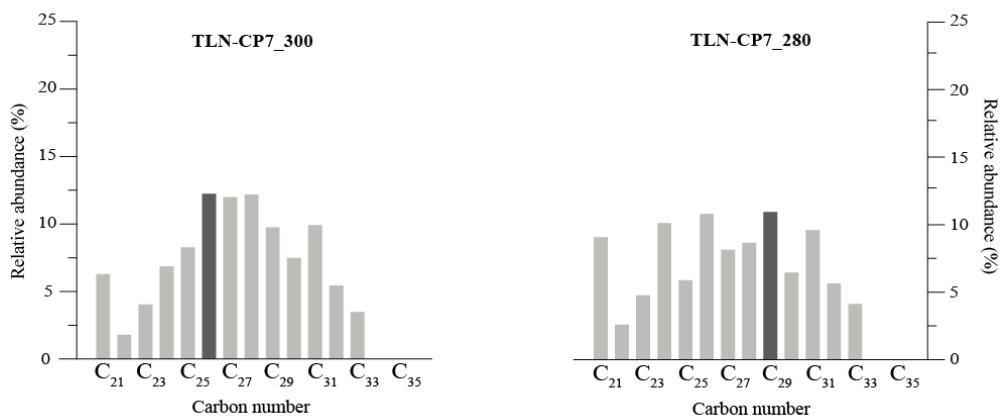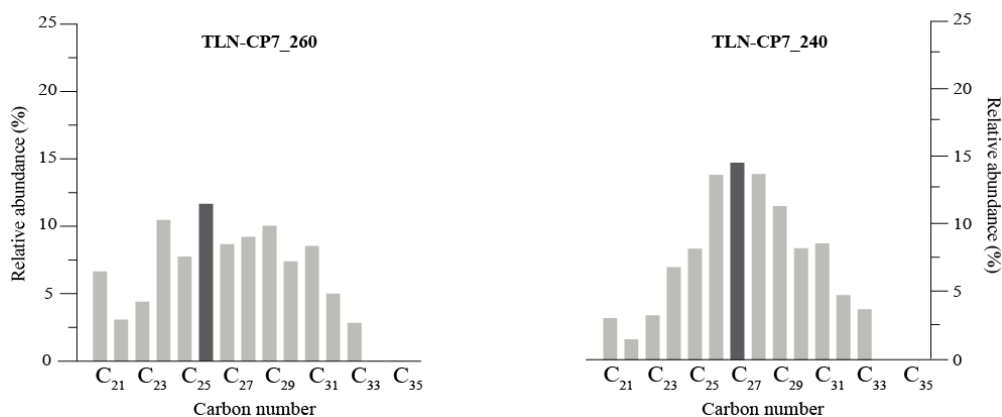
Unit D-2

Figure 32 The distributions of *n*-alkane in the dark grey clay with detrital organic matter of unit D-2.
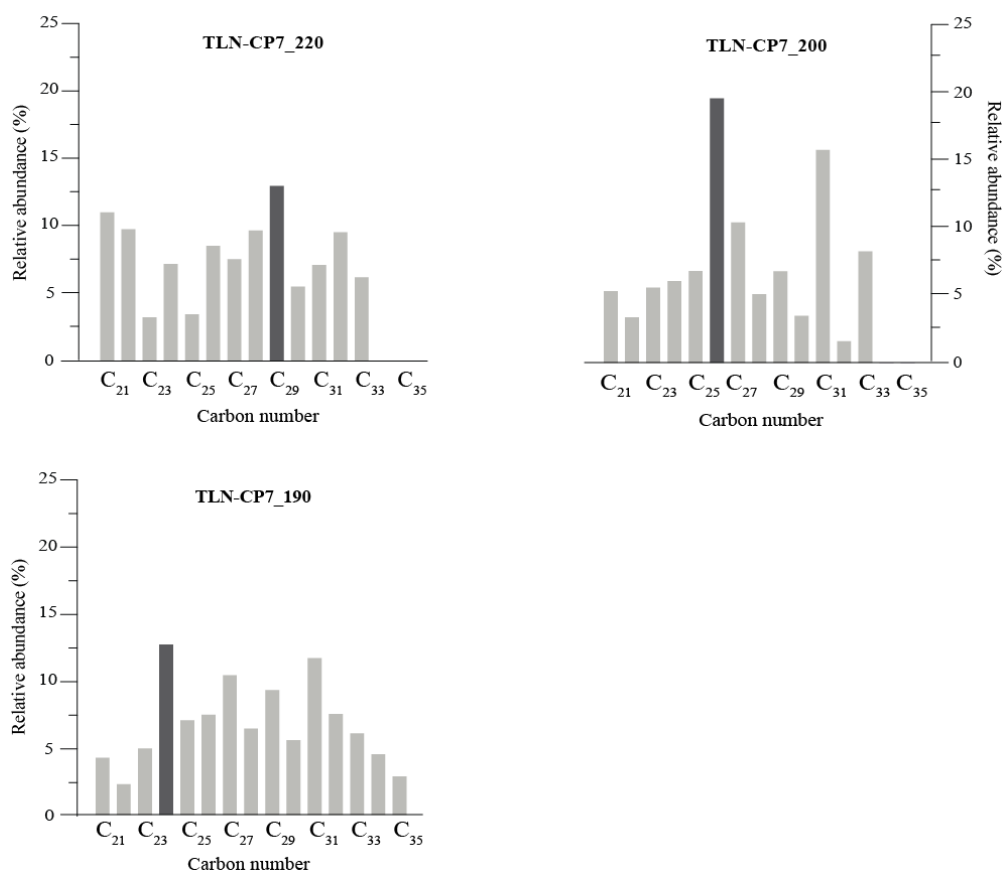
Unit D-3

Figure 33 The distributions of *n*-alkane in the dark grey clay with detrital organic matter of unit D-3.
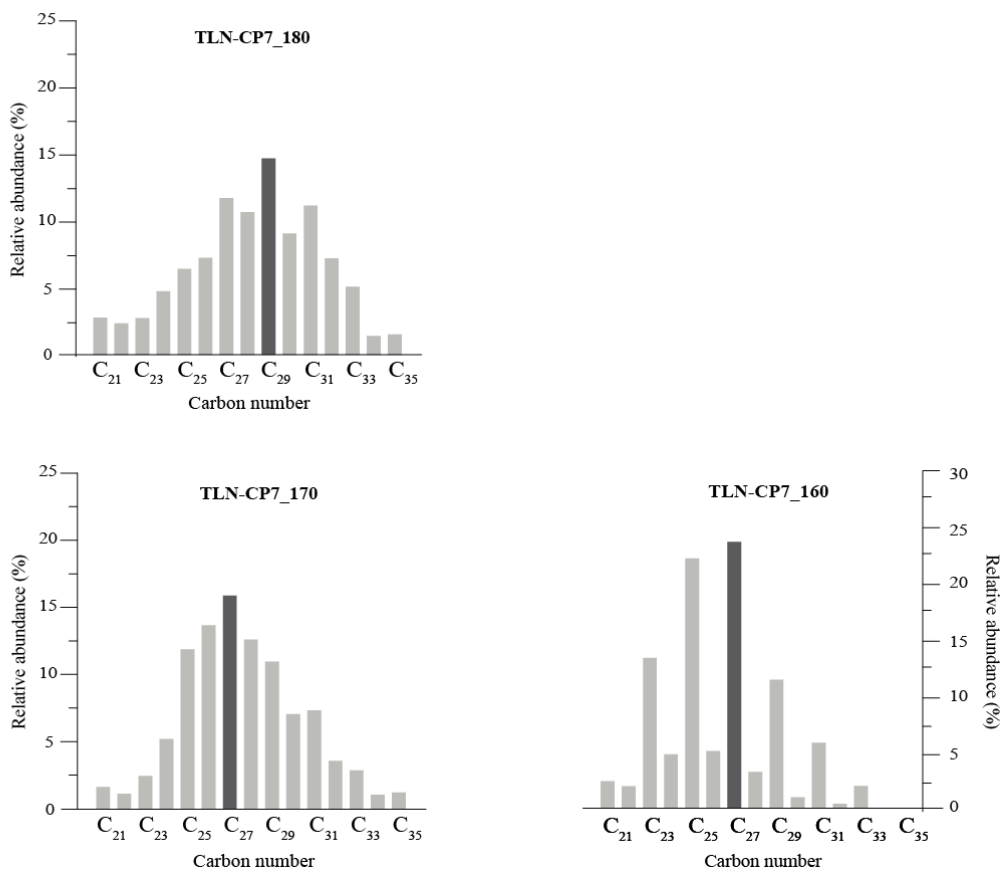
Unit E

Figure 34 The distributions of *n*-alkane in brown gyttja of unit E.

4.3.2 Average chain length, carbon preference index and proportion of aquatic macrophyte

The ACL$_{21-35}$ values are varied from 26.0 to 28.5. The ACL$_{21-35}$ gradually decrease from 28.0 to 26.0 in the sediment unit *C and D between 430 and 320 cm depth below water surface. The ACL$_{21-35}$ in unit D between 300 and 190 cm depth below water surface increase from 26.0 to 28.0 before gradual decrease from 28.0 to 26.0 in unit E (Fig. 35).

The variability of CPI$_{21-35}$ varies from 0.8 to 4.8. The CPI$_{21-35}$ in the unit *C decrease from approximately 1 unit of the value and remained constant at approximately 1.0 in unit D and in the lowermost layer of unit E. The CPI$_{21-35}$ significantly increase in the uppermost layer of unit E that increase from about 1.0 reach to 3.2 (Fig. 35).

The P_{aq} values are varied from 0.2 to 0.7. The lowest P_{aq} is 0.2, which was found at 287 cm depth in the unit *C. Then it becomes increase and remained constant approximately 0.3 to 0.4 in unit D and the lower part of unit E. The P_{aq} in the upper part of unit E is remarkably increased. It becomes an increase from 0.4 to 7.0 (Fig. 35).

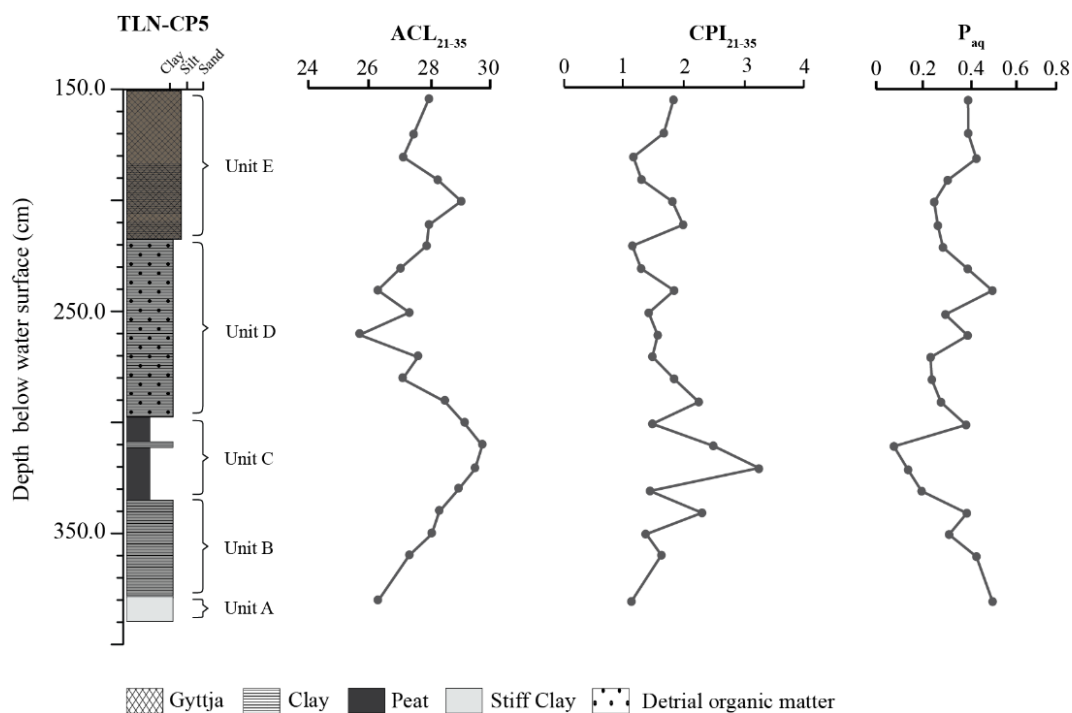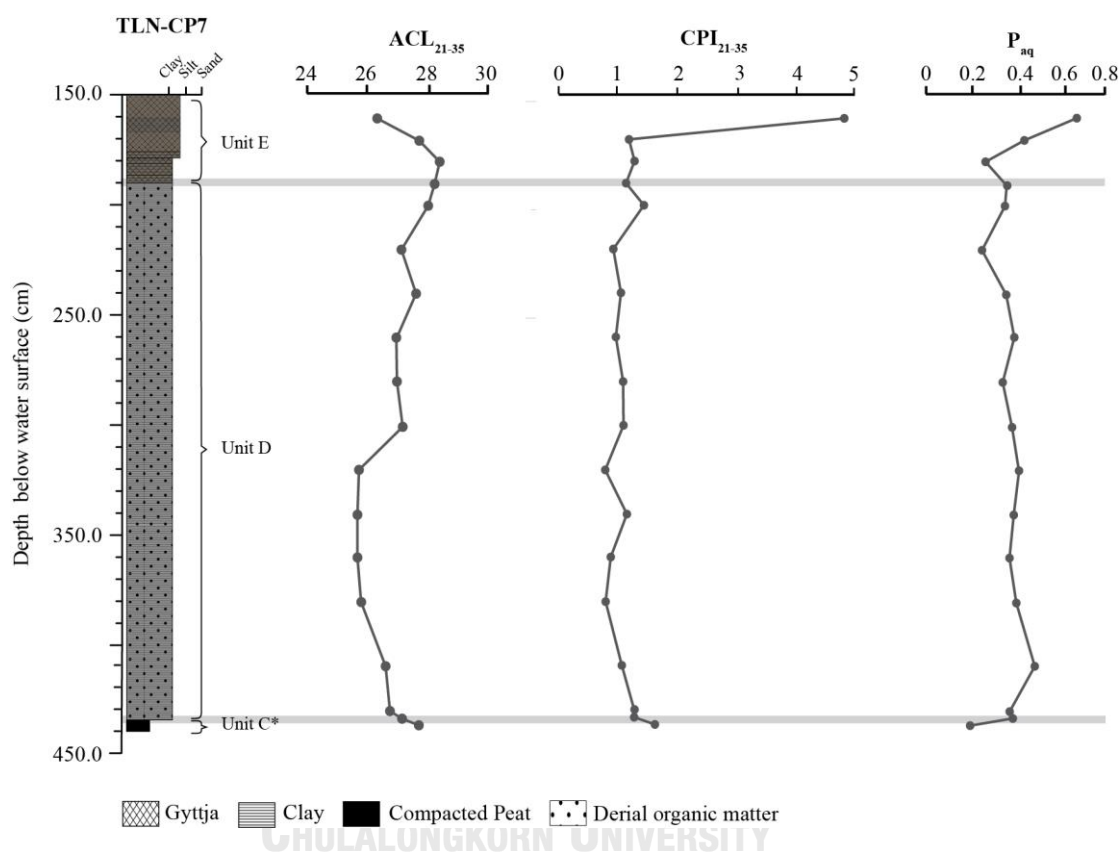**Figure 35** Derived the *n*-alkane biomarker parameters ACL_{21-35}, CPI_{21-35}, and P_{aq} from core TLN-CP7 along with depth (cm).

4.4 Chronology

The radiocarbon dating results were calibrated by InCal13 (Reimer et al., 2013) (Table 7 and Table 8), and then the age-depth models were constructed by BACON (the Bayesian accumulation histories of deposits) (Blaauw and Christen, 2011).

4.4.1 Chronology of TLN-CP5

Chronology of TLN-CP5 based on nine ^{14}C dates of plant remains (Table 7). The dated plant remains to provide ^{14}C age from 8,192 – 8,363 cal yr BP to recent.

The dating results of sample no. 021775, 021774, 021773 and 021776 in sediment unit A, B and C suggest that deposition occurs during 8,192 – 8,363 to 7,962 – 8,072 cal yr BP (Phountong, 2016). And show a gradual deposition of sediments from 368.0 to 298.5 cm depth below water surface. Interestingly, the different dating age between sample no. 021775 and 021776 are about 300 years. Consequently, the accumulation rate is approximately 0.20 cm/yr.

A boundary between unit C and D is sharp, which would suggest a rapid change during the deposition. Sample no. 021776 and 022510 were consequently taken from the top of unit C and bottom of unit D, which are about 7,962 – 8,072 and 7,566 – 7,669 cal yr BP, respectively (Phountong, 2016). The depth interval between no. 021776 and 022510 are approximately 7.5 cm and the different dating age between sample no. 021776 and 022510 are about 400 cal yr BP that suggest the low accumulation rate is approximately 0.02 cm/yr or the presence of a hiatus.

Sample no. 022509, 021777 and 021771 were taken from the middle of unit D, and the bottom and top of unit E, respectively. The dating of no. 022509 and 021777 are about 7,566 – 7,669 and 7,142 – 7,258 cal yr BP (Phountong, 2016). While sample no. 021771 shows a modern age. The dating of sample no. 022509 and 021777 shows a gradual deposition for about 400 cal yr BP. The deposition rate is approximately 0.20 cm/yr.

Table 7 ^{14}C dated for TLN-CP5.

Lab ID	Depth below water surface (cm)	Measured material	^{14}C date age (BP $\pm$ 1σ)	Calibrated age (2σ) (cal yr BP)	Unit	Published in
21771	168.0 - 163.0	leaves	modern		E	Phountong (2016)
21777	206.0 - 211.0	leaves	6,234 ± 44	7,142 - 7,258	E	Phountong (2016)
22509	243.0 - 248.0	leaves	6,690 ± 37	7,486 - 7,616	D	Phountong (2016)
21772	287.5 - 293.0	wood	6,765 ± 34	7,577 - 7,668	D	Phountong (2016)
22510	292.0 - 296.0	leaves	6,744 ± 35	7,566 - 7,669	D	Phountong (2016)
21776	300.0 - 303.0	wood	7,104 ± 35	7,916 - 8,000	C	Phountong (2016)
21773	330.0 - 333.0	wood	7,219 ± 36	7,962 - 8,072	C	Phountong (2016)
21774	365.0 - 368.0	wood	7,359 ± 34	8,041 - 8,219	B	Phountong (2016)
21775	381.0 - 385.0	leaves, charcoal	7,460 ± 37	8,192 - 8,363	A	Phountong (2016)

4.4.2 Chronology of TLN-CP7

The chronology of TLN-CP7 based on four ^{14}C dates obtained on charcoal, leaves, and seed (Table 8). The dated plant remains to provide age from 7,593 – 7,759 cal yr BP to recent.

The dating of charcoal (samples no. 030464) was taken from unit C*, which is a lowermost of the core, is about 7,593 – 7,759 cal yr BP.

Sample no. 030463 and 030462 were taken from unit D at 430.0 and 250.0 cm depth below water surface, respectively. The dating results of sample no. 030463 are about 7,510 – 7,543 cal yr BP. Whereas sample no. 030462, which is an upper layer, is about 7,582 – 7,694 cal yr BP (Table 8). These dating results suggest that the sediment was possibly disturbed by organisms or bioturbating activities e.g. borrowing (Gingras et al., 2015). Alternatively, the occurrence of contamination during dating sample preparation. Nevertheless, the dating results of both samples have a similar range of possibilities (Table 8).

Fortunately, there are the dating results of TLN-CP5 (Phountong, 2016), which can be used to correlate with TLN-CP7 (Fig. 34). The dating result of the top of unit C* in TLN-CP7 and the bottom of unit D in TLN-CP5 are about 7,593 – 7,7590 and 7,582 – 7,694 cal yr BP, which are considered to resemble (Fig. 36). In addition to the lithology of the sediment sequence is reliable evidence that supports the sediment in unit D from both cores beginning to deposition at the same time. According to the dating results, it is possible that unit D of both cores deposits with a similar rate is about 1.50 cm/yr in the initial period. And the thickness of grey clay, which deposited after 7,510 – 7,543 cal yr BP, shows a rapid deposition rate of unit D in TLN-CP7. Unfortunately, we do not collect any plant remains for dating between 250.0 and 175.0 cm depth below water surface, therefore, we cannot specify the time of changing sediment characteristics from unit D to unit E.

The dating of plant remains in sample no. 030461 was taken from the lower part of unit E that suggest the modern age (Table 8).

Table 8 ^{14}C dated for TLN-CP7.

Lab ID	Depth below water surface (cm)	Measured material	[14]C date age (BP ± 1 σ)	Calibrated age (2 σ) (cal yr BP)	Units	Published in
30461	175.0 - 177.0	leaves, charcoals, seed	modern		E	This work
30462	250.0 - 253.0	charcoals	6,808 ± 39	7,582 - 7,694	D	This work
30463	340.0 - 343.0	charcoals	6,729 ± 45	7,510 - 7,543	D	This work
30464	436.0 - 437.0	charcoals	6,843 ± 41	7,593 - 7,759	C*	This work
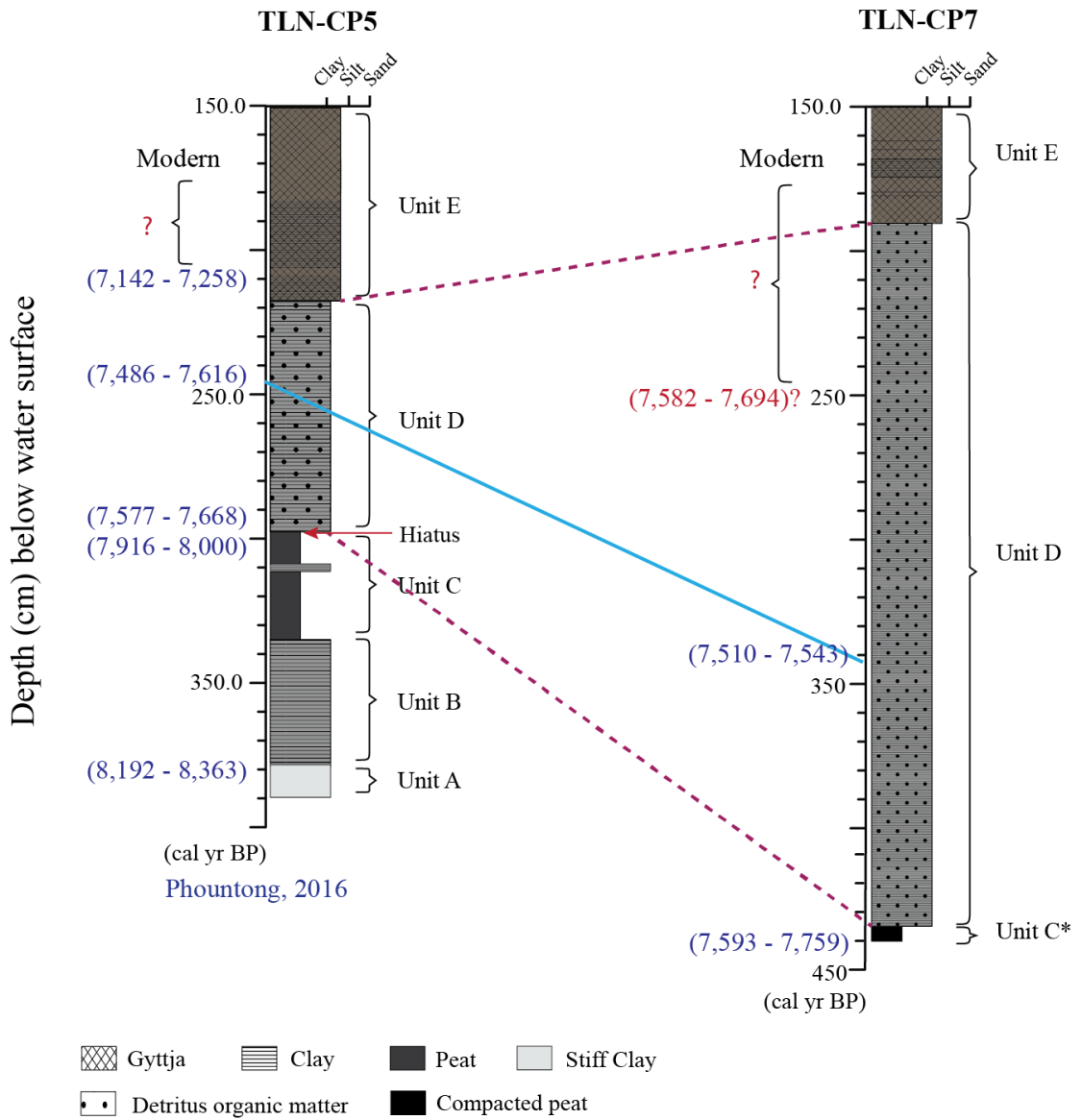
Figure 36 Correlation between core TLN-CP5 and TLN-CP7 (Yoojam, 2015). The calibrated age for TLN-CP5 is according to Phountong (2016). The coring points are shown in figure 11.

CHAPTER V
DISCUSSION

The plants growing around the lake are the major source of organic matter in the sediments (Meyers and Ishiwatari, 1993; Pu et al., 2017). And the vegetation dynamics are important records to assess changes in the environment (Pu et al., 2017; Wang et al., 2017). Consequently, the organic remains to produce by the surrounding plants (pollens and chemical molecules, etc.) can be used for environmental reconstruction.

The plants can be generally classified by their morphology, anatomy, and chemotaxonomy. The chemotaxonomy is a new approach for the classification that is based on the plant chemical constituents producing from their biosynthetic pathways. These chemical constituents are often specific and limited to relate taxonomical organisms (Singh, 2016).

Aliphatic hydrocarbons, especially the *n*-alkanes, are widely used for plant classification (Bush and McInerney, 2013; Ficken et al., 2000) and paleoenvironmental reconstruction (Guo et al., 2014). The *n*-alkanes are the straight-chain hydrocarbons, which are stable and highly resistant molecules, because of their single bond and lack of functional groups. Consequently, the *n*-alkanes can survive in the fossil records for a long time (Eglinton and Hamilton, 1967; Eglinton and Eglinton, 2008). Each plant group generally produced their specific *n*-alkanes patterns (Meyers and Ishiwatari, 1993). Furthermore, the *n*-alkanes can be found in both modern and fossil plants (Bush and McInerney, 2013; Dubois et al., 2014; Ficken et al., 2000), soils and paleosols (Kuhn et al., 2010), and also sediments (Meyers, 2003; Pu et al., 2017; Zhang et al., 2017). Consequently, the *n*-alkanes are wildly used to classify source of organic matter and to reconstruct the past environment.

The discussion in this chapter can be divided into three parts, i.e. the *n*-alkanes in modern plant samples and sediments, and the environmental reconstruction in Thale Noi.

5.1 Modern leaf plant

5.1.1 Distributions of *n*-alkane in modern leaf plants

For the modern plant samples, the *n*-alkanes distributions in true mangrove plants are diverse patterns including the long-, and short-chain predominance, and the bimodal distribution. The *n*-alkane distribution in *Avicennia marina*, *Rhizophora apiculate*, *Rhizophora mucronate* (KSC) and *Sonneratia caseolaris* are the long-chain predominance that agrees well with those of the previous study by Hogg (1984) (Fig 37). Meanwhile, *Barringtonia asiatica* (TLN), *Bruguiera gymnorrhiza, Rhizophora mucronate* (KKB) and *Sesuvium portulacastrum* are dominated by the short-chain *n*-alkanes. *Barringtonia asiatica* (KKB) however shows the bimodal pattern in the *n*-alkanes distribution.

The *n*-alkanes distributions in back mangrove plants can be divided into the long-chain predominance in *Acrostichum aureum*, and short-chain predominance in *Oncusperma tigllarium* and *Xylocarpus granatum*. Despite Poaceae (*Bambusoideae*) and *Casuarina equisetifolia* can be classified to the mangrove associate plants, their *n*-alkane distributions are different. The long-chain *n*-alkane predominance prevails in Poaceae (*Bambusoideae*), which corresponds well with the previous studies (Bush and McInerney, 2013, 2015; Pu et al., 2017; Rommerskirchen et al., 2006). However, *Casuarina equisetifolia* from KKB is dominated by the short-chain *n*-alkanes, while the sample of the same plant from TLN shows the bimodal distribution.

The analysis of *n*-alkanes distributions in this study leaves two interesting points. Firstly, although the epicuticular wax has been generally considered to produce the long-chain n-alkanes, especially from C_{21} to C_{37}, many plant samples are here dominated by the short-chain *n*-alkanes (Herbin and Robins, 1969; Kolattukudy, 1970; Kuhn et al., 2010; Rao et al., 2011). Secondly, the discrepancies of the *n*-alkanes distribution of the same taxon from the different sits have been found in *Sonneratia caseolaris*, *Rhizophora mucronate, Barringtonia asiatica* and *Casuarina equisetifolia* (Fig 37). This inconsistency can possibly be explained by that not only genetic but also external factors play an important role in the *n*-alkane distribution in the plants (Jia et al., 2015; Liu and Liu, 2016).

The assumption of the environmental control is supported by the similarity of the n-alkanes distribution in different plant group that was taken from the same sites.

Most of samples collected from KSC, which is the intertidal zone, for example, demonstrate the *n*-alkane distribution of the long-chain predominance (Fig. 38). The n-alkanes distributions in *Rhizophora mucronate, Rhizophora apiculate, Avicenia marina* and *Sonneratia caseolaris* consist well with those in Hogg et al. (1988) (Fig. 41). The exception is *Sesuvium portulacastrum*, which is dominated by the short-chain *n*-alkanes for this site (Fig. 38)*.*
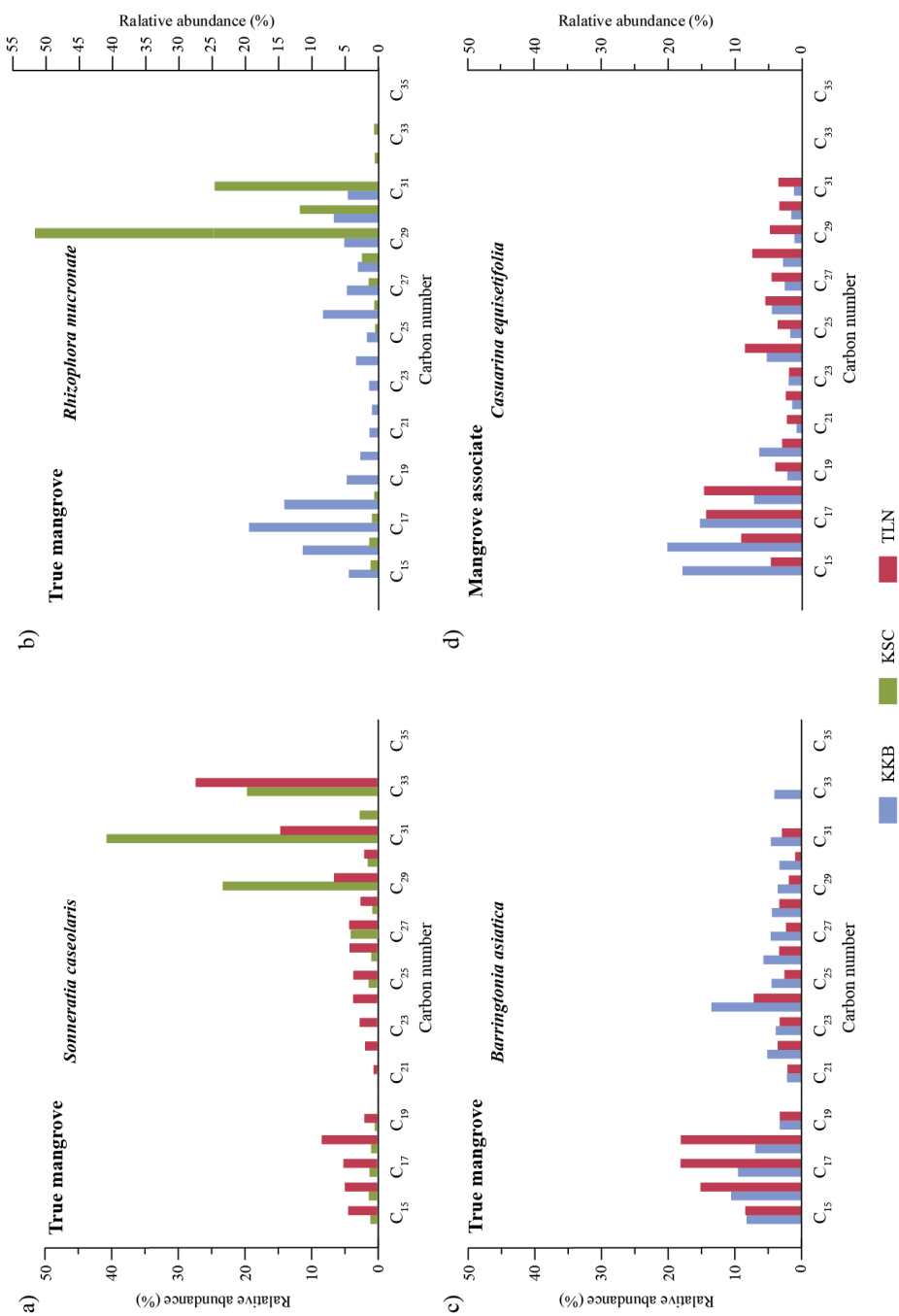
Figure 37 The distributions of n-alkane in same plant species from distinctive sits. The distinctive colored bars represents the plants which collected from distinctive sits; blue bar = Kung Krabaen Bay (KKB), green bar = Khun Samut Chin Temple, and red bar = Thale Noi
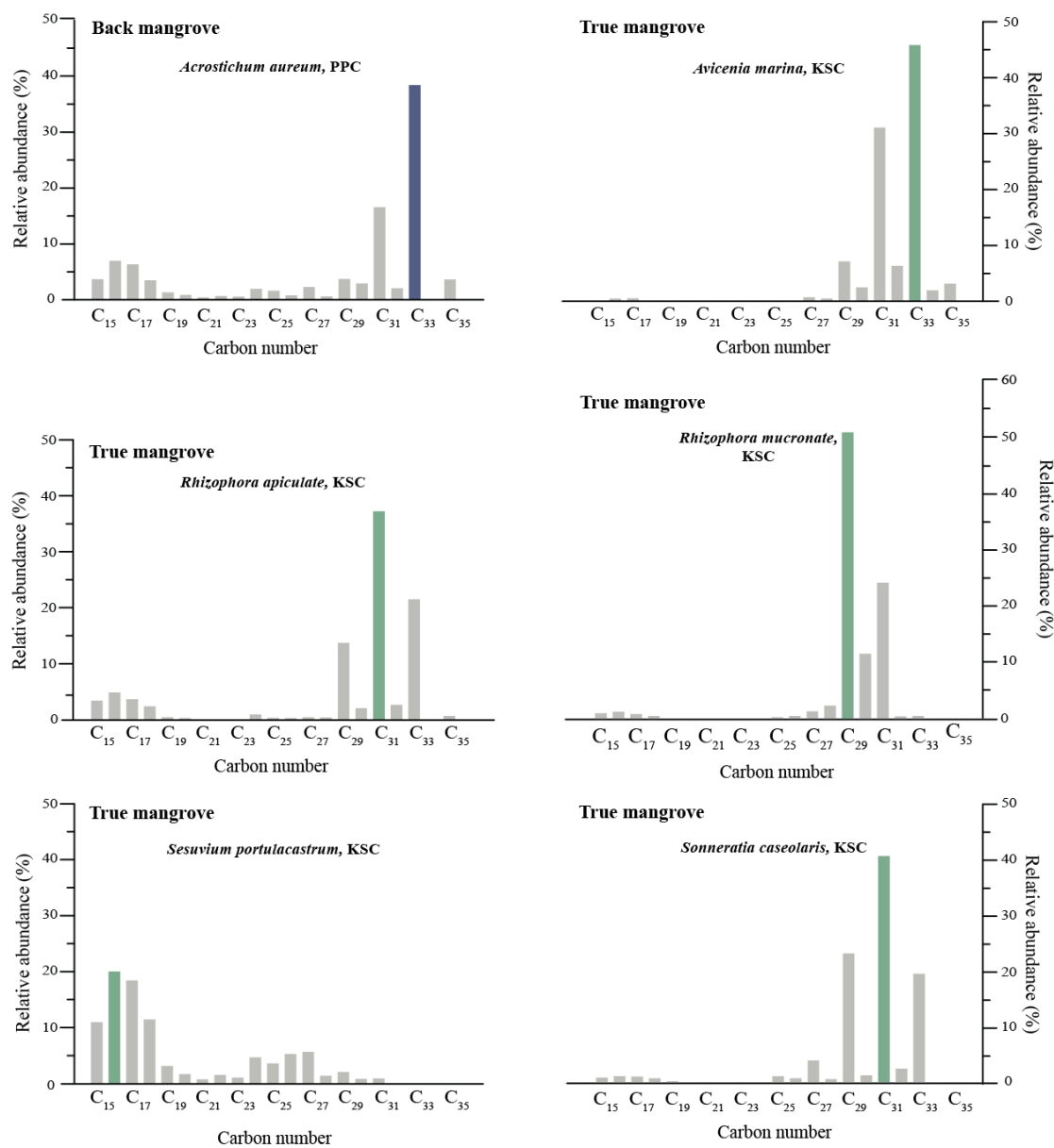
Figure 38 Distributions of *n*-alkane in modern plants, which were collected from Khun Samut Chin Temple (KSC), Samut Prakan Province.
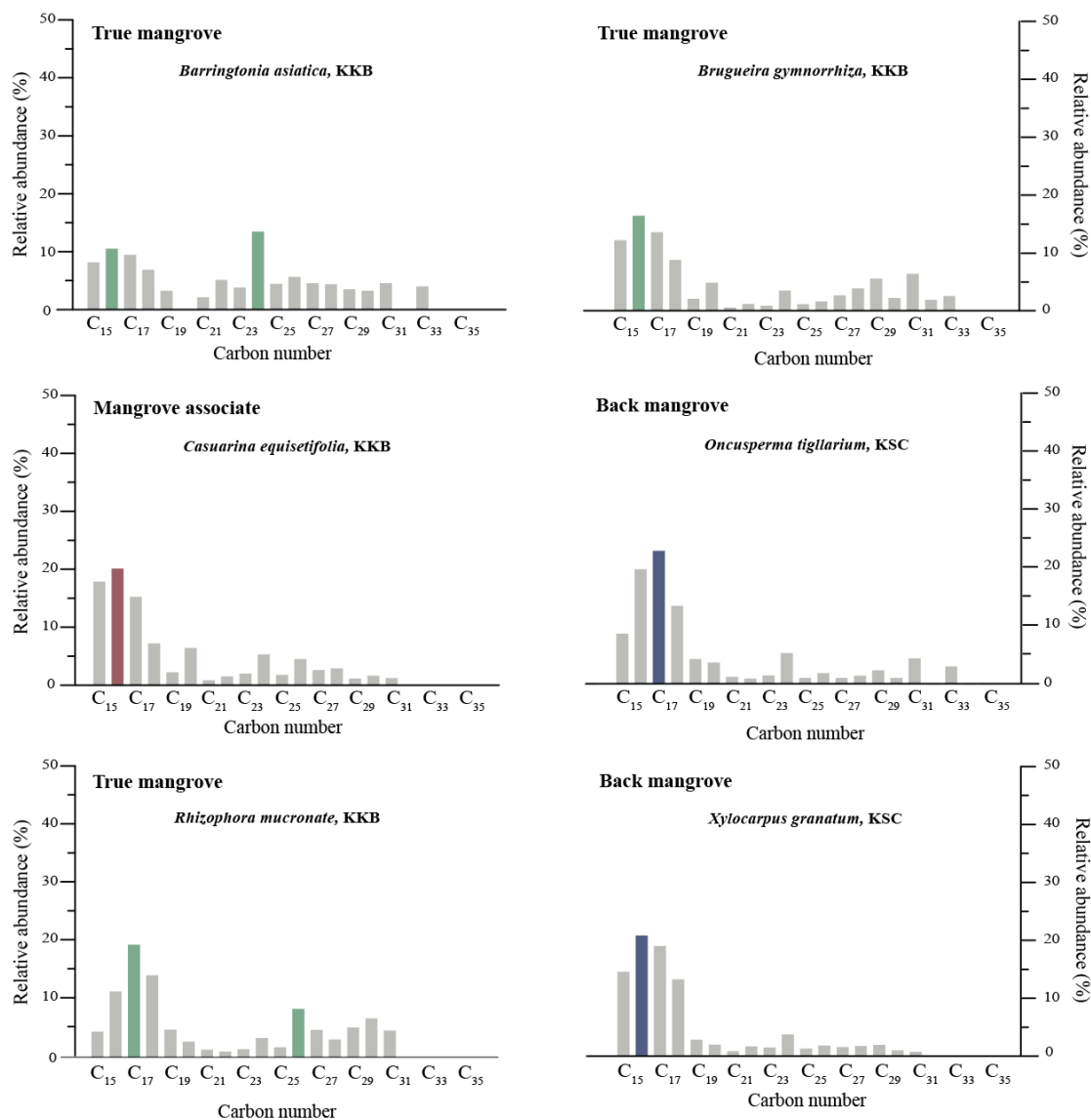
Figure 39 Distributions of *n*-alkane in modern plants, which were collected from Kung Krabaen Bay (KKB), Chantaburi Province.

Another example is the distributions of *n*-alkane in the modern plants taken from KKB, which is the field experiment for mangrove development. The *n*-alkanes distributions in most of the samples from this site are the short-chain predominance, which C_{16} and C_{17} are the most abundant (Fig. 39). The dominance of the short-chain n-alkanes in this experimental field can possibly be explained by the cultivation, such as fertilizers and pesticide (Pitty, 1988).
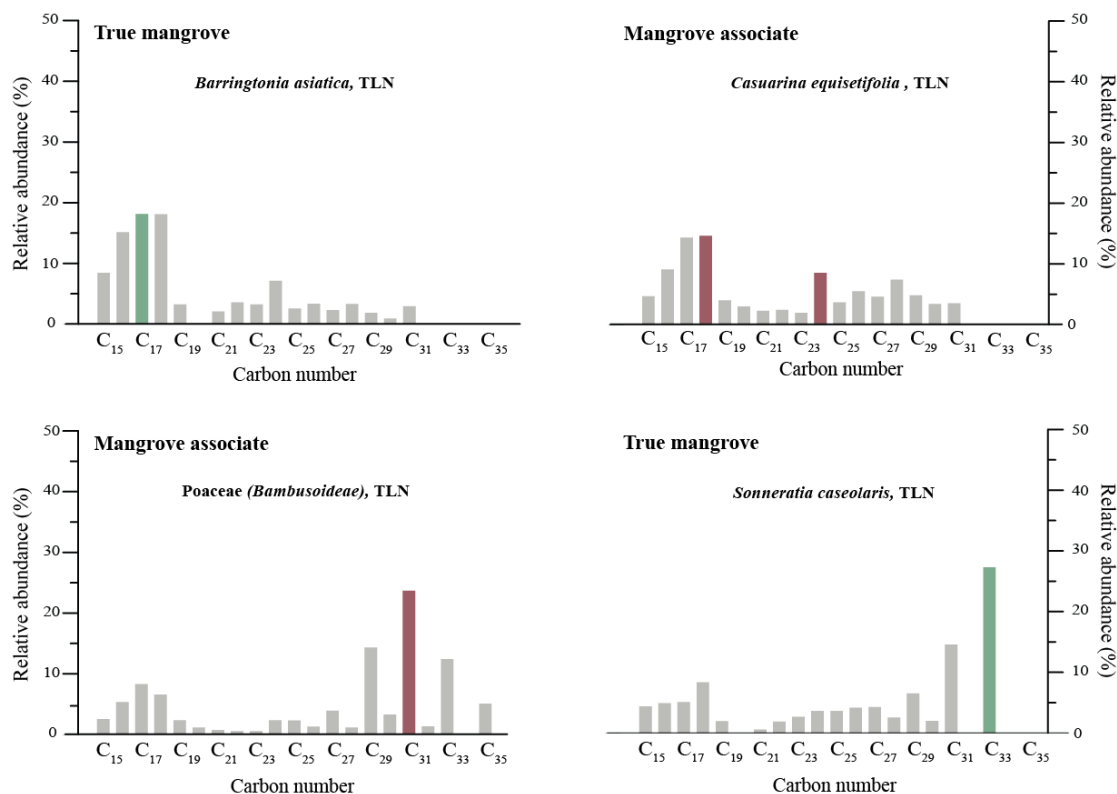
Figure 40 Distributions of *n*-alkane in modern plants, which were collected from Thale Noi (TLN), Phatthalung Province.

However, it is not in all cases that the similar *n*-alkanes distribution can be observed from the same site. The plants were taken from TLN, for example, demonstrate diverse pattern of the *n*-alkane distributions. The distributions of *n*-alkane in Poaceae *(Bambusoideae)* and *Sonneratia caseolaris* are the long-chain predominance that consists well with the previous studies (Bush and McInerney, 2013; Hogg et al., 1988; Rommerskirchen et al., 2006). Bush and McInerney (2013, 2015) suggest that it is difficult to separate grasses from the woody plants since the *n*-alkane are varied in the mangrove associate. Moreover, the n-alkanes distributions in *Barringtonia asiatica* and *Casuarina equisetifolia* are the long-chain predominance and the bimodal distribution, respectively.

The *n*-alkane distributions in the true mangrove plants taken from KSC, KKB, and TLN were further compared with those from Queensland (Hogg et al., 1984) (Fig. 41 to 43). The *n*-alkane distribution patterns in the modern plant from KSC and TLN

agree with Hogg et al (1984) (Fig 41, 42). In contrast, the pattern in the modern plants from KKB is significantly diverse from Hogg et al (1984) (Fig. 43).

These all together also support that the environmental conditions are also an important factor controlling the *n*-alkanes production in the plant epicuticular (Hogg et al., 1988). Despite many studies suggest that a basic genetic potentially controls the composition of the epicuticular wax formation, environmental factors can affect the chemical contents and the specific pattern in some situations (Baker, 1974; Guo et al., 2014; Herbin and Robins, 1969; Pitty, 1988). The environmental factors, e.g. photoperiods, temperature, humidity, and elevation, make a shift in the chain length of the n-alkanes. And each plant responds to the same environmental factors in a different way (Baker, 1974; Maffei et al., 1993; Pitty, 1988; Rao et al., 2011; Wang et al., 2018; Wilkinson, 1972, 1974).
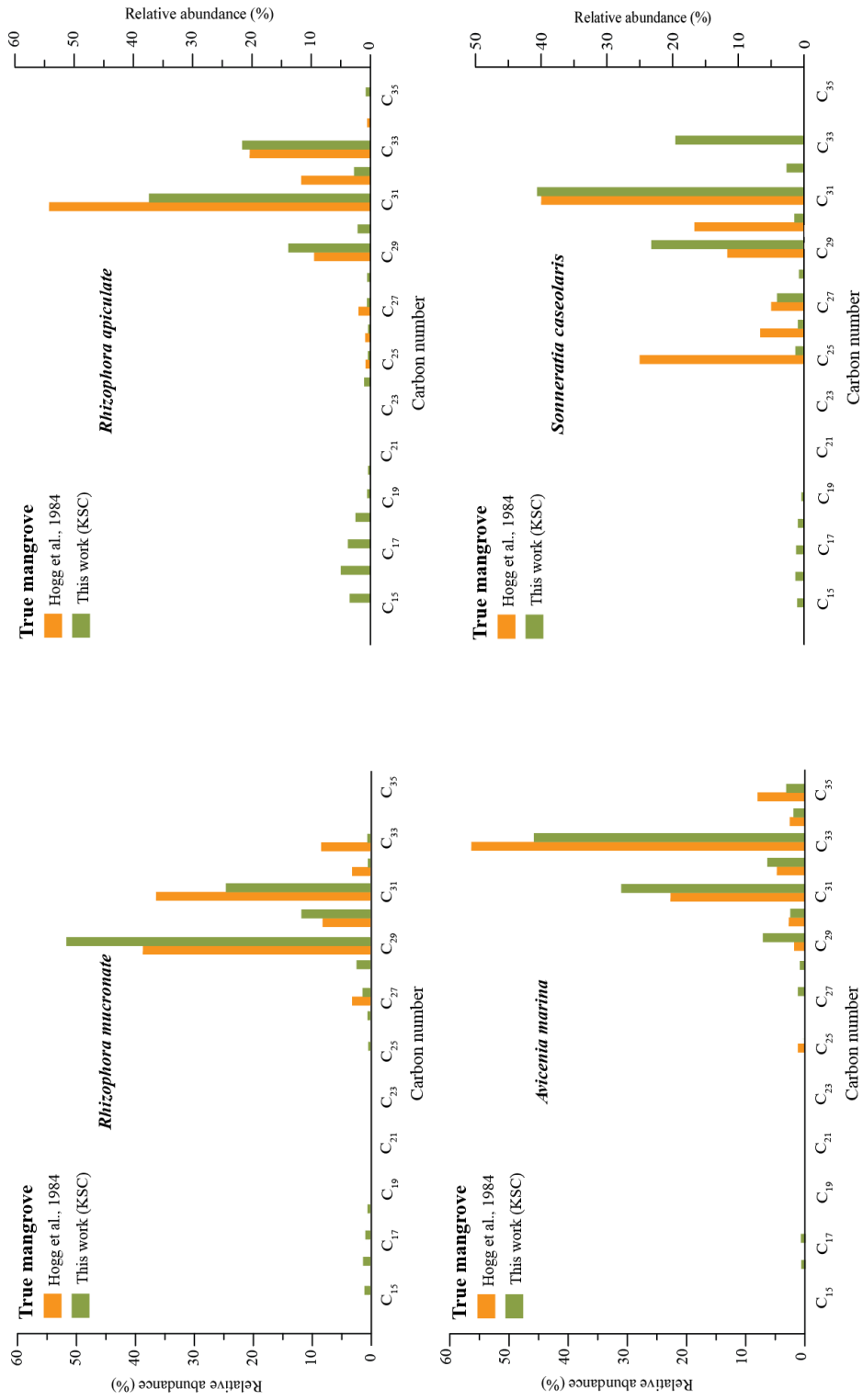
Figure 41 Comparison of similar *n*-alkane distribution between mangrove plants from Khun Samut Chin Temple (KSC) and Hogg et al (1984), including *Rhizophora mucronate, Rhizophora apiculate, Avicenia marina,* and *Sonneratia caseolaris.*
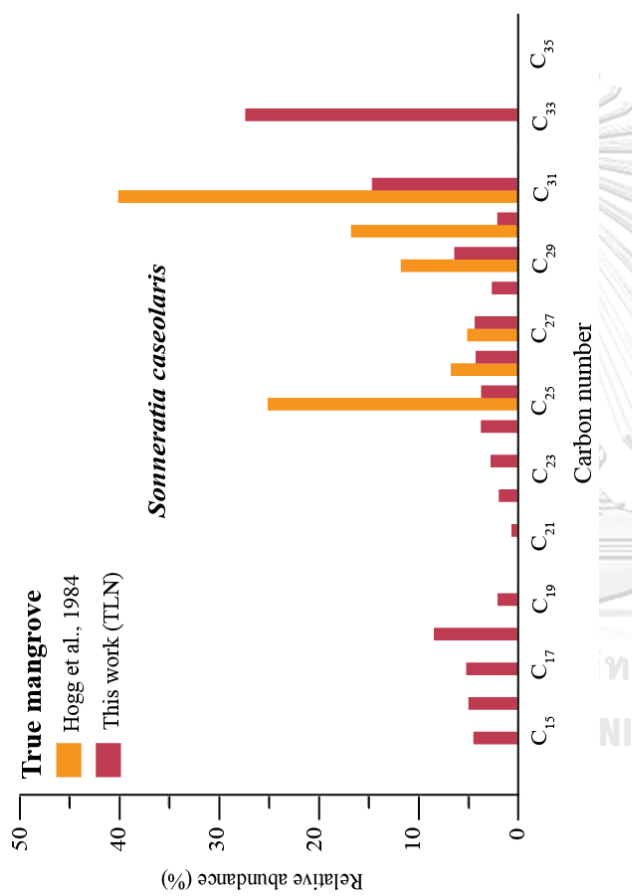
Figure 42 Comparison of similar *n*-alkane distribution between *Sonneratia caseolaris* from Thale Noi (TLN) and (Hogg and Gillan, 1984).
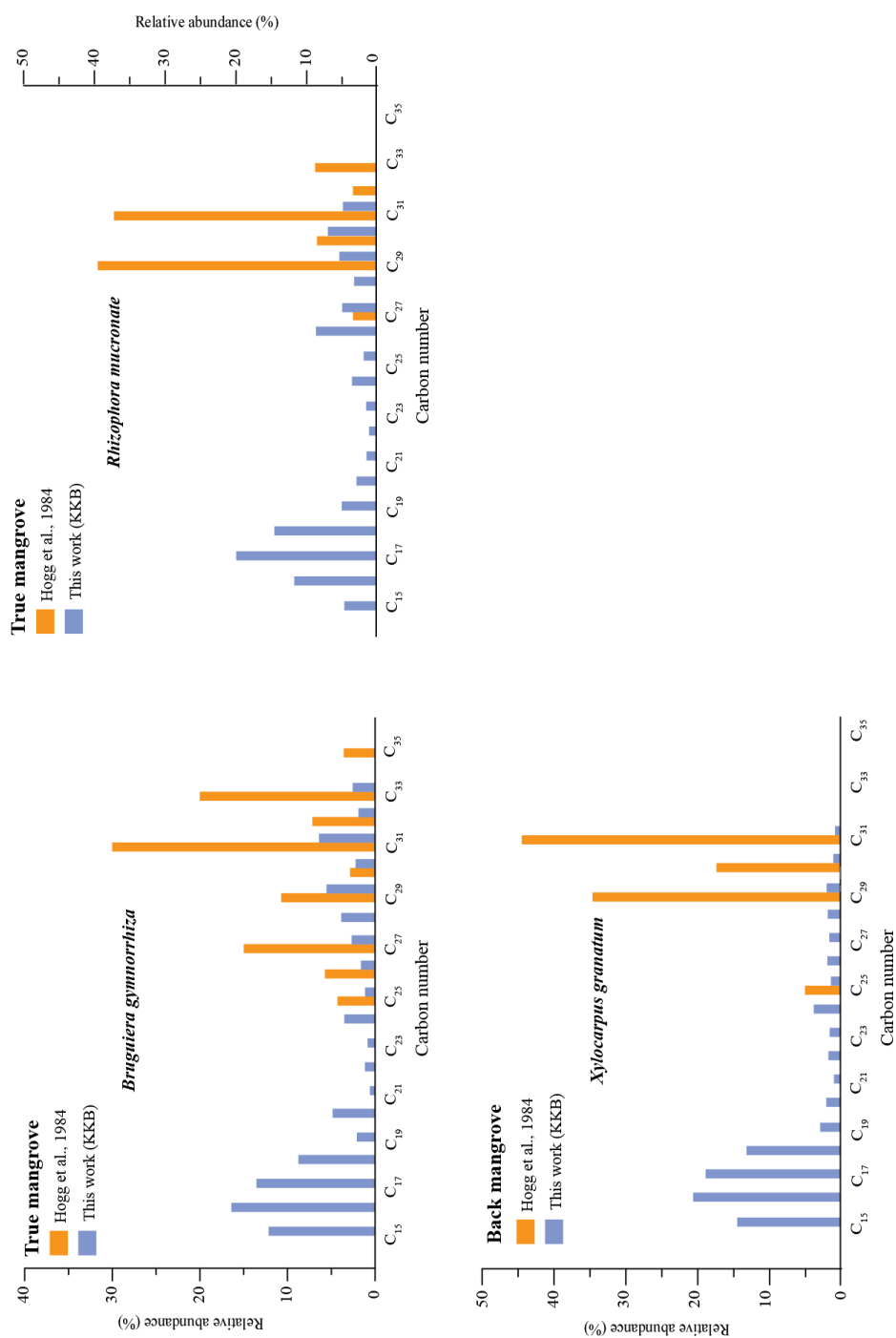
Figure 43 Comparison of dissimilar *n*-alkane distribution between mangrove plants from Kung Krabaen Bay (KKB) and (Hogg and Gillan, 1984), including *Bruguiera gymnorrhiza*, *Rhizophora mucronate*, and *Xylocarpus granatum*.

5.1.2 The average chain length (ACL) and carbon preference index (CPI) in the modern plants

Despite the ACL_T and CPI_T values are diverse in each plant group, these values possibly can be grouped by their locations (Fig. 44). The ACL_T values in the sample taken from KSC, KKB, and TLN are 28.39±4.43, 20.35±1.87, and 24.49±4.45. These results suggest that the long-chain predominance can be observed in the samples from KSC and TLN. However, the ACL_T in the plant samples taken from KKB suggests the predominance of the short-chain *n*-alkanes that consist well with the distribution of the *n*-alkanes in the previous section.

The CPI_T value is obviously different based on the plants sample location. The CPI_T are 5.55±3.54, 0.87±0.09 and 1.80±1.21 in the plant samples taken from KSC, KKB and TLN, respectively. The leaf waxes generally produce CPI value of higher than 1 or the odd over even predominance (OEP) carbon chain length (Bush and McInerney, 2013; Pu et al., 2017). The high CPI values of leaf wax can be explained by the plant physiology (Baker, 1974). The plants growing in the coastal environment, for example, are necessary to produce more leaf wax in order to reduce their transpiration (Rhee et al., 1998). The CPI in the plant samples taken from KSC and TLN suggest that they are the OEP carbon chain length.

However, the CPI value of less than 1 can be found in the samples from KKB. This even over odd predominance (EOP) carbon chain length in leaf waxes are generally explained by a bacteria and fungi contamination or an experimental error owing to the low concentration of *n*-alkanes samples (Herbin and Robins, 1969). During this experiment, the total lipid obtained from *Casuarina equisetifolia* and *Barringtonia asiatica* from KKB and TLN became sticky like gum which is difficult to elute. This is possibly caused by a low concentration of *n*-alkanes and the EOP carbon chain length in these samples. Alternatively, the even over odd predominance (EOP) of carbon chain length can be found in soils, sediments or mature source rocks caused by decomposition or alteration processes (Eglinton and Hamilton, 1967). Some studies suggest that the EOP has been attributed by the highly saline carbonate environments (Dembicki Jr et al., 1976), and anthropogenic fossil fuel pollution (Lichtfouse et al.,1997). Moreover, Kuhn et al. (2009) also report that the productions of the predominance of short-chain *n*-alkanes with EOP carbon chain length can be

observed in the higher plants growing on the biomass burning area. These all together point to another possibility of the growing conditions affected on the production of *n*-alkanes in plants.

Figure 44 demonstrates the scatter plot of ACL_T against CPI_T values based on the sample locations. The samples with low ACL_T values, which range from 18 to 24, are usually low CPI_T of approximately 1 and vice versa. For the modern plant samples taken from KSC, the ACL_T values are slight difference of about 30, while CPI_T values diverse from 1 to 12. However, the ACL_T value of *Sesuvium portulacastrum* from KSC is relatively low compare to those values from other plants. In contrast, the CPI_T values are almost the same of about 1, while ACL_T values are varied from18 to 23. ACL_T and CPI_T can be divided into two groups, i.e. *Casuarina equisetifolia* and *Barringtonia asiatica*, and *Sonneratia caseolaris* and Poaceae (*Bambusoideae*). The CPI_T of lower than 1 can be found in the former plants group. However, the ACL_T of *Casuarina equisetifolia* and *Barringtonia asiatica* are slightly varied of about 21.6 and 19.8, respectively. These values of *Casuarina equisetifolia* and *Barringtonia asiatica* from TLN are comparable with those from KKB. The ACL_T of *Sonneratia caseolaris* and Poaceae (*Bambusoideae*) are almost the same of approximately 28 but CPI_T of these plants are 11.3 and 3.1.

Since the numbers of plant samples are small, the applicable statistic approach on this analysis is possibly not proper. It is a strong suggestion to collect more samples together with diverse plant species for the future study, Alternatively, the chemotaxonomy is necessary to be validated with the other biomarkers, i.e. fatty acids, aldehyde, ketone, alcohol, alkane, etc. It is because the proportion of wax components are distinctively different in each plant species, e.g. a low alkane concentration in sugar cane leaf wax and a high concentration of alkanes in the leaf wax of *Cotyledon orbicularis* (Eglinton and Hamilton, 1967). Fatty acids and fatty acid-derived compounds are major compositions in Geranium and Erodium, therefore, they were used as a marker in the intergeneric (Herbin and Robins, 1969; Hogg and Gillan, 1984; Vogts et al., 2009), etc. Despite the chemotaxonomy based on the *n*-alkanes distributions are possibly not work in all species (Vogts et al., 2009), the *n*-

alkanes have been appropriately applied for paleoenvironmental reconstruction owing to their high resistance (Bush and McInerney, 2013).
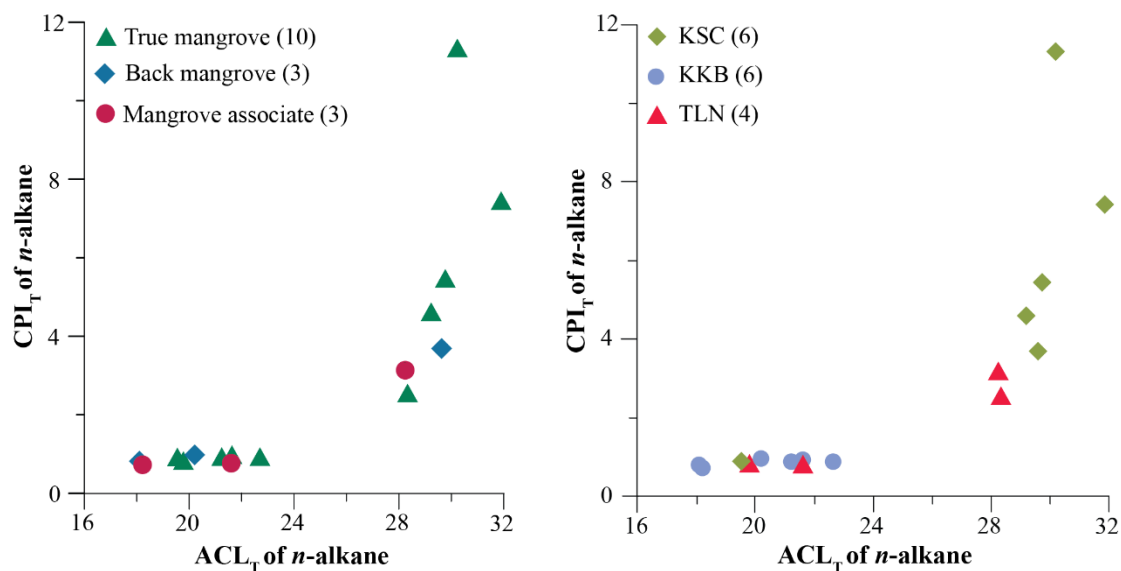
Figure 44 Scatter plots of ACL_T versus CPI_T of *n*-alkane in modern plants based on plant groups (left) and locations (right).

5.2 Sediment

5.2.1 Distributions of *n*-alkane in sediment

The long-chain *n*-alkanes (C_{21} to C_{35}) in epicuticular waxes of leaves are generally produced by higher plants and highly resistant to microbial degradation after deposition. Consequently, the *n*-alkanes ranging from C_{21} to C_{35} in sediments from Thale Noi were here focused. The *n*-alkanes in the modern plants were subsequently compared with those in the sediment successions TLN-CP5 and TLN-CP7 in order to assess the environmental history in Thale Noi.

The n-alkane distributions in the sediment from core TLN-CP5

The sediment core TLN-CP5 was taken from the western sub-basin of Thale Noi. Yoojam (2015) constructed the lithostratigraphy of this core. The grain-sized distribution and loss on ignition were further analyzed by Phountong (2016), and

pollen analysis was studied by Nudnara (2016). These results are discussed together with the *n*-alkanes analysis in this section.

C_{28} is the most abundant *n*-alkanes in the lowermost layer of core TLN-CP5, which is a stiff light grey clay of unit A (Fig. 21). A high concentration of C_{28} is possibly derived from non-photosynthetic bacteria (Tanner et al., 2007; Tanner et al., 2010) in a deep water environment. This unit is a barren zone of pollen (Nudnara, 2016). But it is partly similar with the intertidal sediments based on Chaimanee et al. (1985). These all together suggest that Thale Noi was under flooding.

The most abundant *n*-alkanes in unit B are C_{25}, C_{29} and C_{31} (at 360, 350 and 340 cm depth below water surface, respectively). The predominance of the long-chained n-alkanes suggests that their provenances are from higher plants (Ficken et al., 2000; Pu et al., 2017; Ratnayake et al., 2017). According to the loss on ignition, the dark grey clay of unit B consists of slightly higher organic matter content than those in unit A (Phountong, 2016).

However, the sediment sample at 360 cm depth below water surface is dominance of C_{25}, which was not found its dominant in the modern plant samples. This depth is also a barren zone of pollen (Nudnara, 2016). These all together possibly suggest that C_{25} is originated from other plants that do not include in this study. Since the high runoff can be reconstructed based on grain size analysis, the organic matter with dominated C_{25} was transported to the site (Phountong, 2016).

The most abundant *n*-alkane in the sample at 350 cm depth below water surface is C_{29}, which is resembled with *Rhizophora mucronate* from KSC (Fig. 22). However, *Brugueira, Rhizophora, Stenochlaena,* and *Acrostichum* have been found in pollen analysis at this depth (Nudnara, 2016). *Brugueira, Rhizophora* and *Stenochlaena* are the true mangrove plants. Their concentration is much higher that of *Acrostichum*, which is the back mangrove plant. Consequently, the mangrove plants are a possibly major source of C_{29}.

C_{31} is the most abundant in a sample at 340 cm depth below water surface. This n-alkane is the main peak in *Brugueira* and *Rhizophora apiculate*, which are the mangrove plants. However, the most abundance pollen at this depth is *Acrostichum*, which is about 80%. Despite the main peak of *Acrostichum* is C_{33}, C_{31} has been found in a high concentration. Therefore, C_{31} is here supposed to be produced by both the

mangrove and back mangrove plants. The dominant of C_{31} possibly indicate shrinkage of mangrove forest and expansion of back mangrove comparing to the preceding sample at 350 cm depth below water surface.

C_{31} is also predominance in the samples at 330, 320 and 310 cm depth below water surface of unit C, and at 290, 280 and 270 cm depth below water surface of unit D-1 reflecting a presence of both mangrove and back mangrove plants. Pollen records also suggest the dominance of back mangrove plants from 340 to 330 cm depth below water surface and mangrove plants from 310 to 270 cm depth below water surface (Nudnara, 2016).

The sample at 300 cm depth below water surface is near a boundary between unit C and D at about 298.5 cm depth below water surface, which expected to be a hiatus by Phountong (2016). Despite *Rhizophora* is the highest pollen concentration in this sample, the most abundant n-alkane is C_{27}, which C_{27} is not significantly recognized in the modern plant analysis (Nudnara, 2016). Since C_{27} has generally considered being produced by the terrestrial plant, this alkane is possibly coming from the vegetation that is not including in this study (Bush and McInerney, 2013; Meyers, 1997).

The concentration of C_{21}, which is mainly originated from aquatic plants, is remarkably high in the samples from 260 to 240 cm depth below water surface (unit D-2) (Ficken et al., 2000). However, C_{21} has been found in the very low concentration in all the modern plant samples. This depth has been considered to be an abundance of mangrove plants in regarding to the pollen analysis (Nudnara, 2016). The limited number of data in this study cannot explain these discrepancies between *n*-alkanes and pollen analysis. However, the prevailing C_{21} was here hypothesized that it was transported from the wetland further in the coastal zone.

The *n*-alkane distribution in the sediment at 230 cm depth below water surface is dominated by C_{26}, which is the even carbon number and inconsistent with the modern plant sample analysis. The predominance of the even carbon number in *n*-alkanes is possibly caused by either decomposition of the organic matter due to microbial activities (Reddy et al., 2000). However, pollen records indicate a dominant of mangrove forest and a stillstand of sea level at this depth (Nudnara et al., 2016).

The further investigations for the even carbon number *n*-alkanes, therefore, are necessitated.

C$_{31}$ become again predominance from 220 to 190 cm depth below water surface that agrees well with the abundance of *Rhizophora* in the pollen analysis (Nudnara, 2016). The C$_{27}$ was replaced from 190 to 155 cm depth below water surface indicating woody or tree abundance. The sediments of the middle to the uppermost of unit E have C$_{27}$ predominance, indicating woody or tree abundance. This result compares well with the occupation of Poaceae in the pollen stratigraphy (Nudnara, 2016), and increase in runoff into the lake (Phountong, 2016).
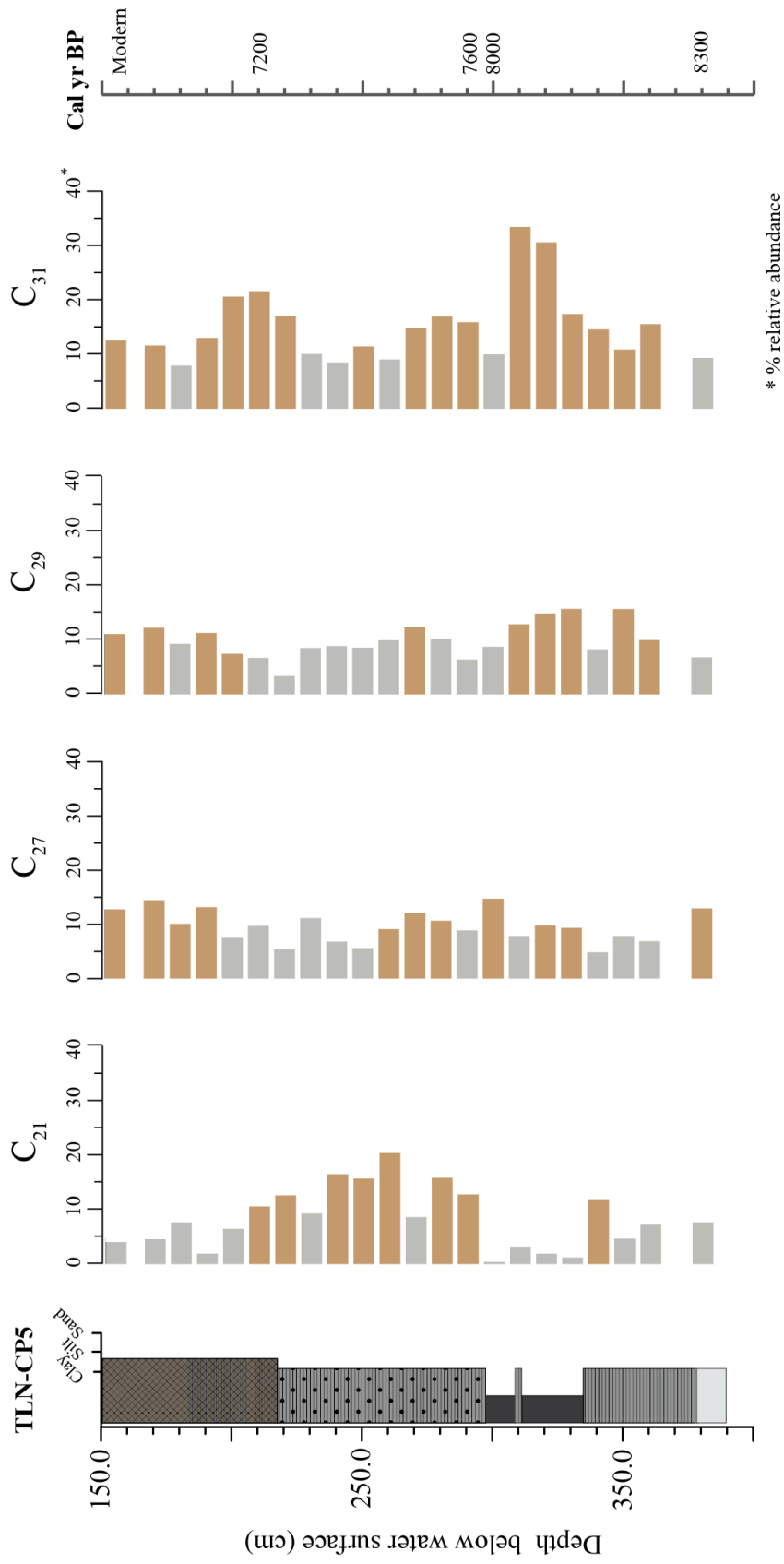
Figure 45 Distributions of *n*-alkane in sediment from TLN-CP5 along with age depth. Lithostratigraphy reported by Yoojam (2015). And age depth reported by Phountong (2016).

The n-alkane distributions in the sediment from core TLN-CP7

TLN-CP7 is a sediment core, which was taken from the eastern part of Thale Noi. This core consists of three sediment units, i.e. unit C*, D and E from bottom to top. The lithostratigraphy for this core was constructed by Yoojam (2015).

The compacted peat of unit C* at 437 cm depth below water surface is dominated by C_{29}, which is generally produced by the terrestrial plants（Meyers and Ishiwatari, 1993）. However, the modern plant samples together with the interpretation with pollen analysis in core TLN-CP5 suggest that C_{29} is the dominant peak in *Rhizophora mucronate* and/or mainly produced by the mangrove plants. This sediment layer is therefore presumed to deposit under the intertidal environment. The C_{21} is the most abundant in the sediment unit D from 433 to 320 cm depth below water surface. According to the interpretation in core TLN-CP5, the C_{21} is mainly produced by the higher plant and transports to the lake. Consequently, the dominance of indicates an increase in runoff to the lake. This high runoff period was possibly interrupted by an environmental shift between 410 and 380 cm depth below water surface in regarding to the predominance of the even carbon number of C_{26} and C_{24}. The abundance of the even carbon number in *n*-alkanes (C_{12} - C_{26}) is present in lacustrine sediments and coastal soils (Ekpo et al., 2005). However, C_{24} was possibly derived from *Xylocarpus granatum*, which their pollens were found in the lowermost of unit D from TLN-CP5. However, the limited information here does not allow us to specify the source of these even number *n*-alkanes.

The environment fluctuations can be observed between 300 and 160 cm depth below water surface, since the carbon numbers in the *n*-alkanes are varied from C_{24} to C_{29}. The even carbon number of C_{26} and C_{24} are again dominance at 300, 260 and 200 cm depth below water surface, and 190 cm depth below water surface, respectively. The abundance of C_{26} suggests microorganism presence. The predominance of these even carbon numbers in sediments has been attributed to special sources found under different conditions or its microbial alteration (Wang et al., 2010). The odd carbon number of C_{27} and C_{29} are abundance at 240, 170 and 160 cm depth below water surface, and 280, 220, and 180 cm depth below water surface. The C_{27} and C_{29} are mainly produced by terrestrial plants. According to the *n*-alkane in modern plants and

the interpretation in core TLN-CP5, C_{29} is here possibly obtained from *Rhizophora* and indicate the intertidal environment. However, C_{27} in the samples from 170 to 160 cm depth below water surface is more likely to be originated from the terrestrial plants since it can be correlated well with those in core TLN-CP5. Alternatively, the *n*-alkane distribution at 160 cm depth below water surface shows the odd carbon number predominance (C_{23}, C_{25}, C_{27} C_{29}) which also possibly reflects the combination of organic matter inputs (Pearson et al., 2007).
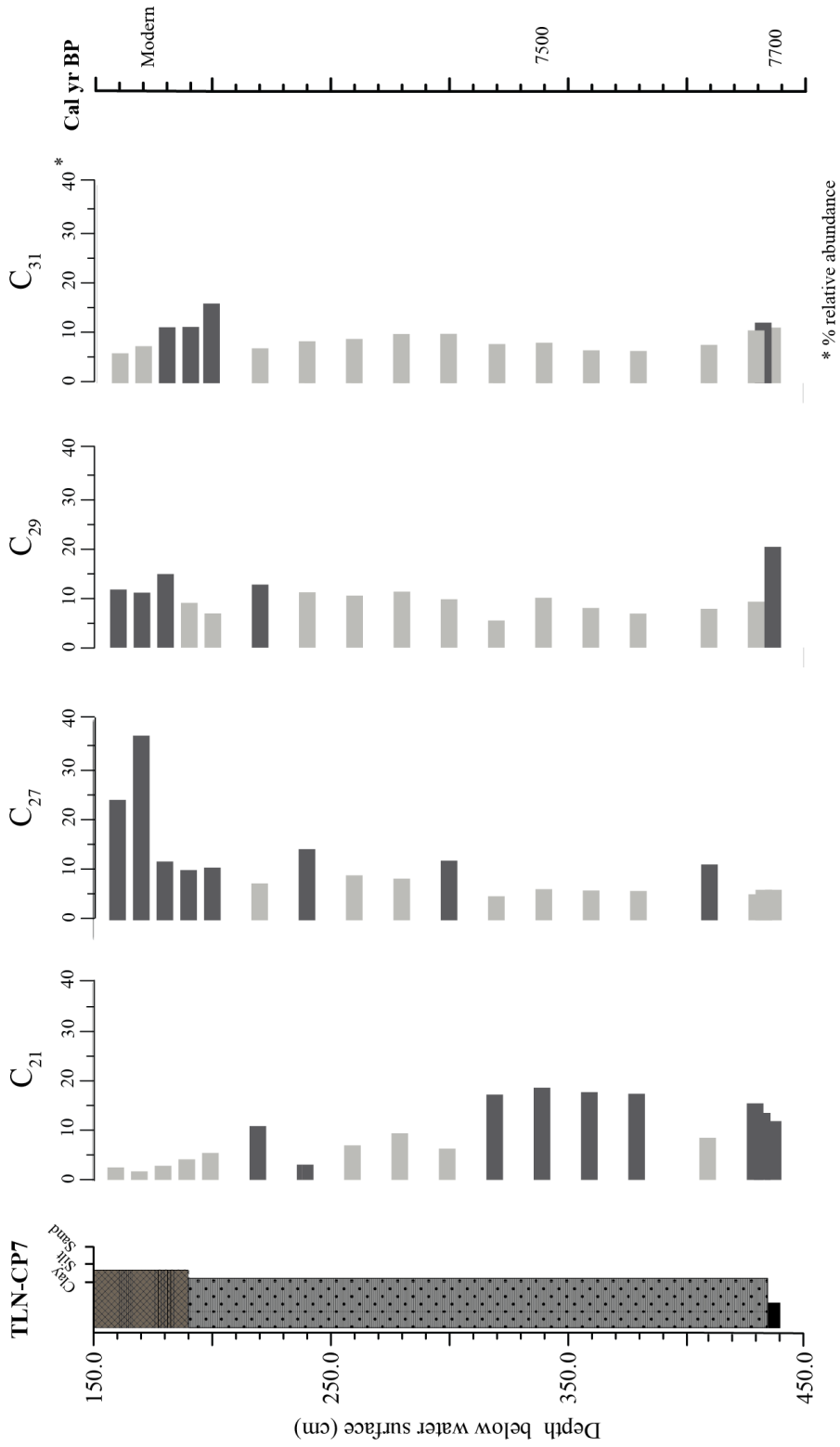
Figure 46 Distributions of *n*-alkane in sediment from TLN-CP7 along with age depth. Lithostratigraphy reported by Yoojam (2015).
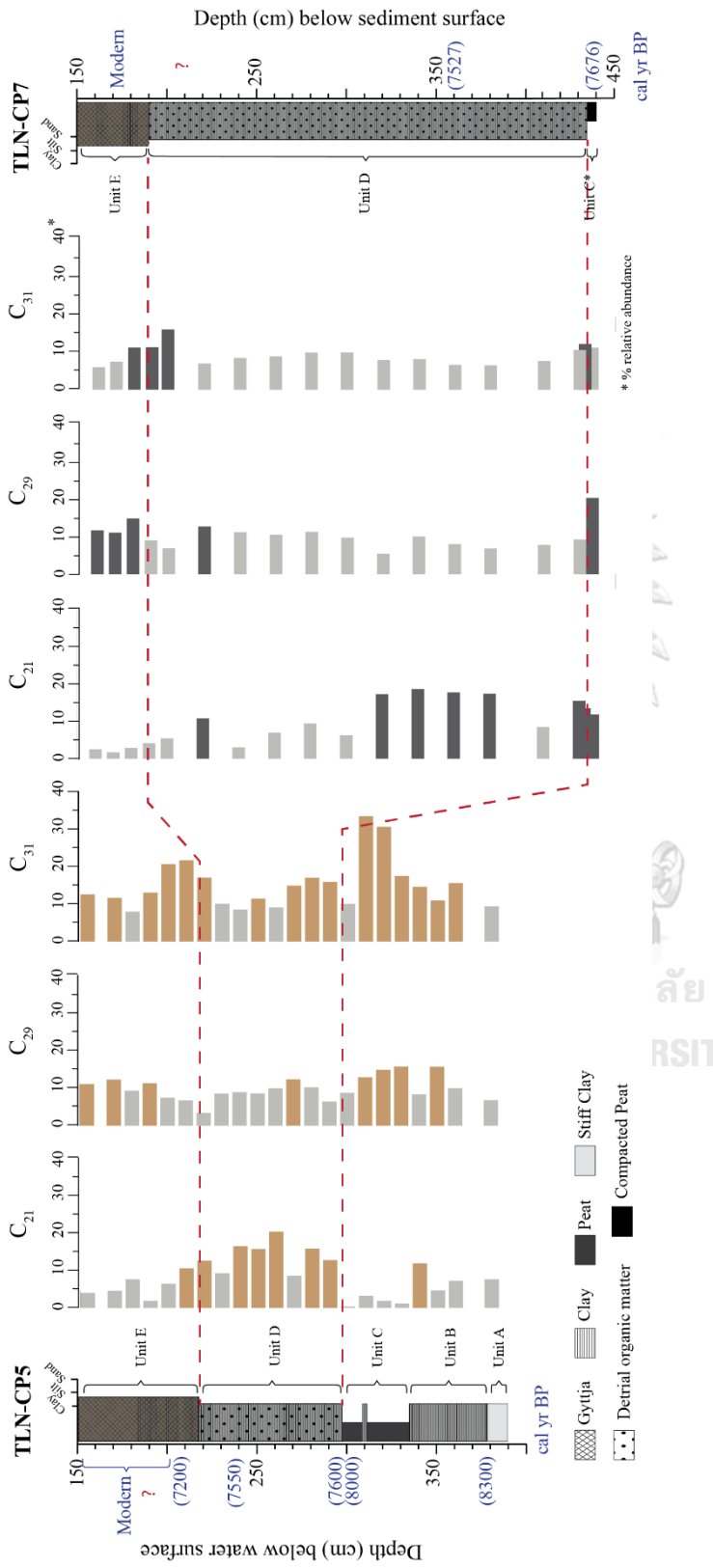
Figure 47 Correlation of distribution of C_{21}, C_{29}, and C_{31} chain length in sediments between TLN-CP5 and TLN-CP7 based on sedimentary unit.

5.2.2 The average chain length (ACL), carbon preference index (CPI), and proportion of aquatic plants (P_{aq}) in sediment

In general, the average chain length (ACL) values can be used to indicate types of vegetation and organism (Andersson et al., 2011; Pu et al., 2017). The recent studies including our modern plant samples suggest that the ACL is not the good biomarkers for chemotaxonomy because this parameter is possibly affected by growing environment (Maffei et al., 1993; Rao et al., 2011). In the current study, ACL_{21-35} in sediments were calculated to compare with those in the modern plants in order to examine the origin of organic matters in Thale Noi (Bush and McInerney, 2013; Pu et al., 2017).

However, the ACL_{21-35} ranges in the cores TLN-CP5 and TLN-CP7 are similar with those values from the modern plants. This result suggests that the plants surrounding the lake are the major sources of the organic matter (Meyers, 1997; Pu et al., 2017). Nevertheless, the classification of plant group based on only the ACL_{21-35} is very difficult. The ACL_{21-35} in *Sesuvium portulacastrum* and *Casuarina equisetifolia*, which is a true mangrove and mangrove associate plants, for example, are approximately 26. Meyers and Ishiwatari (1993), and Ficken et al. (2000) suggest that ACL_{21-35} values of lower than 20, from 21 to 25, and higher than 27 correspond to microorganisms, aquatic plants, and land plants, respectively.

The ACL_{21-35} in TLN-CP5 are gradually increased from the bottom of unit A to the top of unit C. Then they gradually decrease to the middle of unit D and subsequently, the values rise from the middle of unit D to unit E. The uppermost of unit E have a lower value than the previous layer.

The ACL_{21-35} values in the TLN-CP7 are similar to the ACL_{21-35} in unit D of TLN-CP5. The ACL_{21-35} are gradually fallen from the lowermost of unit C* to the middle of unit D and subsequently increase from the middle to the uppermost of unit D. Then they decrease again in unit E.

In sediments, CPI is used to indicate the diagenesis of straight-chain lipid hydrocarbon by microbial organism (Meyers and Ishiwatari, 1993). The CPI value of higher than 1.5, about 1, and less than 1 correspond to plant wax, marine microorganisms, and petroleum residue contaminations, respectively (Kennicutt et al., 1987).

The CPI_{21-35} values from sediment samples are relatively low compared to those in the modern plants. This can be explained by the complicate decomposition pathways in the sediment (Meyers, 1997). However, the corresponding of CPI_{21-35} is ACL_{21-35} suggest that the CPI_{21-35} is possibly response to the environmental changes. The sediment in TLN-CP5 shows a fluctuation of CPI_{21-35} in sediment unit A to C. The exception is at 310 cm depth below water surface that CPI_{21-35} increase and reach its maximum of 3.2 that suggest a rapid accumulation rate or a low decomposition rate of organic matter. This parameter becomes a similar pattern to the ACL_{21-35} variation in the sediment unit D and E.

The proportion of aquatic plant component (P_{aq}) is a biomarker parameter, which is used to distinguish land plant from aquatic plants in freshwater lakes (Andersson et al., 2011). According to Ficken et al. (2000), the P_{aq} value of less than 0.1 indicates the terrestrial plants. The P_{aq} value from 0.1 to 0.4 corresponds to the emergent plants, wetland plants or long-shore plants. And P_{aq} value from 0.4 to 1 represent the submerge/floating macrophytes (Ficken et al., 2000). In addition, this mediate P_{aq} value possibly corresponds to a mixed supply from terrestrial, emergent and submerged/floating plants (Ficken et al., 2000). Furthermore, some studies, P_{aq} value has been used to reconstruct the past water levels in peat bogs (Zheng et al., 2007). The predominance of emergent and submerged/floating plants can be used to consider water level of the lake, emergent plants grow well in the shallow lake because emergent plants are rooted in the lake bottom. Therefore, the shallow lake is possibly dominated by both emergent and floating plants, whereas, the deep lake could be dominated by floating plants.

The P_{aq} is always opposing to the ACL_{21-35} and CPI_{21-35}. The P_{aq} in most of the sediments from TLN-CP5 is about 0.1 to 0.4, representing mixed input from diverse plant groups. However, a low P_{aq} of about 0.1 can be found in the sample from 290 to 340 cm depth below water surface that relate to land plants. The dominant terrestrial plants correspond with the results from the *n*-alkane distribution and ACL_{21-35}. Moreover, P_{aq} reached its maximum value of 0.67 in the uppermost layer of TLN-CP7 suggest that the submerge or floating plants are abundance corresponding to the recent conditions of Thale Noi, which is a freshwater swamp.
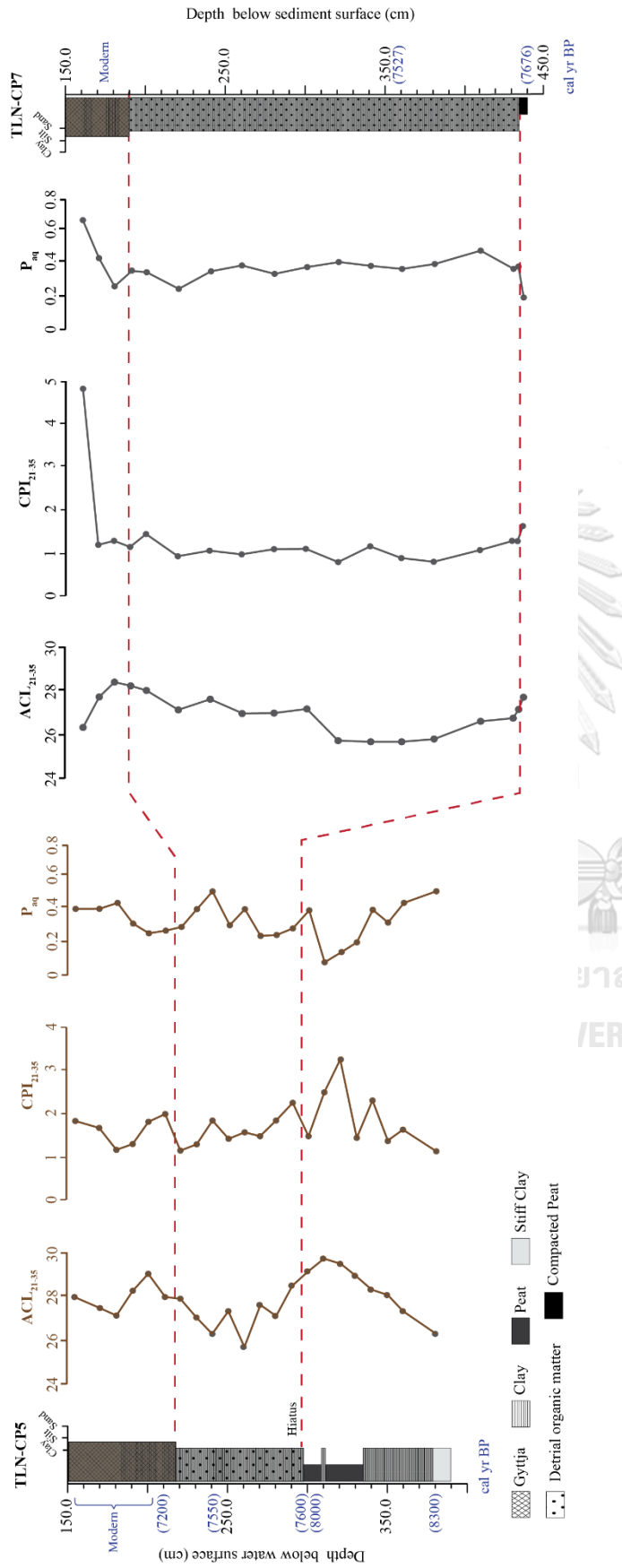
Figure 48 Correlation of ACL$_{21-35}$, CPI$_{21-35}$, and P$_{aq}$ in sediment between TLN-CP5 and TLN-CP7. Lithostratigraphy reported by Yoojam (2015). And age depth of TLN-CP5 reported by Phountong (2016).
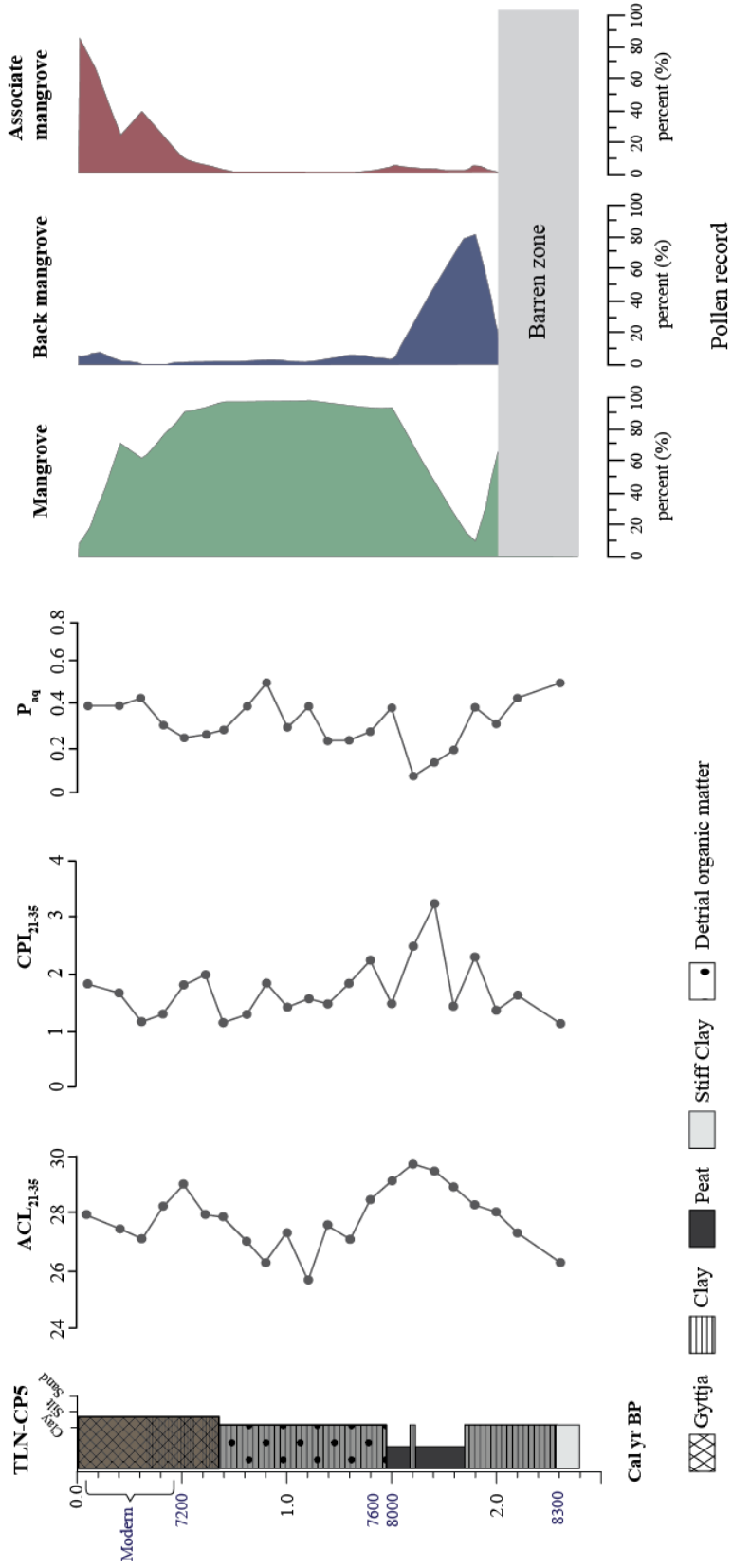
Figure 49 ACL_{21-35}, CPI_{21-35}, and P_{aq} along with age depth of TLN-CP5 compare the pollen record (Nudnara, 2016)

5.3 Environmental reconstruction in Thale Noi

The results of *n*-alkane biomarker analysis along with ^{14}C AMS dating of TLN-CP5 (Phountong, 2016), it shows the environmental change in Thale Noi during the Holocene. Before 8,300 cal yr BP, C_{28} is the most abundant in the sediment that possibly derived from non-photosynthetic bacteria (Tanner et al., 2010), suggesting a deepwater environment, in accord with pollen disappearance (Nudnara, 2016). Consequently, we speculate that is possible the whole area was covered by a high sea level (Nudnara, 2016; Phountong, 2016). Otherwise, several studies reported the transgression in the Gulf of Thailand at about 8,500 yr BP (Chaimanee et al., 1986; Horton et al., 2005).

After 8,300 cal yr BP, the $ACL_{21-35,}$ and CPI_{21-35} values increased gradually, while P_{aq} values decreased until about 8,100 cal yr BP, suggesting that the sea level gradually decline which relate to the presence of back mangrove (Nudnara, 2016). But Horton et al (2005) reported that during about 8,420 – 8,190 cal yr BP, true mangrove pollen predominance, representing the sea level transgression.

About 8,100 – 8,000 cal yr BP, sediments in TLN-CP5 are dominated by $C_{27,}$ $C_{29,}$ and C_{31} that is the representative of a woody plant. That corresponding to the high concentration of true mangrove pollen taxa (Nudnara, 2016). A hiatus presents at 298 cm depth below water surface in the TLN-CP5, it approximately extended from 8,000 – 7,600 for 400 years (Phountong, 2016). Subsequently, a transgression had begun at about 7,600 – 7,500 cal yr BP based on the *n*-alkane distribution (Fig. 45), and their parameters (Fig. 48). In addition to *Rhizophora and Brugeuira* pollens were vast dominant in western sub-basin (Nudnara, 2016). On the other hand, Horton et al (2005) reported that regression had begun at about 7,880 – 7,680 cal yr BP.

Freshwater more supplied into the lake meanwhile effect of sea level was decline, according to the change from C_{31} to C_{21} are consistent with the decreased ACL_{21-35} while P_{aq} is increased. They suggest that aquatic macrophytes are widely predominant during 7,500 – 7,200 cal yr BP. About 7,200 cal yr BP, C_{21} turn to C_{31} again that represent freshwater supply was gradually declining to correspond to the increased ACL_{21-35} and decreased P_{aq}. Accordingly, the concentration of freshwater pollens can support the regression of sea level (Nudnara, 2016).

The shift from C_{31} to C_{27}, the increased ACL_{21-35} and the highest CPI_{21-35} refer to the continental environment. Likewise, constantly P_{aq} which indicate a mixture of aquatic and mangrove associate after 7,200 cal yr BP to recent. These suggest freshwater swamp in the recent.

a) Before 8,300 cal yr BP

b) 8,300 to 7,600 cal yr BP
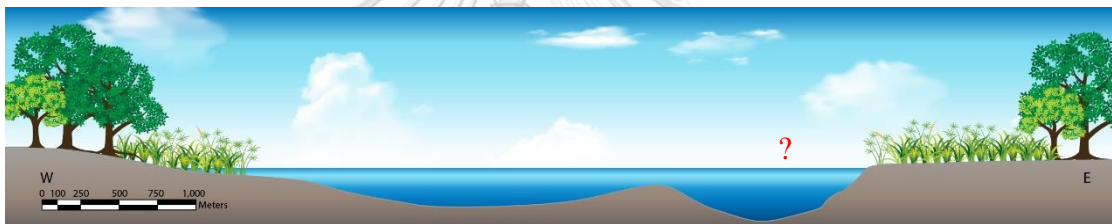
c) 7,600 to 7,200 cal yr BP

d) Recent

Figure 50 Paleoenvironmental change around Thale Noi during 8,300 cal yr BP to recent based on biomarker.

CHAPTER VI
CONCLUSION

6.1 Conclusions

This study has analyzed the *n*-alkane distributions and generality of *n*-alkane parameters in the leaf waxes of 16 recent plant samples (12 species) from Kung Krabaen Bay Royal Development Study Center (KKB), Chantaburi Province, Khun Samut Chin Temple (KSC), Samut Prakan Province, and Thale Noi (TLN), Phatthalung Province. All these plant samples are mangrove forest which reflects the sea level fluctuation and environmental change. The mangrove plants were separated into true mangrove, back mangrove, and mangrove associate based on mangrove zonation (Kamaludin et al., 1988). We expected plants in each group to create a similar *n*-alkane and the characteristic of *n*-alkane in each group will be a biomarker for the chemotaxonomy. And the *n*-alkane can be applied in reconstructing the paleoenvironment. As the results we, therefore, concluded as follows: (Pitty, 1988)

- Despite the *n*-alkanes distribution and their parameters in the modern plant leaves are generally similar in the same species, the shift in the *n*-alkane distributions can be found in some species. These discrepancies can possibly explained by the influence of their local environments.

- The species of modern plant samples in this study are quite multitudinous, there are diverse species. The only *n*-alkane is not a potential biomarker for every plant species. Consequently, the *n*-alkane distribution, average chain length (ACL), and carbon preference index (CPI) cannot be used to classify the modern plant into the groups of mangrove zonation.

- The database of *n*-alkanes distribution derived from mangrove forest around the gulf of Thailand has been report in detail in the Appendix B.

And further analyzed the *n*-alkane distributions and generality of *n*-alkane parameters in 22 and 18 sediment samples from TLN-CP5 and TLN-CP7, respectively at Thale Noi and compared them with *n*-alkane of modern plants in order

to identify vegetation types of organic matters in the lake. Conclusion, our findings and their significance here:

- First, the results illustrate that the n-alkanes in the lake sediments of Thale Noi derive from mixture sources and they reflect environmental changes.
- Second, the major sources of organic matter are derived from surrounding plants, but the n-alkane in sediments cannot be used to accurately interpret as expected plant species (true mangrove, back mangrove, and mangrove associate) because of their biochemical processes. However, they can be used to classify as vegetation types (aquatic plant or terrestrial) which leading to sea level or water inpretation.
- The last one ACL, CPI and P_{aq} values that are a good proxy, reflecting the organic matter types.

This study demonstrates that relationship of the n-alkanes distributions between modern plants and lake sediments is complicated. Because n-alkanes of lake sediment are the mixture sources, not only plant and their geo-biochemical processes. In addition to growing environment of modern plant and fossil plants are different. Consequently, n-alkane of both cannot use to compare each other. However, the advantage of using n-alkane and their parameters is that they can provide comprehensive information for the environmental reconstruction.

6.2 Suggestion and recommendation

Since the proportion of components in the wax is different in each plant species, therefore, more than one compound should be used for chemotaxonomy. And should limit the family of plant samples in order to not allowing each group to have a variety of plant. Alternatively, the number of plant samples in the same species should be increased to ensure that the n-alkane distribution has been represented by those plants.

REFERENCES

Andersson, R.A., Kuhry, P., Meyers, P., Zebühr, Y., Crill, P., and Mörth, M. 2011. Impacts of paleohydrological changes on n-alkane biomarker compositions of a Holocene peat sequence in the eastern European Russian Arctic. Organic Geochemistry 42: 1065-1075.

Baker, E. 1974. The influence of environment on leaf wax development in Brassica oleracea var. gemmifera. New Phytologist 73: 955-966.

Berlyn, G.P. 1986. The botany of mangroves. Science 234: 373-374.

Blaauw, M., and Christen, J.A. 2011. Flexible paleoclimate age-depth models using an autoregressive gamma process. Bayesian analysis 6: 457-474.

Brock, F., Higham, T., Ditchfield, P., and Ramsey, C.B. 2010. Current pretreatment methods for AMS radiocarbon dating at the Oxford Radiocarbon Accelerator Unit (ORAU). Radiocarbon 52: 103-112.

Bush, R.T., and McInerney, F.A. 2013. Leaf wax n-alkane distributions in and across modern plants: Implications for paleoecology and chemotaxonomy. Geochimica et Cosmochimica Acta 117: 161-179.

Bush, R.T., and McInerney, F.A. 2015. Influence of temperature and C 4 abundance on n -alkane chain length distributions across the central USA. Organic Geochemistry 79: 65-73.

Chaimanee, N., Disyaphun, S., and Teerasikul, N. 1986. Geology of Cha-uat and Ranot District Trans.). In (Ed.),^(Eds.),   (ed., Vol. pp.). Department of Mineral Resources. (Reprinted from.

Chawchai, S., et al. 2013. Lake Kumphawapi – an archive of Holocene palaeoenvironmental and palaeoclimatic changes in northeast Thailand. Quaternary Science Reviews 68: 59-75.

Cranwell, P.A. 1973. Chain-length distribution of n-alkanes from lake sediments in relation to post-glacial environmental change. Freshwater Biology 3: 259-265.

Dembicki Jr, H., Meinschein, W., and Hattin, D.E. 1976. Possible ecological and environmental significance of the predominance of even-carbon number C20-C30n-alkanes. Geochimica et Cosmochimica Acta 40: 203-208.

Dubois, N., et al. 2014. Indonesian vegetation response to changes in rainfall seasonality over the past 25,000 years. Nature Geoscience 7: 513-517.

Easterling, W.E., Crosson, P.R., Rosenberg, N.J., McKenney, M.S., Katz, L.A., and Lemon, K.M. 1993. Paper 2. Agricultural impacts of and responses to climate change in the Missouri-Iowa-Nebraska-Kansas (MINK) region. Climatic Change 24: 23-61.

Eglinton, G., and Hamilton, R.J. 1967. Leaf epicuticular waxes. Science 156: 1322-1335.

Eglinton, T.I., and Eglinton, G. 2008. Molecular proxies for paleoclimatology. Earth and Planetary Science Letters 275: 1-16.

Fairall, C., Bradley, E.F., Hare, J., Grachev, A., and Edson, J. 2003. Bulk parameterization of air–sea fluxes: Updates and verification for the COARE algorithm. Journal of climate 16: 571-591.

Ficken, K.J., Li, B., Swain, D., and Eglinton, G. 2000. An n-alkane proxy for the sedimentary input of submerged/floating freshwater aquatic macrophytes. Organic geochemistry 31: 745-749.

Gelpi, E., Schneider, H., Mann, J., and Oro, J. 1970. Hydrocarbons of geochemical significance in microscopic algae. Phytochemistry 9: 603-612.

Gingras, M.K., Pemberton, S.G., and Smith, M. 2015. Bioturbation: reworking sediments for better or worse. Oilfield Review 26: 46-58.

Guo, N., Gao, J., He, Y., Zhang, Z., and Guo, Y. 2014. Variations in leaf epicuticular n-alkanes in some Broussonetia, Ficus and Humulus species. Biochemical Systematics and Ecology 54: 150-156.

Han, J., McCarthy, E.D., Van Hoeven, W., Calvin, M., and Bradley, W. 1968. Organic geochemical studies, II. A preliminary report on the distribution of aliphatic hydrocarbons in algae, in bacteria, and in a recent lake sediment. Proceedings of the National Academy of Sciences of the United States of America 59: 29.

Hao, D.C., Gu, X.-J., and Xiao, P.G. 2015. Chemotaxonomy. In Medicinal Plants, pp. 1-48.

Herbin, G., and Robins, P. 1969. Patterns of variation and development in leaf wax alkanes. Phytochemistry 8: 1985-1998.

Hoegh-Guldberg, O., et al. 2007. Coral reefs under rapid climate change and ocean acidification. science 318: 1737-1742.

Hogg, R.W., and Gillan, F.T. 1984. Fatty acids, sterols and hydrocarbons in the leaves from eleven species of mangrove. Phytochemistry 23: 93-97.

Horton, B.P., Gibbard, P.L., Mine, G., Morley, R., Purintavaragul, C., and Stargardt, J.M. 2005. Holocene sea levels and palaeoenvironments, Malay-Thai Peninsula, southeast Asia. The Holocene 15: 1199-1213.

Jia, G., et al. 2015. Biogeochemical evidence of Holocene East Asian summer and winter monsoon variability from a tropical maar lake in southern China. Quaternary Science Reviews 111: 51-61.

Kolattukudy, P. 1970. Plant waxes. Lipids 5: 259-275.

Kuhn, T.K., Krull, E.S., Bowater, A., Grice, K., and Gleixner, G. 2010. The occurrence of short chain n-alkanes with an even over odd predominance in higher plants and soils. Organic Geochemistry 41: 88-95.

Kunst, L., and Samuels, A. 2003. Biosynthesis and secretion of plant cuticular wax. Progress in lipid research 42: 51-80.

Last, W.M., and Smol, J.P. 2006. Tracking environmental change using lake sediments: volume 2: physical and geochemical methods. Springer Science & Business Media.

Li, J., Huang, J., Ge, J., Huang, X., and Xie, S. 2013. Chemotaxonomic significance of n-alkane distributions from leaf wax in genus of Sinojackia species (Styracaceae). Biochemical Systematics and Ecology 49: 30-36.

Liu, H., and Liu, W. 2016. n-Alkane distributions and concentrations in algae, submerged plants and terrestrial plants from the Qinghai-Tibetan Plateau. Organic Geochemistry 99: 10-22.

Maffei, M., Mucciarelli, M., and Scannerini, S. 1993. Environmental factors affecting the lipid metabolism in Rosmarinus officinalis L. Biochemical systematics and ecology 21: 765-784.

Marzi, R., Torkelson, B., and Olson, R. 1993. A revised carbon preference index. Organic Geochemistry 20: 1303-1306.

Meyers, P.A. 1997. Organic geochemical proxies of paleoceanographic, paleolimnologic, and paleoclimatic processes. Organic geochemistry 27: 213-

250.

Meyers, P.A. 2003. Applications of organic geochemistry to paleolimnological reconstructions: a summary of examples from the Laurentian Great Lakes. Organic geochemistry 34: 261-289.

Meyers, P.A., and Ishiwatari, R. 1993. Lacustrine organic geochemistry—an overview of indicators of organic matter sources and diagenesis in lake sediments. Organic geochemistry 20: 867-900.

Nikolić, B., Tešević, V., Bojović, S., and Marin, P.D. 2013. Chemotaxonomic Implications of the n-Alkane Composition and the Nonacosan-10-ol Content in Picea omorika, Pinus heldreichii, and Pinus peuce. Chemistry & biodiversity 10: 677-686.

Nishimura, M., and Baker, E.W. 1986. Possible origin of n-alkanes with a remarkable even-to-odd predominance in recent marine sediments. Geochimica et Cosmochimica Acta 50: 299-305.

Norström, E., Katrantsiotis, C., Smittenberg, R.H., and Kouli, K. 2017. Chemotaxonomy in some Mediterranean plants and implications for fossil biomarker records. Geochimica et Cosmochimica Acta 219: 96-110.

Nudnara, W. 2016. Paleoenvironmental reconstruction based on palynology in Thale Noi, Phatthalung. Bachelor Geology Chulalongkorn university.

Pearson, E.J., Farrimond, P., and Juggins, S. 2007. Lipid geochemistry of lake sediments from semi-arid Spain: relationships with source inputs and environmental factors. Organic Geochemistry 38: 1169-1195.

Peters, K.E., Walters, C.C., and Moldowan, J.M. 2004. The Biomarker Guide.

Phountong, K. 2016. Reconatruction of sea level changes in Changwat Phatthalung. Bachelor, Geology Chulalongkorn university.

Pitty, A. 1988. Effect of environmental conditions on velvetleaf and giant foxtail epicuticular wax quantity and quality and the relationship to herbicide penetration.

Pradit, S., Wattayakorn, G., Angsupanich, S., Baeyens, W., and Leermakers, M. 2009. Distribution of Trace Elements in Sediments and Biota of Songkhla Lake, Southern Thailand. Water, Air, and Soil Pollution 206: 155-174.

Pramojanee, P., Hastings, P., Liengsakul, M., and Engakul, V. 1986. The Holocene transgression in Peninsular Thailand.

Pu, Y., Wang, C., and Meyers, P.A. 2017. Origins of biomarker aliphatic hydrocarbons in sediments of alpine Lake Ximencuo, China. Palaeogeography, Palaeoclimatology, Palaeoecology 475: 106-114.

Rao, Z., Wu, Y., Zhu, Z., Jia, G., and Henderson, A. 2011. Is the maximum carbon number of long-chain n-alkanes an indicator of grassland or forest? Evidence from surface soils and modern plants. Chinese Science Bulletin 56: 1714-1720.

Ratnayake, A.S., Sampei, Y., Ratnayake, N.P., and Roser, B.P. 2017. Middle to late Holocene environmental changes in the depositional system of the tropical brackish Bolgoda Lake, coastal southwest Sri Lanka. Palaeogeography, Palaeoclimatology, Palaeoecology 465: 122-137.

Reddy, C.M., et al. 2000. Even carbon number predominance of plant wax n-alkanes: a correction. Organic geochemistry 31: 331-336.

Rhee, Y., Hlousek-Radojcic, A., Ponsamuel, J., Liu, D., and Post-Beittenmiller, D. 1998. Epicuticular wax accumulation and fatty acid elongation activities are

induced during leaf development of leeks. Plant physiology 116: 901-911.

Rommerskirchen, F., Eglinton, G., Dupont, L., and Rullkötter, J. 2006. Glacial/interglacial changes in southern Africa: Compound-specific δ13C land plant biomarker and pollen records from southeast Atlantic continental margin sediments. Geochemistry, Geophysics, Geosystems 7: n/a-n/a.

Singh, R. 2016. Chemotaxonomy: a tool for plant classification. Journal of Medicinal Plants 4: 90-93.

Somboon, J. 1990. Palynological study of mangrove and marine sediments of the Gulf of Thailand. Journal of Southeast Asian Earth Sciences 4: 85-97.

Tanner, B.R., Uhle, M.E., Kelley, J.T., and Mora, C.I. 2007. C3/C4 variations in salt-marsh sediments: An application of compound specific isotopic analysis of lipid biomarkers to late Holocene paleoenvironmental research. Organic Geochemistry 38: 474-484.

Tanner, B.R., et al. 2010. Comparison of bulk and compound-specific δ13C analyses and determination of carbon sources to salt marsh sediments using n-alkane distributions (Maine, USA). Estuarine, Coastal and Shelf Science 86: 283-291.

Tjia, H., and Liew, K. 1996. Changes in tectonic stress field in northern Sunda Shelf basins. Geological Society, London, Special Publications 106: 291-306.

Vogts, A., Moossen, H., Rommerskirchen, F., and Rullkötter, J. 2009. Distribution patterns and stable carbon isotopic composition of alkanes and alkan-1-ols from plant waxes of African rain forest and savanna C3 species. Organic Geochemistry 40: 1037-1054.

Wang, G., et al. 2017. Climate conditions and relative abundance of C3 and C4 vegetation during the past 40 ka inferred from lake sediments in Wudalianchi, northeast China. Journal of Paleolimnology 58: 243-256.

Wang, J., et al. 2018. Temperature effect on abundance and distribution of leaf wax n-alkanes across a temperature gradient along the 400 mm isohyet in China. Organic Geochemistry 120: 31-41.

Wang, Y., et al. 2010. Predominance of even carbon-numbered n-alkanes from lacustrine sediments in Linxia Basin, NE Tibetan Plateau: Implications for climate change. Applied Geochemistry 25: 1478-1486.

Wilkinson, R.E. 1972. Sicklepod hydrocarbon response to photoperiod. Phytochemistry 11: 1273-1280.

Wilkinson, R.E. 1974. Sicklepod surface wax response to photoperiod and S-(2, 3-dichloroallyl) diisopropylthiocarbamate (diallate). Plant physiology 53: 269-275.

Yoojam, N. 2015. Paleoenvironmental reconstruction based on lake sediments from Thale Noi, Changwat Pattalung. Bachelor, Geology Chulalongkorn university.

Zeisler-Diehl, V., Müller, Y., and Schreiber, L. 2018. Epicuticular wax on leaf cuticles does not establish the transpiration barrier, which is essentially formed by intracuticular wax. Journal of plant physiology 227: 66-74.

Zhang, Y., Su, Y., Liu, Z., Yu, J., and Jin, M. 2017. Lipid biomarker evidence for determining the origin and distribution of organic matter in surface sediments of Lake Taihu, Eastern China. Ecological Indicators 77: 397-408.

Zheng, Y., Zhou, W., Meyers, P.A., and Xie, S. 2007. Lipid biomarkers in the Zoigê-Hongyuan peat deposit: Indicators of Holocene climate changes in West China. Organic Geochemistry 38: 1927-1940.

APPENDICS

APPENDIX A

CORE LOCATIONS

Table 1 Core locations.

Core Name	Latitude	Longitude	UTM (WGS)		Water depth (cm)	Core depth (cm)
			X	Y		
TLN-CP3	7°47′2″	100°07′40″	624351	861217	150	234
TLN-CP4	7°47′11″	100°09′00″	626802	860855	200	184
TLN-CP5	7°47′15″	100°09′00″	625668	860975	150	238
TLN-CP7	7°47′03″	100°09′60″	628641	860615	150	292
TLN-CP8	7°47′34″	100°09′04″	626923	861562	200	168
TLN-CP9	7°48′05″	100°09′07″	627012	862515	200	231
TLN-CP10	7°46′38″	100°09′07″	627019	859842	200	143
TLN-CP11	7°47′06″	100°09′32″	627783	860704	200	139

APPENDIX B

N-ALKANE DATABASE IN MANGROVE FOREST

Abbreviations for plant species

Acrostichum aureum (Aa)   *Avicennia marina (Am)*

Barringtonia asiatica (Ba)   *Bruguira gymnorrhiza (Bg)*

Casuarina equisetifolia (Ce)   *Oncusperma tigllarium (Ot)*

Poaceae (*Bambusoideae*) *(PB)*   *Rhizophora apiculate (Ra)*

Rhizophora mucronate (Rm)   *Sesuvium portulacastrum (Sp)*

Sonneratia caseolaris (Sc)   *Xylocarpus granatum (Xg)*

Carbon chain length	Aa	Am	Ba (KKB)	Ba (TLN)	Bg	Ce (KKB)	Ce (TLN)	Ot	PB	Ra	Rm (KSC)	Rm (KKB)	Sp	Sc (KSC)	Sc (TLN)	Xg
C$_{14}$	0.98	-	2.27	3.62	8.32	5.73	2.32	1.93	0.85	2.75	1.26	1.38	5.2	0.43	1.64	9.54
C$_{15}$	3.7	-	8.2	8.43	12.2	17.84	4.68	8.67	2.54	3.5	1.14	4.45	11.1	1.05	4.38	14.6
C$_{16}$	6.97	0.49	10.54	15.15	16.4	20.1	9.08	19.81	5.34	4.99	1.4	11.39	20.1	1.3	4.89	20.8
C$_{17}$	6.35	0.52	9.49	18.13	13.5	15.23	14.31	22.97	8.31	3.78	1	19.48	18.5	1.2	5.11	19
C$_{18}$	3.49	-	6.91	18.11	8.75	7.18	14.63	13.45	6.58	2.51	0.64	14.17	11.5	0.94	8.36	13.3
C$_{19}$	1.32	-	3.27	3.24	2.07	2.2	3.99	4.31	2.34	0.55	-	4.78	3.23	0.41	1.96	2.85
C$_{20}$	0.87	-	-	-	4.83	6.42	2.98	3.7	1.16	0.39	-	2.74	1.76	-	-	1.97
C$_{21}$	0.43	-	2.17	2.08	0.58	0.83	2.26	1.22	0.73	-	-	1.35	0.83	-	0.57	0.88
C$_{22}$	0.69	-	5.15	3.56	1.15	1.49	2.43	0.94	0.54	-	-	1	1.62	-	1.85	1.67
C$_{23}$	0.58	-	3.84	3.26	0.85	2.01	1.95	1.47	0.55	-	-	1.4	1.15	-	2.66	1.5
C$_{24}$	1.96	-	13.5	7.15	3.5	5.28	8.53	5.32	2.36	1.04	-	3.37	4.75	-	3.63	3.75
C$_{25}$	1.65	-	4.47	2.56	1.14	1.78	3.64	1.04	2.33	0.43	0.52	1.75	3.66	1.32	3.62	1.32

Carbon chain length	Aa	Am	Ba (KKB)	Ba (TLN)	Bg	Ce (KKB)	Ce (TLN)	Ot	PB	Ra	Rm (KSC)	Rm (KKB)	Sp	Sc (KSC)	Sc (TLN)	Xg
C$_{26}$	0.79	-	5.7	3.34	1.6	4.51	5.47	1.87	1.29	0.39	0.63	8.37	5.35	0.93	4.16	1.84
C$_{27}$	2.29	0.73	4.61	2.31	2.68	2.58	4.57	1.02	3.91	0.56	1.48	4.75	5.76	4.11	4.26	1.56
C$_{28}$	0.6	0.47	4.41	332	3.87	2.86	7.42	1.4	1.15	0.54	2.51	3.11	1.47	0.76	2.54	1.78
C$_{29}$	3.71	7.09	3.54	1.87	5.53	1.14	4.8	2.36	14.3	13.9	51.7	5.15	2.16	23.22	6.51	1.94
C$_{30}$	2.95	2.47	3.3	0.94	2.23	1.61	3.41	1.05	3.29	2.16	11.85	6.73	0.9	1.46	1.99	1
C$_{31}$	16.6	31	4.58	2.92	6.39	1.22	3.52	4.42	23.7	37.4	24.65	4.63	0.97	40.62	14.57	0.74
C$_{32}$	2.07	6.34	-	-	1.89	-	-	-	1.32	2.77	0.56	-	-	2.66	-	-
C$_{33}$	38.4	45.8	4.05	-	2.55	-	-	3.04	12.4	21.7	0.66	-	-	19.59	27.28	-
C$_{34}$	-	1.94	-	-	-	-	-	-	-	-	-	-	-	-	-	-
C$_{35}$	3.66	3.15	-	-	-	-	-	-	5.06	0.77	-	-	-	-	-	-

APPENDIX C

GAS CHROMATOGRAPHY/MASS SPECTROSCOPY

Gas chromatogram m/z 85 (Normal alkane homologous)

Peak	Carbon No.	IUPAC	Peak	Carbon No.	IUPAC
1	n-C_{12}		16	n-C_{27}	Heptacosane
2	n-C_{13}		17	n-C_{28}	Octacosane
3	n-C_{14}	Tetradecane	18	n-C_{29}	Nonacosane
4	n-C_{15}	Pentadecane	19	n-C_{30}	Triacontane
5	n-C_{16}	Hexadecane	20	n-C_{31}	Hentriacontane
6	n-C_{17}	Heptadecane	21	n-C_{32}	Dotriacontane
7	n-C_{18}	Octadecane	22	n-C_{33}	Tritriacontane
8	n-C_{19}	Nonadecane	23	n-C_{34}	Tetratriacontane
9	n-C_{20}	Eicosane	24	n-C_{35}	Pentatriacontane
10	n-C_{21}	Heneicosane	25	n-C_{36}	
11	n-C_{22}	Docosane	26	n-C_{37}	
12	n-C_{23}	Tricosane	27	n-C_{38}	
13	n-C_{24}	Tetracosane	28	n-C_{39}	
14	n-C_{25}	Pentacosane	29	n-C_{40}	
15	n-C_{26}	Hexacosane			

Standard C_{12}-C_{40} *n*-alkane
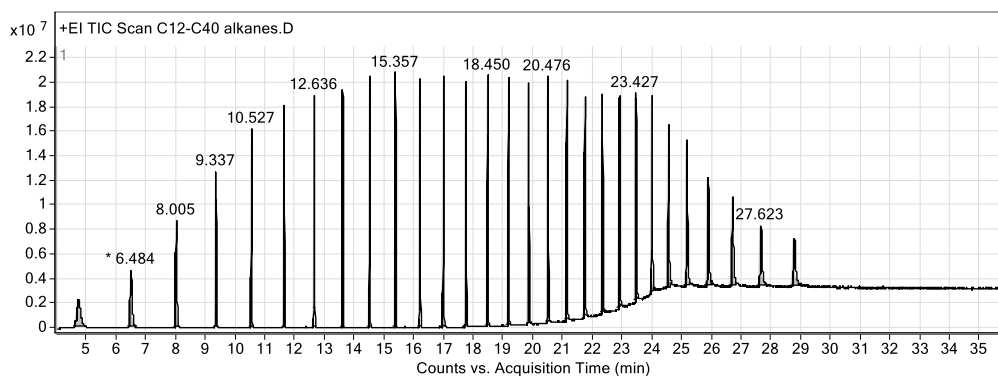
Location: Khun Samut Chin Temple (KSC), Samut Prakan Province

Sample ID: *Avicennia marina* (long-chain predominance)
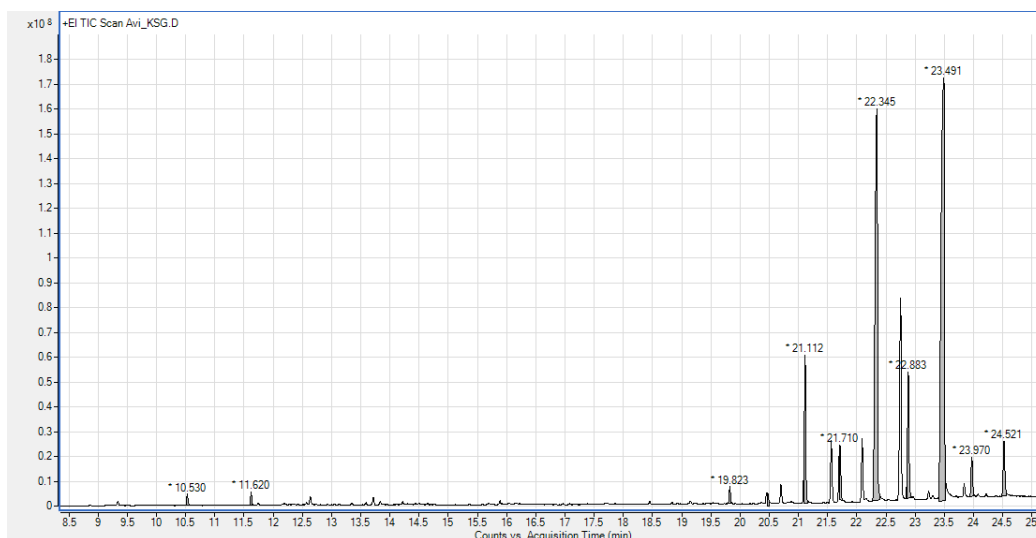
Peak	Carbon No.	RT	Area	Total area	%area
1	$n\text{-}C_{14}$			1464896356	0.000000
2	$n\text{-}C_{15}$			1464896356	0.000000
3	$n\text{-}C_{16}$	10.53	7116382.54	1464896356	0.485794
4	$n\text{-}C_{17}$	11.62	7690344.38	1464896356	0.524975
5	$n\text{-}C_{18}$			1464896356	0.000000
6	$n\text{-}C_{19}$			1464896356	0.000000
7	$n\text{-}C_{20}$			1464896356	0.000000
8	$n\text{-}C_{21}$			1464896356	0.000000
9	$n\text{-}C_{22}$			1464896356	0.000000
10	$n\text{-}C_{23}$			1464896356	0.000000
11	$n\text{-}C_{24}$			1464896356	0.000000
12	$n\text{-}C_{25}$			1464896356	0.000000
13	$n\text{-}C_{26}$			1464896356	0.000000
14	$n\text{-}C_{27}$	19.823	10700493.45	1464896356	0.730461
15	$n\text{-}C_{28}$	20.474	6886565.47	1464896356	0.470106
16	$n\text{-}C_{29}$	21.112	103868448.3	1464896356	7.090498
17	$n\text{-}C_{30}$	21.71	36207171.18	1464896356	2.471654
18	$n\text{-}C_{31}$	22.345	454378460.8	1464896356	31.017789
19	$n\text{-}C_{32}$	22.883	92864348.67	1464896356	6.339312
20	$n\text{-}C_{33}$	23.491	670702671.5	1464896356	45.784991

21	$n\text{-}C_{34}$	23.97	28405941.4	1464896356	1.939109
22	$n\text{-}C_{35}$	24.521	46075528.43	1464896356	3.145310

Location: Khun Samut Chin Temple (KSC), Samut Prakan Province

Sample ID: *Sesuvium portulacastrum* (short-chain predominance)
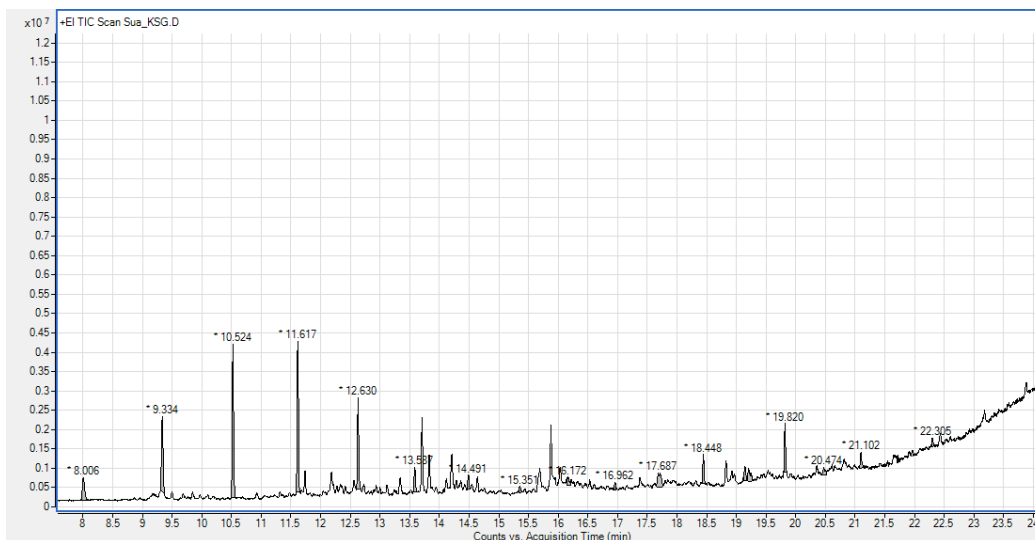
Peak	Carbon No.	RT	Area	Total area	%area
1	$n\text{-}C_{14}$	8.006	1627047.23	31303633	5.197631
2	$n\text{-}C_{15}$	9.334	3460831.25	31303633	11.055686
3	$n\text{-}C_{16}$	10.524	6292871.8	31303633	20.102689
4	$n\text{-}C_{17}$	11.617	5796732.77	31303633	18.517764
5	$n\text{-}C_{18}$	12.63	3607741.45	31303633	11.524993
6	$n\text{-}C_{19}$	13.587	1010223.55	31303633	3.227177
7	$n\text{-}C_{20}$	14.491	552076.21	31303633	1.763617
8	$n\text{-}C_{21}$	15.351	258383.15	31303633	0.825409
9	$n\text{-}C_{22}$	16.172	505784.1	31303633	1.615736
10	$n\text{-}C_{23}$	16.962	359615.56	31303633	1.148798
11	$n\text{-}C_{24}$	17.687	1487492.59	31303633	4.751821
12	$n\text{-}C_{25}$	18.448	1146833.22	31303633	3.663579
13	$n\text{-}C_{26}$	19.145	1676045.81	31303633	5.354158
14	$n\text{-}C_{27}$	19.82	1802164.12	31303633	5.757045
15	$n\text{-}C_{28}$	20.474	458727.4	31303633	1.465413
16	$n\text{-}C_{29}$	21.102	676696.62	31303633	2.161719
17	$n\text{-}C_{30}$	21.717	282103.33	31303633	0.901184
18	$n\text{-}C_{31}$	22.305	302262.61	31303633	0.965583
19	$n\text{-}C_{32}$			31303633	0.000000
20	$n\text{-}C_{33}$			31303633	0.000000

21	$n\text{-}C_{34}$	31303633	0.000000
22	$n\text{-}C_{35}$	31303633	0.000000

Location: Kung krabaen bay (KKB), Chantaburi Province

Sample ID: *Casuarina equisetifolia* (bimodal distribution)
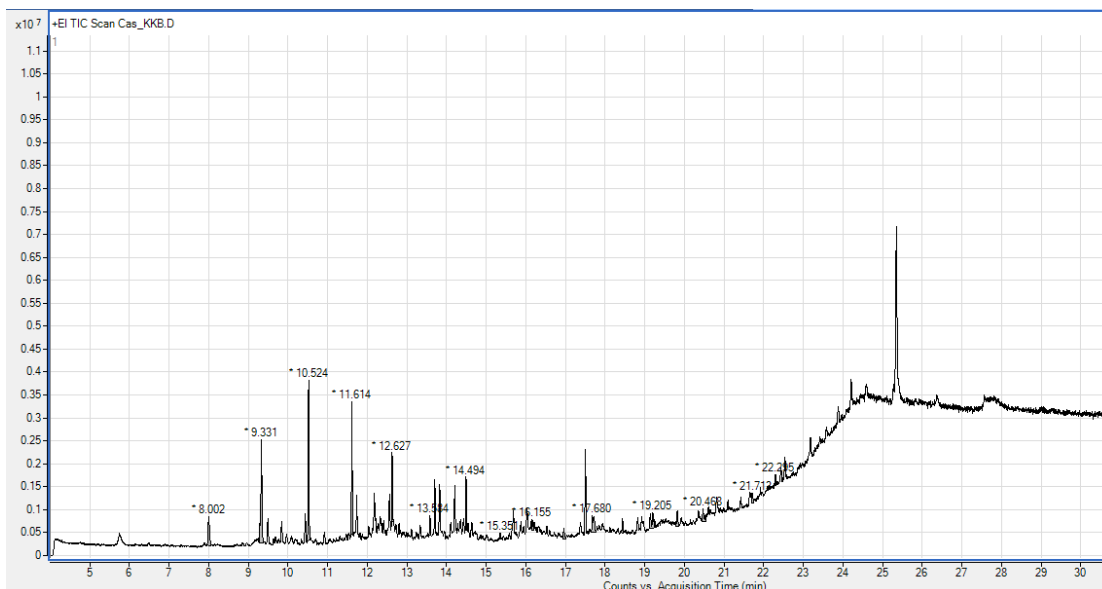
Peak	Carbon No.	RT	Area	Total area	%area
1	$n\text{-}C_{14}$	8.002	1567756.17	27376368	5.726677
2	$n\text{-}C_{15}$	9.331	4885088.67	27376368	17.84418
3	$n\text{-}C_{16}$	10.524	5503597.73	27376368	20.10346
4	$n\text{-}C_{17}$	11.614	4169416.06	27376368	15.22998
5	$n\text{-}C_{18}$	12.627	1965675.91	27376368	7.180192
6	$n\text{-}C_{19}$	13.584	603018.34	27376368	2.202697
7	$n\text{-}C_{20}$	14.494	1757203.96	27376368	6.418689
8	$n\text{-}C_{21}$	15.351	226341.19	27376368	0.826776
9	$n\text{-}C_{22}$	16.155	407569.82	27376368	1.488765
10	$n\text{-}C_{23}$	16.962	549286.25	27376368	2.006425
11	$n\text{-}C_{24}$	17.68	1444406.63	27376368	5.276108
12	$n\text{-}C_{25}$	18.441	486838.2	27376368	1.778316
13	$n\text{-}C_{26}$	19.205	1233525.91	27376368	4.505806
14	$n\text{-}C_{27}$	19.82	706174.18	27376368	2.579503
15	$n\text{-}C_{28}$	20.468	783962.29	27376368	2.863646
16	$n\text{-}C_{29}$	21.099	312764.5	27376368	1.142462
17	$n\text{-}C_{30}$	21.713	439811.86	27376368	1.606538
18	$n\text{-}C_{31}$	22.295	333930.31	27376368	1.219776
19	$n\text{-}C_{32}$			27376368	0

20	n-C$_{33}$	27376368	0
21	n-C$_{34}$	27376368	0
22	n-C$_{35}$	27376368	0

จุฬาลงกรณ์มหาวิทยาลัย

CHULALONGKORN UNIVERSITY

Location: Thale Noi, Phatthalung Province

Sample ID: TLN-CP5_230 (380 cm depth below water), Unit A
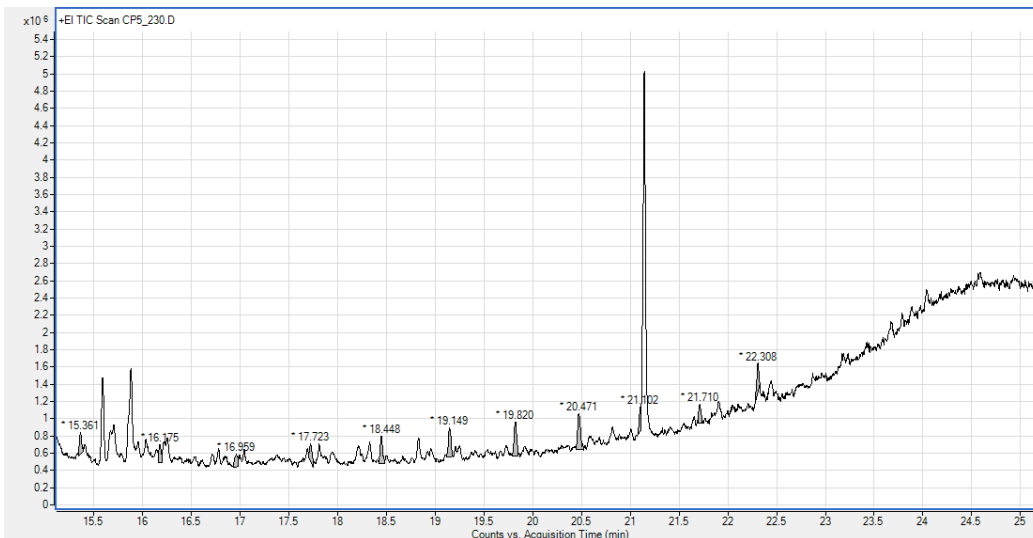
Peak	Carbon No.	RT	Area	Total area	%area
8	n-C_{21}	15.361	414787.49	5409939	7.667138
9	n-C_{22}	16.175	348994.97	5409939	6.450997
10	n-C_{23}	16.959	301759.13	5409939	5.577866
11	n-C_{24}	17.723	401160.14	5409939	7.415244
12	n-C_{25}	18.448	600123.01	5409939	11.092972
13	n-C_{26}	19.149	587971.23	5409939	10.868353
14	n-C_{27}	19.82	696499.11	5409939	12.874436
15	n-C_{28}	20.471	819460.53	5409939	15.147316
16	n-C_{29}	21.102	368144.8	5409939	6.804972
17	n-C_{30}	21.71	366330.73	5409939	6.771439
18	n-C_{31}	22.308	504707.7	5409939	9.329268
19	n-C_{32}			5409939	0.000000
20	n-C_{33}			5409939	0.000000
21	n-C_{34}			5409939	0.000000
22	n-C_{35}			5409939	0.000000

Location: Thale Noi, Phatthalung Province

Sample ID: TLN-CP5_200 (350 cm depth below water), Unit B
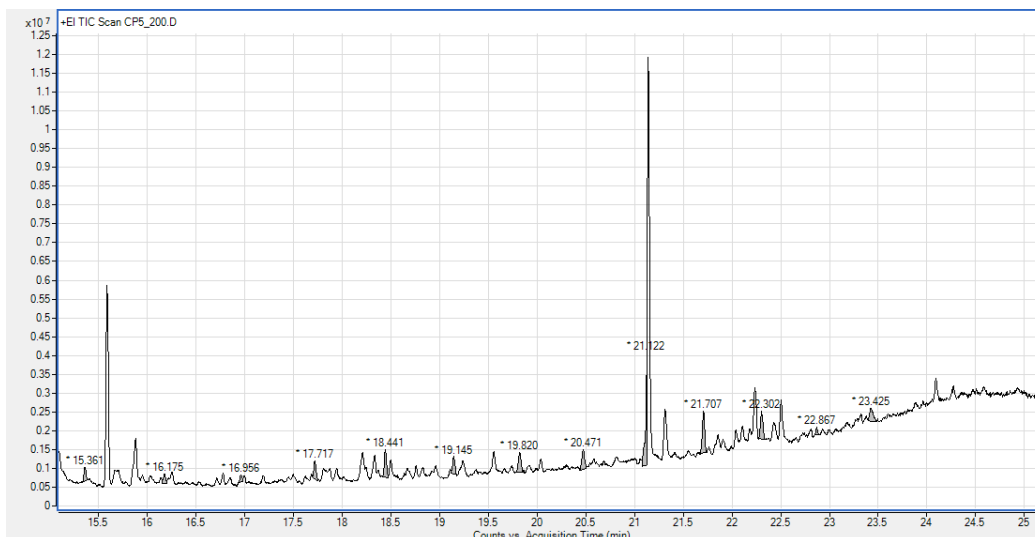
Peak	Carbon No.	RT	Area	Total area	%area
8	$n\text{-}C_{21}$	15.361	572802.92	12234724.7	4.681780
9	$n\text{-}C_{22}$	16.175	434518.74	12234724.7	3.551520
10	$n\text{-}C_{23}$	16.956	294985.8	12234724.7	2.411054
11	$n\text{-}C_{24}$	17.717	813343.41	12234724.7	6.647828
12	$n\text{-}C_{25}$	18.441	1204742.96	12234724.7	9.846915
13	$n\text{-}C_{26}$	19.145	720821.47	12234724.7	5.891604
14	$n\text{-}C_{27}$	19.82	954187.5	12234724.7	7.799011
15	$n\text{-}C_{28}$	20.471	995983.97	12234724.7	8.140632
16	$n\text{-}C_{29}$	21.122	1919357.38	12234724.7	15.687786
17	$n\text{-}C_{30}$	21.707	1860981.27	12234724.7	15.210651
18	$n\text{-}C_{31}$	22.302	1334178.67	12234724.7	10.904852
19	$n\text{-}C_{32}$	22.867	213332.16	12234724.7	1.743661
20	$n\text{-}C_{33}$	23.425	915488.44	12234724.7	7.482706
21	$n\text{-}C_{34}$			12234724.7	0.000000
22	$n\text{-}C_{35}$			12234724.7	0.000000

Location: Thale Noi, Phatthalung Province

Sample ID: TLN-CP5_150 (300 cm depth below water), Unit C
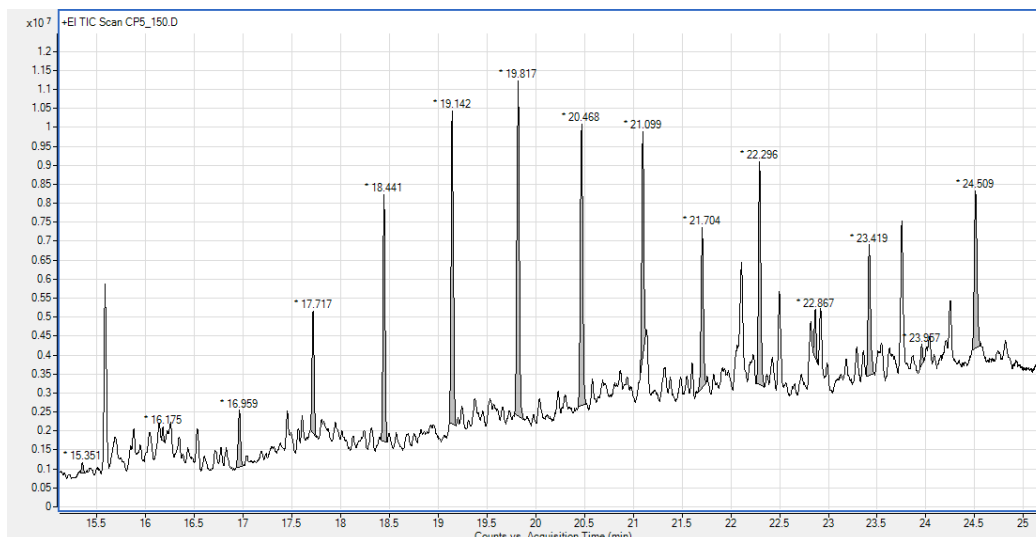
Peak	Carbon No.	RT	Area	Total area	%area
8	$n\text{-}C_{21}$	15.351	381957.15	102510147.9	0.372604
9	$n\text{-}C_{22}$	16.175	355496.84	102510147.9	0.346792
10	$n\text{-}C_{23}$	16.959	2574270.7	102510147.9	2.511235
11	$n\text{-}C_{24}$	17.717	4947061.8	102510147.9	4.825924
12	$n\text{-}C_{25}$	18.441	10173658.22	102510147.9	9.924538
13	$n\text{-}C_{26}$	19.142	12902696.2	102510147.9	12.586750
14	$n\text{-}C_{27}$	19.817	15013044.39	102510147.9	14.645423
15	$n\text{-}C_{28}$	20.468	12348147.61	102510147.9	12.045781
16	$n\text{-}C_{29}$	21.099	8960688.47	102510147.9	8.741270
17	$n\text{-}C_{30}$	21.704	7248672.57	102510147.9	7.071176
18	$n\text{-}C_{31}$	22.296	10266314.26	102510147.9	10.014925
19	$n\text{-}C_{32}$	22.867	1740652.78	102510147.9	1.698030
20	$n\text{-}C_{33}$	23.419	6379843.6	102510147.9	6.223621
21	$n\text{-}C_{34}$	23.957	741069.81	102510147.9	0.722923
22	$n\text{-}C_{35}$	24.509	8476573.5	102510147.9	8.269009

Location: Thale Noi, Phatthalung Province

Sample ID: TLN-CP5_120 (270 cm depth below water), Unit D
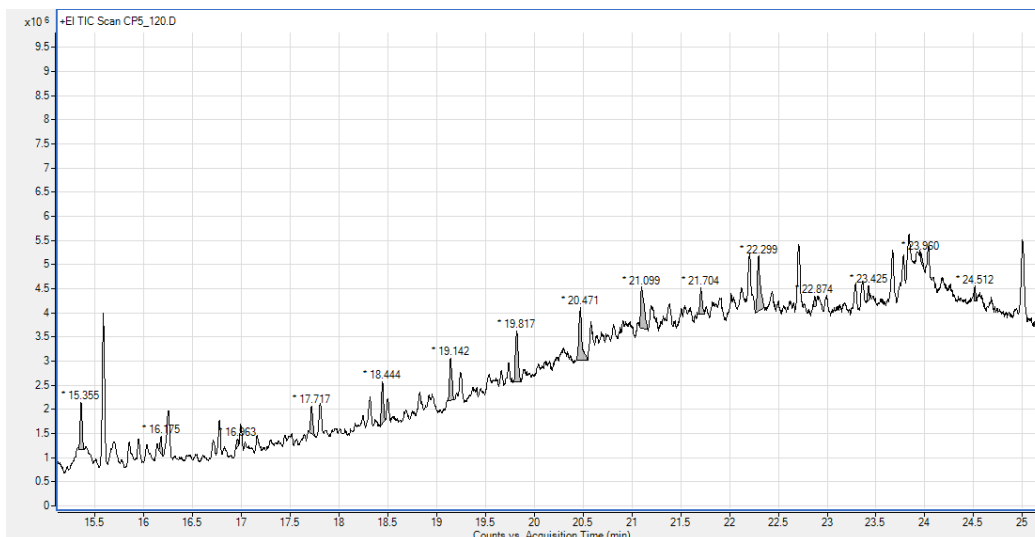
Peak	Carbon No.	RT	Area	Total area	%area
8	n-C_{21}	15.354	1422610.69	16483687	8.630416
9	n-C_{22}	16.175	411488.9	16483687	2.496340
10	n-C_{23}	16.963	211813.12	16483687	1.284986
11	n-C_{24}	17.717	900817.11	16483687	5.464901
12	n-C_{25}	18.444	1289024.1	16483687	7.819999
13	n-C_{26}	19.142	1424655.81	16483687	8.642822
14	n-C_{27}	19.817	1981226.92	16483687	12.019319
15	n-C_{28}	20.471	2306040.46	16483687	13.989834
16	n-C_{29}	21.099	2038401.04	16483687	12.366172
17	n-C_{30}	21.704	907180.55	16483687	5.503505
18	n-C_{31}	22.299	2449264.56	16483687	14.858718
19	n-C_{32}	22.874	243877.23	16483687	1.479507
20	n-C_{33}	23.425	327108.58	16483687	1.984438
21	n-C_{34}	23.96	264226.48	16483687	1.602957
22	n-C_{35}	24.512	305951.57	16483687	1.856087

Location: Thale Noi, Phatthalung Province

Sample ID: TLN-CP5_40 (190 cm depth below water), Unit E
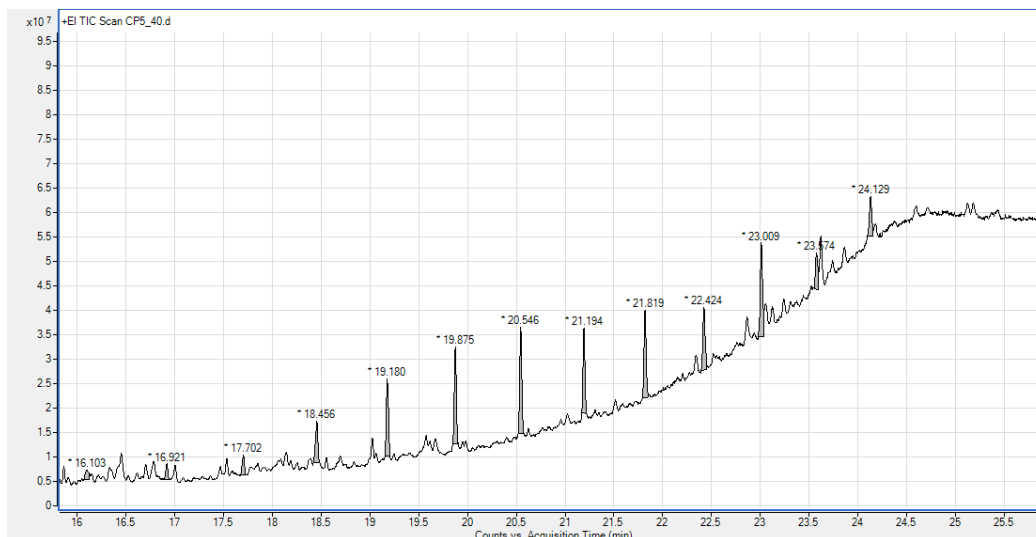
Peak	Carbon No.	RT	Area	Total area	%area
8	$n\text{-}C_{21}$	16.103	4706004	248281470.3	1.895431
9	$n\text{-}C_{22}$	16.921	4811975	248281470.3	1.938113
10	$n\text{-}C_{23}$	17.702	6047394	248281470.3	2.435701
11	$n\text{-}C_{24}$	18.456	13771552	248281470.3	5.546750
12	$n\text{-}C_{25}$	19.180	22812230	248281470.3	9.188052
13	$n\text{-}C_{26}$	19.875	30161987	248281470.3	12.148304
14	$n\text{-}C_{27}$	20.546	32566252	248281470.3	13.116666
15	$n\text{-}C_{28}$	21.194	24605226	248281470.3	9.910214
16	$n\text{-}C_{29}$	21.819	28098678	248281470.3	11.317268
17	$n\text{-}C_{30}$	22.424	21019470	248281470.3	8.465984
18	$n\text{-}C_{31}$	23.009	32338003	248281470.3	13.024735
19	$n\text{-}C_{32}$	23.574	13319478	248281470.3	5.364669
20	$n\text{-}C_{33}$	24.129	14023221	248281470.3	5.648114
21	$n\text{-}C_{34}$			248281470.3	0.000000
22	$n\text{-}C_{35}$			248281470.3	0.000000

Location: Thale Noi, Phatthalung Province

Sample ID: TLN-CP7_287 (437 cm depth below water), Unit C*
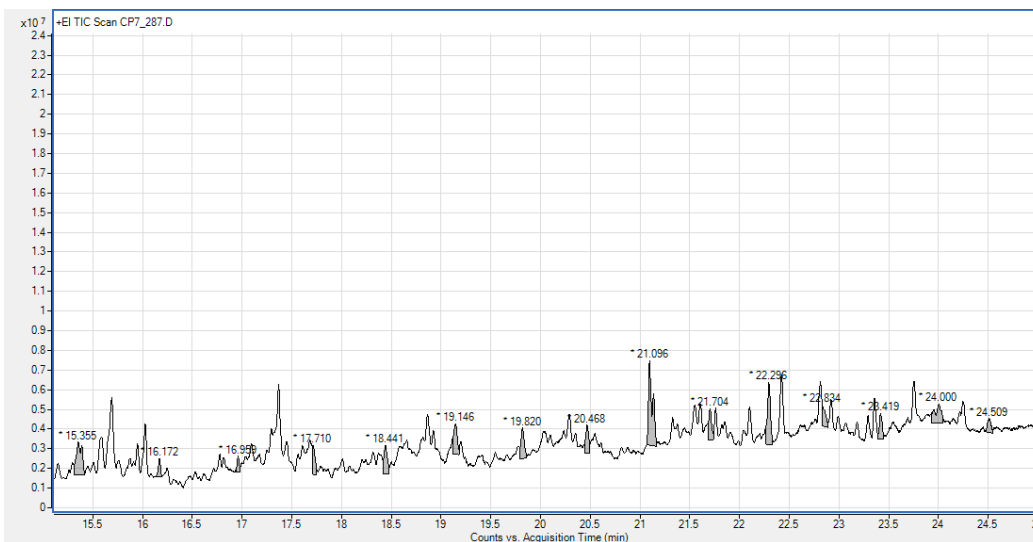
Peak	Carbon No.	RT	Area	Total area	%area
8	$n\text{-}C_{21}$	15.355	6838886.77	57786050	11.834840
9	$n\text{-}C_{22}$	16.172	1493874.01	57786050	2.585181
10	$n\text{-}C_{23}$	16.959	1191106.88	57786050	2.061236
11	$n\text{-}C_{24}$	17.71	2660887.41	57786050	4.604723
12	$n\text{-}C_{25}$	18.441	3310694.45	57786050	5.729228
13	$n\text{-}C_{26}$	19.146	3893704.84	57786050	6.738140
14	$n\text{-}C_{27}$	19.82	3545085.16	57786050	6.134846
15	$n\text{-}C_{28}$	20.468	2755979.17	57786050	4.769281
16	$n\text{-}C_{29}$	21.096	11752414.94	57786050	20.337806
17	$n\text{-}C_{30}$	21.704	3289311.3	57786050	5.692224
18	$n\text{-}C_{31}$	22.296	6479505.18	57786050	11.212923
19	$n\text{-}C_{32}$	22.834	2095029.85	57786050	3.625494
20	$n\text{-}C_{33}$	23.419	2492081.8	57786050	4.312601
21	$n\text{-}C_{34}$	24	4268223.4	57786050	7.386252
22	$n\text{-}C_{35}$	24.509	1719264.52	57786050	2.975224

Location: Thale Noi, Phatthalung Province

Sample ID: TLN-CP7_90 (240 cm depth below water), Unit D
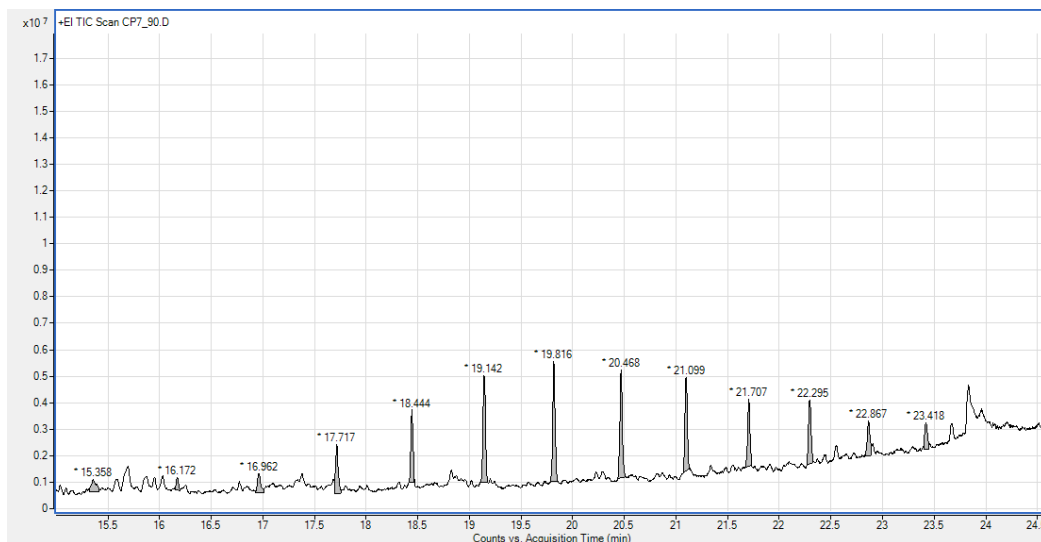
Peak	Carbon No.	RT	Area	Total area	%area
8	n-C_{21}	15.358	1529207.55	50247247	3.043366
9	n-C_{22}	16.172	753043.62	50247247	1.498676
10	n-C_{23}	16.962	1631029.65	50247247	3.246008
11	n-C_{24}	17.717	3386125.54	50247247	6.738927
12	n-C_{25}	18.444	4060049.57	50247247	8.080143
13	n-C_{26}	19.142	6753563.97	50247247	13.440665
14	n-C_{27}	19.816	7199352.32	50247247	14.327854
15	n-C_{28}	20.468	6785803.04	50247247	13.504825
16	n-C_{29}	21.099	5611046.3	50247247	11.166873
17	n-C_{30}	21.707	4073012.39	50247247	8.105941
18	n-C_{31}	22.295	4247286.23	50247247	8.452774
19	n-C_{32}	22.867	2366910.86	50247247	4.710528
20	n-C_{33}	23.418	1850816.14	50247247	3.683418
21	n-C_{34}			50247247	0.000000
22	n-C_{35}			50247247	0.000000

Location: Thale Noi, Phatthalung Province

Sample ID: TLN-CP7_20 (170 cm depth below water), Unit E
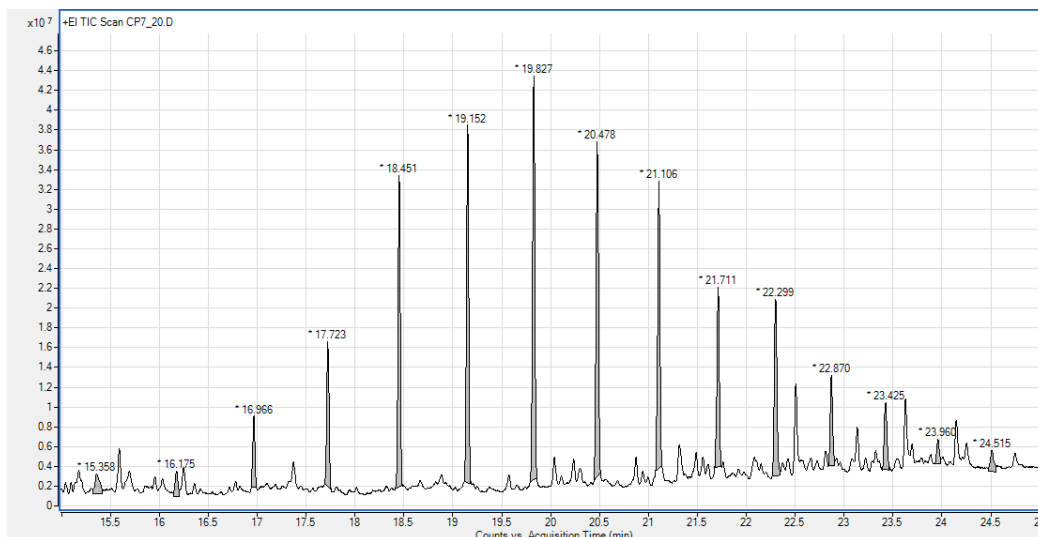
Peak	Carbon No.	RT	Area	Total area	%area
8	n-C_{21}	15.358	7278596.77	431021921.8	1.688684
9	n-C_{22}	16.175	5041874.52	431021921.8	1.169749
10	n-C_{23}	16.966	10873299.23	431021921.8	2.522679
11	n-C_{24}	17.723	22818955.7	431021921.8	5.294152
12	n-C_{25}	18.451	51836706.52	431021921.8	12.026466
13	n-C_{26}	19.152	59614994.83	431021921.8	13.831082
14	n-C_{27}	19.827	69189039.86	431021921.8	16.052325
15	n-C_{28}	20.478	55006566.79	431021921.8	12.761895
16	n-C_{29}	21.106	47840275.01	431021921.8	11.099267
17	n-C_{30}	21.711	30861500.41	431021921.8	7.160077
18	n-C_{31}	22.99	32088484.56	431021921.8	7.444745
19	n-C_{32}	22.87	15715024.29	431021921.8	3.645992
20	n-C_{33}	23.425	12647375.99	431021921.8	2.934277
21	n-C_{34}	23.96	4710262.1	431021921.8	1.092813
22	n-C_{35}	24.515	5498965.26	431021921.8	1.275797

BIOMARKER VALUE

Table 4.3 Biomarker parameters of TLN-CP5

Depth (cm)	Units	$ACL_{21\text{-}35}$	ACL_T	P_{aq}	$CPI_{21\text{-}35}$	CPI_T
155	E	27.94	24.60	0.41	1.83	1.81
170	E	27.42	24.62	0.41	1.67	1.51
180	E	27.15	23.48	0.44	1.16	1.11
190	E	28.22	26.89	0.32	1.28	1.22
200	E	29.05	25.38	0.26	1.80	1.07
210	E	28.01	23.63	0.27	2.00	1.07
220	D	27.89	23.61	0.31	1.15	1.04
230	D	27.00	24.18	0.41	1.27	1.04
240	D	26.22	22.03	0.51	1.79	1.18
250	D	27.31	23.07	0.31	1.36	1.17
260	D	25.62	23.72	0.42	1.58	1.21
270	D	27.63	25.71	0.25	1.42	1.28
280	D	27.08	24.67	0.25	1.87	1.12
290	D	28.53	24.67	0.29	2.21	1.65
300	C	29.12	28.19	0.40	1.43	1.43
310	C	29.75	28.74	0.08	2.54	2.18
320	C	29.47	27.88	0.15	3.24	2.21
330	C	28.93	26.31	0.20	1.43	1.52
340	B	28.27	24.70	0.41	2.31	1.71
350	B	28.06	25.99	0.32	1.37	1.25
360	B	27.30	25.48	0.44	1.66	1.63
380	A	26.26	24.04	0.51	1.06	1.22

Table Biomarker parameters of TLN-CP7

Depth (cm)	Units	ACL_{21-35}	ACL_T	P_{aq}	CPI_{21-35}	CPI_T
160	E	26.33	24.32	0.67	4.83	3.16
170	E	27.65	26.93	0.44	1.19	1.23
180	E	28.35	27.46	0.26	1.26	1.01
190	D	28.15	26.36	0.36	1.14	0.96
200	D	27.99	24.50	0.35	1.44	0.96
220	D	27.11	24.99	0.25	0.92	0.92
90	D	27.59	26.01	0.37	1.05	1.02
240	D	26.96	23.26	0.40	0.97	0.92
280	D	27.00	23.78	0.34	1.08	1.09
300	D	27.18	24.05	0.39	1.10	1.08
320	D	25.71	20.82	0.42	0.80	1.16
340	D	25.70	21.01	0.39	1.14	1.22
360	D	25.71	21.03	0.39	0.88	1.23
380	D	25.79	21.27	0.40	0.80	1.10
410	D	26.57	22.78	0.49	1.03	1.23
430	D	26.71	23.40	0.38	1.27	1.32
433	C*	27.18	23.89	0.39	1.27	1.38
437	C*	27.69	23.97	0.20	1.62	1.76

VITA

NAME   Assuma Sainakum

DATE OF BIRTH   13 February 1987

PLACE OF BIRTH   Lampang, Thailand

HOME ADDRESS   298 JP. Residence Ratchadiphisek 14
Ratchadiphisek Rd.
Huai Khwang, Bangkok 10310